Requirement for Lis1 in Normal and Malignant Stem Cell Renewal

by

Bryan Jeffrey Zimdahl

Department of Pharmacology and Cancer Biology
Duke University

Date:_____

Approved:

_____
Tannishtha Reya, Co-Supervisor

_____
Ann Marie Pendergast, Co-Supervisor

_____
Xiao-Fan Wang

_____
David Kirsch

_____
John Chute

Dissertation submitted in partial fulfillment of
the requirements for the degree of Doctor
of Philosophy in the Department of
Pharmacology and Cancer Biology in the Graduate School
of Duke University

2013

ABSTRACT

Requirement for Lis1 in Normal and Malignant Stem Cell Renewal

by

Bryan Jeffrey Zimdahl

Department of Pharmacology and Cancer Biology
Duke University

Date:_____

Approved:

_____
Tannishtha Reya, Co-Supervisor

_____
Ann Marie Pendergast, Co-Supervisor

_____
Xiao-Fan Wang

_____
David Kirsch

_____
John Chute

An abstract of a dissertation submitted in partial
fulfillment of the requirements for the degree
of Doctor of Philosophy in the Department of
Pharmacology and Cancer Biology in the Graduate School of
Duke University

2013

Abstract

Stem cells are defined by their ability to make more stem cells, a property known as self-renewal and their ability to generate cells that enter differentiation. One mechanism by which fate decisions can be effectively controlled in stem cells is through asymmetric division and the correct partitioning and inheritance of cell fate determinants. While hematopoietic stem cells have the capacity to divide through asymmetric division, the molecular machinery that regulates this process is unknown and whether its activity is required *in vivo* remains unclear. Here we show that Lis1, a dynein-binding protein and regulator of asymmetric division, is critically required for blood development and for hematopoietic stem cell renewal in fetal and adult life. In particular, conditional deletion of *Lis1* led to a severe bloodless phenotype and embryonic lethality *in vivo*. In both fetal and adult mice, loss of Lis1 led to a failure of normal self-renewal, which included impaired colony-forming ability *in vitro* and defects in long-term reconstitution ability following transplantation. As a possible mechanism, we find that the absence of Lis1 in hematopoietic cells, in part, accelerates differentiation linked to the incorrect inheritance of cell fate determinants. Furthermore, using a live cell imaging strategy, we find that the incorrect inheritance of cell fate determinants observed following the loss of Lis1 is due defects in spindle positioning and orientation. Finally, using two animal models of undifferentiated myeloid leukemia, we show that Lis1 is critical for the aberrant cell growth that occurs in cancer. Deletion of *Lis1* both at the early and late stages of myeloid leukemia blocked its propagation *in vivo* and led to a marked improvement in survival. Together, these data identify Lis1 and the directed control of asymmetric division as key regulators of normal and malignant hematopoietic development.

Dedication

For Mary Kay Francis and my father.

Everyday I am drenched with their love and support that shower down from Heaven.

Contents

List of Tables

List of Figures

List of Abbreviations

AML	Acute Myelogenous Leukemia
BrdU	5-bromo-2′-deoxyuridine
BFU-E	Burst Forming Unit-Erythroid
CFU-GM	Colony-Forming Unit-Granulocyte Macrophage
CFU-GEMM	Colony-Forming Unit-Granulocyte, Erythrocyte, Monocyte/macrophage, Megakaryocyte
CML	Chronic Myelogenous Leukemia
FACS	Fluorescence Activated Cell Sorting
HSC	Hematopoietic Stem Cell
PCR	Polymerase Chain Reaction
RT-PCR	Real-time Polymerase Chain Reaction
TNR	Transgenic Notch Reporter

Acknowledgements

My dissertation would not have been possible without the help of numerous individuals. I am grateful to Brigid Hogan, John Chang, Arshad Desai, Joseph Gleeson, Ji Eun Lee, MingFu Wu, Maike Sander, and Janel Koop for experimental advice and reagents. I would also like to thank Marcie Kritzik for advice and comments on my written work and Mike Cook, Lynn Matinek, Beth Harvat, Eric O'Conner and Karl Marquez for cell sorting. I would also like to thank the following individuals who generously provided either mice or constructs: Warren Pear, Ann Marie Pendergast, Gary Gilliland, Scott Armstrong, Christopher Counter, Sarah Russell, Geoffrey Wahl and Dimitris Kioussis.

I would like to thank David Rizzieri, Charles Chuah and Vivian G. Oehler for providing us with human leukemia patient samples. I would also like to thank Roman Sasik and Gary Hardiman from BIOGEM at the University of California, San Diego for performing the analysis on our Lis1 microarray data. I am grateful for experimental help from numerous members of the Reya lab including: Joi Weeks, Claire Koechlein, Hyog Young Kwon, Omead Arami and Mai Nakamura. A special thanks to Takaaki Konuma for independently performing, for the most part, the majority of the Lis1 human leukemia experiments. I would also like to thank Jeevisha Bajaj who helped perform experiments as well as helped establish the live imaging method we used to track spindle orientation in real time.

I'm extremely grateful to Allen Blevins, who over the past few years almost on a daily basis has provided excellent technical help. I sincerely appreciate all the time Allen devoted to the Lis1 project especially with the management of the Lis1 mouse colony. I am deeply indebted to Takahiro Ito. For the past six years, Takahiro has taught me how to effectively plan and perform experiments. Over the years, his willingness to continually participate in rigorous discussions on a variety of scientific topics has helped me more critically think about and properly interpret experimental data. He has played an integral part in the development and success of the Lis1 story. I cannot thank him enough.

I am especially grateful for all the time and advice provided by my thesis committee members including: Ann Marie Pendergast, Xiao-Fan Wang, David Kirsch and John Chute. Over the years, they have given invaluable advice and suggestions on my project and future career goals.

Last but not least, I sincerely thank my thesis mentor, Tannishtha Reya for giving me the opportunity to train and grow as a scientist in her laboratory. She always had great advice and suggestions when it came to designing experiments, preparing talks, writing grants and abstracts, or how to build professional relationships with potential collaborators. Most importantly, Tannishtha fostered a work environment where I felt completely comfortable voicing my own suggestions, comments and concerns and

confidently knew that they would be listen to and taken into consideration. Tannishtha has been a strong and supportive mentor to me throughout my graduate school career. Importantly, she has always given me great freedom to purse independent work. As a result, I feel that I have become a more independent and confident scientist and individual. Thank you Tannishtha.

1. Introduction

1.1 Hematopoiesis and hematopoietic stem cells

The hematopoietic system is a regulated developmental cascade that produces distinct cell lineages that differentiate into the mature cell types of the blood and generates roughly 100 billion blood cells every day (Orkin 2000). This process is maintained throughout the lifetime of an individual by hematopoietic stem cells (HSC). HSCs are defined by their unique ability to make more stem cells, a property known as self-renewal and their ability to differentiate into all blood cell lineages (Weissman 2000). The ability of HSCs to balance self-renewal with differentiation is critical not only when the body replaces cells to maintain homeostasis, but also during development when a substantial increase in HSC numbers is required to ensure enough HSCs are generated for postnatal life and for the essential geometric expansion of differentiated blood cells that are immediately required for embryonic growth and development (Lessard et al. 2004). In addition, the capacity of HSCs to balance self-renewal with differentiation is also important after acute injury when an exponential rise in the HSC population is needed for rapid and effective regeneration (Morrison 2009).

1.1.1 Hematopoietic stem cell development

Blood cell production during embryonic development manifests in numerous anatomical sites that are separated both temporally and spatially. The first definitive HSCs appear in mice around embryonic day (E) 10.5 in very low numbers in the aorta-

gonad mesonephros region, which is composed of the dorsal aorta, its surrounding mesenchyme and the urogenital ridges (Cumano et al. 1996; Godin et al. 1999; Medvinsky and Dzierzak 1996; Muller et al. 1994). Additionally, HSCs are generated in the vitelline and umbilical arteries that connect the dorsal aorta with the yolk sac and the placenta, respectively (de Bruijn et al. 2000). The placenta also has the capacity for *de novo* generation of HSCs and accrues a reservoir of HSCs during mid-gestation (Alvarez-Silva et al. 2003; Gekas et al. 2005; Ottersbach and Dzierzak 2005). However, HSCs derived from the aorta-gonad mesonephros region, placenta and yolk sac eventually colonize the fetal liver, which serves as the main site for HSC expansion and differentiation during mid-gestation (Ema and Nakauchi 2000). In late gestation, however, hematopoietic activity moves to the bone marrow, which supports both self-renewal and differentiation of HSCs in specialized microenvironmental niches, including well-defined endothelial/perivascular and osteoblastic niches (Orkin and Zon 2008).

1.1.2 Properties of fetal and adult hematopoietic stem cells

During development, the HSC pool expands rapidly in the fetal liver and therefore, most HSCs in the fetal liver are actively cycling (Morrison et al. 1995). However, the movement of hematopoietic activity from the fetal liver to the bone marrow is accompanied by a shift from a proliferative fetal HSC to a quiescent, conservatively self-renewing adult HSC (Mikkola and Orkin 2006; Orkin and Zon 2008).

In addition to differences in proliferative capacity between fetal and adult HSCs, there are several phenotypic and functional differences between fetal and adult HSCs. Fetal liver HSCs differ from adult bone marrow HSCs in the expression of specific surface markers, in their gene expression profiles and in their self-renewal and developmental potential (Harrison et al. 1997; Ikuta et al. 1990; Ivanova et al. 2002; Kantor et al. 1992; Kim et al. 2005; Morrison et al. 1995; Phillips et al. 2000). Several genes including *Rae28* (Kim et al. 2004; Ohta et al. 2002), *Meis1* (Azcoitia et al. 2005; Hisa et al. 2004; Kirito et al. 2004), *c-myb* (Mucenski et al. 1991; Sandberg et al. 2005) and *Cbp* (Rebel et al. 2002) regulate the maintenance of HSCs throughout fetal and adult life. In contrast, a number of transcriptional regulators including Gfi-1 (Hock et al. 2004a), Tel/Etv6 (Hock et al. 2004b) and Bmi1 (Park et al. 2003) maintain adult but not fetal HSCs, whereas the transcription factor and endodermal marker Sox17 is required for fetal and neonatal, but not adult HSCs (Kim et al. 2007).

1.2 Asymmetric cell division

Both during embryogenesis and in adult life, stem cells are defined by their ability to make more stem cells, a property known as self-renewal and their ability to generate cells that undergo differentiation. One attractive strategy stem cells employ to accomplish these two tasks is asymmetric division, whereby a stem cell divides and gives rise to one daughter cell that maintains the stem cell fate and one daughter cell

that differentiates (Morrison and Kimble 2006). By contrast, a symmetric division generates daughter cells that are destined to acquire the same fate.

1.2.1 Principle mechanisms that govern asymmetric cell division

Two principle mechanisms govern asymmetric division: intrinsic or extrinsic. During an "intrinsic" asymmetric division, a dividing cell asymmetrically segregates fate determinants so that the daughter cells inherit different levels, thus generating daughter cells that adopt distinct cell fates. For an intrinsic asymmetric division to occur, a cell must initially set up an axis of polarity via extrinsic and/or intrinsic cues and subsequently use this axis of polarity to partition fate determinants to one side of the cell (Knoblich 2008). Finally, the dividing cell must orient the mitotic spindle along the axis of asymmetry to facilitate differential inheritance of fate determinants into the two incipient daughter cells (Congdon and Reya 2008).

Alternatively, an "extrinsic" mechanism can promote an asymmetric division however, unlike an intrinsically-motivated division, an extrinsic mechanism relies on the asymmetric placement of daughter cells relative to external cues (Morrison and Kimble 2006). In this context, the stem cell is in close contact with the stem cell niche and depends on localized niche-derived signals to maintain stem cell identity. Importantly, regulated orientation of the mitotic spindle during division retains only one of the two daughter cells in the stem cell niche and thus only one of the daughter cells is adequately exposed to extrinsic cues necessary to maintain stem cell identity. Thus, an

extrinsic mechanism attains an asymmetric outcome even though the division itself is intrinsically symmetric.

1.2.2 Asymmetric cell division in invertebrates

The fruitfly *Drosophila melanogaster* is a model system for asymmetric division (Neumuller and Knoblich 2009). Neuroblasts, which are stem cell-like progenitor cells of the *Drosophila* central nervous system, divide asymmetrically to generate one daughter cell that retains neuroblast properties and one ganglion mother cell (GMC), which further divides to generate two differentiating neurons (Neumuller and Knoblich 2009). During an asymmetric division, apical-basal polarity is established and maintained by an evolutionarily conserved protein-complex, the Par complex, which consists of Bazooka/Par-3 (Schober et al. 1999; Wodarz et al. 1999), Par-6 (Petronczki and Knoblich 2001) and atypical protein kinase C (aPKC) (Rolls et al. 2003; Wodarz et al. 2000). Apical positioning of the Par complex first occurs in the neurogenic ectoderm of the *Drosophila* embryo and is maintained during neuroblast delamination (Betschinger and Knoblich 2004). This apical localization of the Par complex is required to drive the segregation of cell fate determinants to the opposite, basal side of the cell and to direct the orientation of the mitotic spindle.

Basal localization of the cell fate determinant Numb is driven by a cascade of phosphorylation events triggered by the mitotic kinase Aurora A (Wirtz-Peitz et al. 2008). Specifically, at the onset of mitosis, Aurora A phosphorylates Par-6, which is

initially in complex with aPKC and lethal (2) giant larvae (Lgl). This phosphorylation event leads to the phosphorylation of Lgl by aPKC. Phosphorylated Lgl no longer binds aPKC, and this allows for the exchange of Lgl for Par-3 into the Par complex. This complex remodeling permits aPKC to now phosphorylate Numb which triggers its release from the apical neuroblast cortex and its subsequent accumulation on the opposite, basal side of the cell (Smith et al. 2007; Wirtz-Peitz et al. 2008). This mechanism may also explain how other segregating determinants, including Brain Tumor (Brat) and Prospero (Pros) localize asymmetrically. Once inherited by the differentiated daughter cell, Numb represses Notch signaling (Knoblich 2008) and Pros acts as both a transcriptional activator and inhibitor to promote a differentiated state (Choksi et al. 2006). The molecular function of Brat in neuroblasts is currently unknown, however, recent evidence suggest Brat may serve as a transcriptional activator of Pros or influence cell fate by regulating microRNAs (Bello et al. 2006; Knoblich 2008).

Proper orientation of the mitotic spindle is required to ensure unequal inheritance of cell fate determinants. Two pathways are known to control neuroblast spindle orientation: the Gα-Pins-Mud pathway and the Pins-Dlg-Khc73 pathway (Siller and Doe 2009). The Gα-Pins-Mud pathway involves an adaptor protein called Inscuteable (Insc), which localizes apically and associates with the Par complex by binding to Par-3 and recruits a GoLoco domain protein called Pins. The GoLoco domains of Pins serve as binding sites for the heterotrimeric G protein subunit Gαi,

which when bound leads to a conformational change in Pins that allows for its subsequent interaction with mushroom body defective (Mud). The mammalian orthologue of Mud (NuMA) interact with the dynein-dynactin complex, which includes Lis1 (Merdes et al. 1996). This association is required for spindle rocking movements and spindle orientation in *Drosophila* larval neuroblasts (Siller and Doe 2008b). Although definitive evidence is lacking, it is thought that the Gα-Pins-Mud pathway regulates spindle orientation by recruiting the dynein-dynactin-Lis1 complex to the apical cortex. The dynenin-dynactin-Lis1 complex is intimately associated with astral microtubules emanating from the centrosome, and thus, the recruitment of this complex to the apical cortex generates a pulling force to lock one centrosome at the apical pole, which subsequently leads to the proper alignment of the mitotic spindle along the apical/basal polarity axis (Siller and Doe 2009). A second spindle orientation pathway requires Pins, the membrane-bound guanylate kinase Dlg (disc large) and its interaction partner Khc-73, a microtubule plus-end-directed kinesin motor heavy chain (Siegrist and Doe 2005). Implementation of this pathway involves the localization of Khc73 to microtubule plus-ends where it binds to Dlg, which associate with Pins to facilitate cortical microtubule anchoring and subsequent stabilization of the mitotic spindle (Siegrist and Doe 2005).

1.2.2 Asymmetric cell division in the Hematopoietic System

Although the intricate molecular machineries controlling asymmetric division are well characterized in *Drosophila*, a comprehensive understanding of asymmetric

division and its regulation in the blood system is lacking. Pioneering studies in the hematopoietic system using a clone-splitting technique demonstrated that the progeny of hematopoietic precursor cells could adopt asymmetric fates (Ema et al. 2000; Punzel et al. 2003). However, these earlier studies did not provide constitute evidence of an intrinsically-driven asymmetric cell division. That is, following an intrinsically symmetric division, two identical daughter cells could be differentially exposed to an extrinsic cue, thus changing the fate of one of the two daughter cells without being linked to the mitosis itself. The challenge of definitively showing that hematopoietic stem cells can asymmetric divide via an intrinsic mechanism is that, for the most part, dependable markers for the prospective and noninvasive discrimination of differentiating and immature hematopoietic cells is lacking. This obstacle was overcome by using transgenic notch reporter (TNR) mice, in which GFP expression indicates notch pathway activation (Mizutani et al. 2007). The TNR system revealed that hematopoietic stem cells (HSC) highly express GFP and that GFP expression is down-regulated as HSCs differentiate (Duncan et al. 2005). Thus, these data indicate that GFP expression could serve as a surrogate marker for HSC identity and that the fate of daughter cells could be determined by tracking dividing GFP-positive HSCs in real-time via time-lapse microscopy. This approach convincingly demonstrated that HSCs could undergo both symmetric division (two GFP^+ progeny) and asymmetric division (one GFP^+ and one GFP^- daughter) (Wu et al. 2007).

1.2.2.1 Numb is an important cell fate determinant in the hematopoietic system

Following the observation that HSCs could, in fact, undergo both symmetric and asymmetric division came the discovery that the balance between asymmetric and symmetric division of HSCs is responsive to intrinsic cues linked to mitosis. Specifically, the cell fate determinant Numb was shown to be selectively partitioned into the differentiating daughter cell during an asymmetric division (Wu et al. 2007). Mechanistically, Numb induces differentiation by inhibiting Notch signaling, most likely by controlling the intracellular trafficking of Notch intermediates (Berdnik et al. 2002). In line with this, Notch reporter activity in HSCs was increasingly more repressed with increasing levels of Numb (Wu et al. 2007). Furthermore, ectopic expression of Numb enhances the differentiation of HSCs *in vitro* (Wu et al. 2007). These data support a role for Numb as a cell fate determinant in the hematopoietic system, in part by inhibiting Notch signaling.

1.2.2.1 Regulators of asymmetric division implicated in hematopoietic stem cell function

In addition to Numb, several polarity proteins and cell fate determinants implicated in asymmetric cell division in other stem cell model systems have recently been shown to play a role in HSC activity. Genetic deletion or shRNA-mediated knockdown of the cell fate determinant Musashi2 (Msi2) leads to a reduction in the frequency and absolute number of HSC-enriched cells (de Andres-Aguayo et al. 2011;

Ito et al. 2010). Furthermore, *Msi2*-deficient HSCs have impaired repopulation ability *in vivo* and undergo premature differentiation *in vitro* (de Andres-Aguayo et al. 2011; Hope et al. 2010; Kharas et al. 2010). An RNAi screen identified *Pard6a,* one of the four mammalian pard6 proteins that are homologs of the *C. elegans* PARD6, and *Prkcz*, one of the two mammalian homologs of *aPKC*, as necessary for the maintenance of HSCs in adult life (Hope et al. 2010). In addition, *Prox1*, the vertebrate cognate of *Drosophila* Prospero, was shown to promote differentiation at the expense of HSC maintenance (Hope et al. 2010). The cell polarity gene *Llgl1* (lethal giant larvae homolog 1) plays an important role in regulation of HSCs. Conditional deletion of *Llgl1* leads to expansion of HSCs and increased cell fitness (Heidel et al. 2013). Interestingly, recent studies suggest fatty acid oxidation (FAO) plays a role in the regulation of asymmetric HSC division. Specifically, genetic deletion of the FAO regulator *Pml,* induced the differentiation of HSCs in part due to an increase in symmetric, differentiating divisions (Ito et al. 2012). Collectively, these data suggest that several previously identified asymmetric division regulators play a critical functional role in normal HSC activity.

1.2.2.2 Balance of the modes of hematopoietic stem cell division depends on the microenvironment

Along with data showing HSCs can asymmetrically divide via intrinsic mechanisms, it has also been shown that the balance between symmetric and asymmetric division in part, depends on the microenvironment. Studies driven largely

by the utilization of the clone-splitting technique demonstrated that the type of stroma or cytokines used in culture influence the frequencies of division patterns (Ema et al. 2000; Punzel et al. 2003; Takano et al. 2004). Later work, using the transgenic notch reporter system, which did not require any micromanipulation of progeny cells, further showed that when HSCs were cultured on a pro-differentiation osteoblastic cell line, HSCs predominately undergo asymmetric division. In contrast, HSCs placed on a stromal cell line previously shown to maintain HSCs fate *in vitro*, preferentially divide symmetrically (Wu et al. 2007). Collectively, these data suggest that the balance between modes of division is not hardwired in HSCs, but instead is responsive to extrinsic cues.

1.2.2.3 Asymmetric cell division during activation of the immune system

In addition to HSCs, certain differentiated hematopoietic cells, under the right conditions, can undergo asymmetric division as well. Following antigenic stimulation, naïve T and B cell of the adaptive immune system respond by generating terminally differentiated effector and stem cell-like memory daughter cells. In context of T lymphocytes, a naïve T cell becomes activated when it engages with an antigen-presenting cell via the immunological synapse (Saito and Yokosuka 2006). The formation of the immunological synapse results in facultative polarity of the lymphocyte, which permits the T cell to direct its mitotic spindle perpendicular to the synapse. Subsequently, several molecules asymmetrically distribute to one side of the cell including the immune receptors leukocyte function-associated-1 (LFA-1), CD8 and CD3.

In addition, the cell fate determinant Numb and members of the aPKC-Par3-Par6 complex and the Scrib-Dlg-Lgl family of polarity proteins polarize in the T cell, indicating that previously defined mechanisms of asymmetric division were most likely conserved in lymphocytes (Chang et al. 2007). As the naïve T cell divides, the incipient daughter cells inherit unequal amounts of several of these proteins. Phenotypic and functional analyses indicated that the daughter "proximal" to the antigen-presenting cell undergoes transit amplification and eventually terminally differentiates into an effector cell, whereas the daughter "distal" to the contact site becomes a self-renewing memory cell that maintains the capacity to asymmetrically divide if re-challenged (Chang et al. 2007). Collectively, these data indicate that asymmetric division of activated T cells was responsible in part, for the production of functionally distinct daughter cells and that previously defined mechanisms of asymmetric division were most likely conserved in lymphocytes.

1.2.3 Dysregulation of asymmetric division in cancer

In context of oncogenesis, stem cells play a crucial role in the formation and maintenance of human tumors (Clarke and Fuller 2006; Reya et al. 2001). The observation that only a small population of tumor cells, which have stem cell-like properties, can reinitiate tumor formation in immunocompromised mice has led to the cancer stem cell hypothesis, which predicts that tumors are maintained by so-called cancer stem cells that give rise to all the other tumor cell-types (Bonnet and Dick 1997;

Lapidot et al. 1994; Reya et al. 2001). Furthermore, this hypothesis raises the possibility that stem cells might even be at the origin of a tumor, and therefore, defects in stem cells might be among the earliest events that induce tumor formation (Clarke and Fuller 2006). In homeostasis, asymmetric cell division is one mechanism stem cells employ to properly control self-renewal activity and ensure normal stem cell maintenance. Since uncontrolled self-renewal can be a hallmark of oncogenesis (Reya et al. 2001), dysregulation of asymmetric cell division may account for this aberrant self-renewal activity in cancer.

1.2.3.1 Asymmetric division regulators implicated in tumor formation

In *Drosophila*, defects in asymmetric cell division can transform neural stem cells into tumor-initiating cells and thus, several of the critical regulators of asymmetric cell division, including Brat, Numb and Pros, act as tumor suppressors (Bello et al. 2006; Betschinger et al. 2006; Caussinus and Gonzalez 2005; Gonzalez 2007; Lee et al. 2006a; Lee et al. 2006b; Wang et al. 2007; Wang et al. 2006). When any of these genes are mutated, neuroblasts, in part, begin dividing symmetrically which leads to the production of excess neuroblasts at the expense of differentiating neurons. Importantly, vertebrate homologs of genes regulating asymmetric cell division in *Drosophila* have been shown to be dysregulated in human malignancies. For example, loss of Numb is responsible for the hyperactivation of Notch signaling observed in breast cancer (Pece et al. 2004). Atypical PKCι is overexpressed in non-small cell lung cancer (Regala et al.

2005), human Lgl (Hugl-1) and atypical PKCζ fail to asymmetrically localize in ovarian epithelial cancers (Grifoni et al. 2007), and both human Scrib and Dlg mislocalize in colon cancer (Gardiol et al. 2006). Recently it was shown, in a mouse mammary tumor model, that transformed mammary stem cells mislocalized Numb and therefore, loss the ability to effectively divide asymmetrically (Cicalese et al. 2009). Instead, these cells perpetually underwent symmetric renewal divisions, which lead to the formation of a tumor.

1.2.3.2 Dysregulation of asymmetric cell division in malignant hematopoietic development

In context of hematopoietic malignancy, it was recently shown that certain leukemia-associated oncogenes could influence the balance of symmetric and asymmetric division. While the tyrosine kinase BCR-ABL, which is the hallmark genetic abnormality in chronic myelogenous leukemia (CML) has a specific and profound impact on cell proliferation and survival, NUP98-HOXA9, an oncogene associated with late stage CML and some *de novo* AMLs, does not influence proliferation and survival and instead, shifts the normal balance of asymmetric and symmetric division towards symmetric renewal divisions (Wu et al. 2007). This may explain why the acquisition of certain oncogenes, such as NUP98-HOXA9, leads to the preferential growth of immature cells and reduced differentiation. Since CML is known to progress from a slow growing chronic phase where the ability to differentiate is maintained (Witte 2001) to an

aggressive, blast crisis stage where the capacity to differentiate is nearly eliminated (Calabretta and Perrotti 2004), the observation that secondary translocations such as NUP98-HOXA9 can cause a significant shift in the pattern of division suggest that dysregulation of HSC division pattern may, in part, be responsible for disease progression.

Whether known regulators of asymmetric division play a role in hematological malignancies is largely unknown, however, recently it was shown that repression of the polarity protein Lgl1 is associated with human leukemia development and an adverse prognosis in cytogentically normal acute myelogenous leukemia (AML) (Heidel et al. 2013). Furthermore, mutations of Llgl2, a close human homologue of Llgl1, have been identified in progression from congenital neutropenia to AML (Beekman et al. 2012). Although the functional consequences of expression changes of Llgl1,2 has not be shown, these data, nevertheless, suggest dysregulation of asymmetric cell division may play a role in malignant hematopoietic development.

1.3 Lis1 (Pafah1b)

The *LIS1* gene encodes a 45-kDA protein that contains a N-terminal Lis-H domain, followed by a coiled-coil region and a C-terminal series of WD repeats. These seven WD repeats form a propeller-like structure that serves as a platform for LIS1 to engage in numerous protein-protein interactions (Cahana et al. 2001; Caspi et al. 2000; Gerlitz et al. 2005; Neer et al. 1994; Reiner et al. 1993; Sapir et al. 1997; Sasaki et al. 2000;

Smith et al. 2000; Tai et al. 2002; Tarricone et al. 2004). LIS1 was first identified as a non-catalytic subunit of the brain cytosolic platelet-activating factor acetylhydrolase (PAFAH) isoform 1b, an enzyme involved in the deactivation of platelet-activating factor (PAF), a lipid messenger that has a critical role in the inflammatory response (Hattori et al. 1994; Reiner et al. 1993). Thus, the formal gene name for *LIS1* is *PAFAH1b*. The 1b isoform of this enzyme, which is composed of LIS1 and two catalytic alpha subunits (α1 and α2), is specific to the brain cytosol and evidence to date has not revealed a definitive role for LIS1 in PAFAH enzymatic regulation. A non-enzymatic function of LIS1 was first identified in the filamentous fungus *Aspergillus nidulans*. Mutations in *nudF*, the fungal homologue of *LIS1*, caused a severe defect in nucleokinesis, a process that involves the migration of nuclei into and within the growing tip of hyphae (Xiang et al. 1995). The *nudF* phenotype was identical to that generated by mutations in genes encoding subunits of the microtubule motor protein cytoplasmic dynein (Willins et al. 1997). This, along with studies in *Saccharomyces cerevisiae* and *Drosophila*, identified LIS1 as part of an evolutionarily conserved pathway that regulates the microtubule motor protein dynein (Lee et al. 2003; Lei and Warrior 2000). LIS1 does, in fact, bind to verterbrate cytoplasmic dynein (Faulkner et al. 2000; Sasaki et al. 2000; Smith et al. 2000) as well as to other proteins including CLIP-70 (Coquelle et al. 2002; Tai et al. 2002), NDEL (Kitagawa et al. 2000), NDEL1 (Niethammer

et al. 2000), and mNudC (Morris et al. 1998). Each of these Lis1-interacting proteins, in turn, dynamically associates with dynein (Aumais et al. 2001; Sasaki et al. 2000).

In cultured mammalian cells, it was shown that LIS1 co-localizes with cytoplasmic dynein at the cell cortex and at the mitotic kinetochores. Functionally, elevated or reduced levels of LIS1 results in a pronounced delay of mitotic progression accompanied with a chromosomal alignment defect in metaphase (Faulkner et al. 2000). Supporting a role for Lis1 in cell division, following either shRNA-mediated knockdown or the controlled genetic deletion of *Lis1* in neural progenitor cells impaired cell cycle progression (Tsai et al. 2005; Yingling et al. 2008). Lis1 also has an important function in spermatogenesis. Using a gene trap mouse line with selective disruption of a testis-specific Lis1 transcript, it was shown that loss of Lis1 leads to a blockade of spermatid differentiation (Nayernia et al. 2003). Recently it was demonstrated that Lis1 regulates BMP signaling and E-cadherin-mediated adhesion to control germline stem cell (GSC) self-renewal and proliferation in the *Drosophila* ovary (Chen et al. 2010). Importantly, complete loss of *Lis1* results in peri-implantation lethality, indicating that *Lis1* is a critical gene (Cahana et al. 2001; Hirotsune et al. 1998).

1.3.1 Role of the *Lis1* gene in lissencephaly

The *PAFAH1b* gene is designated as *LIS1*, because heterozygous mutations of this gene cause a severe brain developmental disorder known as lissencephaly (Lo Nigro et al. 1997; Reiner et al. 1993). Unlike the conspicuous convolutions of the normal brain,

the brain surface of individuals with lissencephaly is completely devoid of the normal sulci and gyri, which accounts for the name of the disease, which translates from Greek to "smooth brain" (Dobyns et al. 1993). During normal cortical development, neurons migrate in an "inside-out" fashion to establish the neuronal layers of the cerebral cortex (Gupta et al. 2002). As a result of proper implementation of this process the brain appears normal. However, during cortical development in individuals with lissencephaly, migratory neurons fail to reach their final cortical position within the cerebral cortex This, consequently, leads to a paucity of gyri and sulci on the brain surface, which accounts for the overall "smooth brain" phenotype (Wynshaw-Boris 2007). Studies in mice have confirmed that a defect in Lis1-mediated neuronal migration is primarily responsible for this gross phenotype. Mice with graded reduction in *Lis1* dosage exhibited a LIS1 dose-dependent disorganization of the cortical layers, the hippocampus and the olfactory bulb (Fleck et al. 2000; Hirotsune et al. 1998; Paylor et al. 1999), and thus, faithfully recapitulated the human disorder. Importantly, mice with reduced levels of *Lis1* display migrational defects (Hirotsune et al. 1998). Furthermore, a requirement for Lis1 in neuronal migration was demonstrated by time-lapse videomicroscopy of neuronal migration in slice cultures from embryonic cortex (Shu et al. 2004; Youn et al. 2009). Mechanistically, LIS1 is required for nuclear movement during neuronal migration by coupling the nucleus to the centrosome in a dynein-dependent manner (Tanaka et al. 2004).

1.3.2 Lis1 in regulation of spindle orientation

A role for Lis1 in spindle orientation and positioning has been demonstrated in the budding yeast *Saccharomyces cerevisiae* (Lee et al. 2003), *C. elegans* (Cockell et al. 2004), *Drosophila* neuroblasts (Siller and Doe 2008a), in cultured epithelial cells (Faulkner et al. 2000) and in the mammalian neuroepithelium (Yingling et al. 2008). In *S. cerevisiae,* Pac1 (related to mammalian Lis1) is required for polarized transport of the astral microtubule plus ends into the mother-bud neck of dividing yeast cells (Lee et al. 2003). Likewise, in *C. elegans,* a membrane-anchored protein complex containing Lis1 and dynein generates pulling forces on the astral microtubules to properly position the mitotic spindle (Cockell et al. 2004). In this system, the protein LIN-5 (Mud in flies; NuMA in mammals) regulates the interaction of the Lis1/dynein complex with the cell cortex (Srinivasan et al. 2003). In cultured mammalian epithelial cells, the mitotic spindles of dividing cells normally lie parallel to the epithelial plane. However, overexpression of LIS1 randomized spindle orientation (Faulkner et al. 2000). These data suggest Lis1 regulates spindle orientation in epithelial cells.

Recently, a role for Lis1 in spindle orientation has extended to the mammalian nervous system. During development, neuroepithelial stem cells (NESCs) perpetually undergo symmetrical renewal divisions until the onset of neurogenesis when NESCs switch to an asymmetric mode of division to generate one radial glial progenitor cell (RGPCs) and one migratory post-mitotic neuron. In order for a NESC to undergo a

symmetric renewal division, it must precisely align its mitotic spindle in such a way to facilitate equal distribution of asymmetrically localized determinants such as β-catenin, aPKC, Numb and cadherins into the incipient daughter cells. However, in the absence of Lis1, spindle cleavage planes of NESCs and RGPCs become randomized and as a result *Lis1* mutant NESCs and RGPCs predominantly divide asymmetrically thereby reducing the progenitor pool population and decreasing the total number of cortical neurons (Yingling et al. 2008). Randomization of spindle orientation occurs in *Lis1* mutant cells because in the absence of Lis1, cortical microtubule capture and stability is impaired and thus, *Lis1*-deficient cells cannot effectively rotate the mitotic spindle to a precise orientation that facilitates symmetric division (Yingling et al. 2008). Collectively, these studies underscore Lis1 as a core component of the spindle-positioning machinery regulating asymmetric cell division in a variety of organisms and cell types.

2. Materials and Methods

2.1 Generation and analysis of mice

Hypomorphic conditional knockout mice (*Lis1*$^{f/f}$, also *Lis1-loxP* or *Pafah1b1-loxP*; Strain: 129-*Pafah1b1*^{tm2awb}/*J*) (Hirotsune et al. 1998) were mated with either *Rosa26-CreERT2* mice (Strain: B6*;129-Gt(ROSA)26Sor*$^{tm1(cre/Esr1)Tyj}$) (Ventura et al. 2007) or *Vav*-Cre transgenic mice(de Boer et al. 2003). *Vav-Cre* reporter mice were generated by crossing Vav-Cre mice to Rosa26-stop-tdTomato mice (Stain: B6.Cg-*Gt(ROSA)26Sor*$^{tm9(CAG-tdTomato)Hze}$/J; Stock #: 007909). B6-CD45.1 (Strain: B6.SJL-*Ptprc*^{a}*Pepc*^{b}/BoyJ) mice were used as transplant recipients. All mice were 6-16 weeks of age. Mice were bred and maintained in the animal care facilities at Duke University Medical Center and the University of California, San Diego. Tamoxifen treatment of mice was done as previously described (Yang et al. 2008). Briefly, adult mice were administered tamoxifen (Sigma) in corn oil (20 mg/ml) daily by oral gavage at ~114 μg tamoxifen per gram of body weight per day for five consecutive days. For leukemia experiments, all recipient mice weighed ~17.5-20 grams and were administered 2 mg of tamoxifen per day for five consecutive days. Embryos were suspended in phosphate-buffered saline and visualized with a Leica MZ16 FA Fluorescence Stereomicroscope. Embryos were fixed in 4% paraformaldehyde and embedded in paraffin according to standard protocols. Sections (5 μm) were obtained for hematoxylin and eosin (H&E) staining. All animal experiments were performed according to protocols approved by the Duke University Institutional

Animal Care and Use Committee and the University of California, San Diego Institutional Animal Care and Use Committee.

2.2 Cell isolation and FACS analysis

Cells were suspended in Hanks' balanced salt solution (HBSS) (Gibco, Life Technologies) containing 5% (vol/vol) fetal bovine serum and 2 mM EDTA and prepared for FACS analysis and sorting as previously described (Domen et al. 2000). The following antibodies were used to define lineage positive cells: 145-2C11 (CD3ε), GK1.5 (CD4), 53-6.7 (CD8), RB6-8C5 (Ly-6G/Gr1), M1/70 (CD11b/Mac-1), TER119 (Ly-76/TER119), 6B2 (CD45R/B220), and MB19-1 (CD19). Red blood cells were lysed using RBC Lysis Buffer (eBioscience) before staining for lineage markers. For fetal liver cell isolation and FACS analysis, single-cell suspensions were prepared by disaggregation and passing through a 74-μm-nylon mesh (Corning). Placentas were prepared as described previously (Gekas et al. 2008). Yolk sacs were prepared as described previously (Yoder et al. 1997). For fetal HSC cell population analysis, the lineage antibody cocktail was used without anti-Mac-1. The following additional antibodies were used to define HSC populations: 2B8 (CD117/c-kit), D7 (Ly-6A/E/Sca-1), AA4.1 (CD93/C1qRp), HM48-1 (CD48/BCM1), TC15-12F12.2 (CD150), A2F10 (CD135/Flt3) and RAM34 (CD34). Fetal HSCs were defined as c-Kit$^+$ Lin$^-$ AA4.1$^+$ (KL AA4.1$^+$). Yolk sac HSCs/progenitors were defined as CD34$^+$. Placenta HSCs/progenitors were defined as c-Kit$^+$ CD34$^+$. Adult HSCs were defined as either c-Kit$^+$ Lin$^-$ Sca1$^+$ CD48$^-$ CD150$^+$ (KLS

CD48$^-$ CD150$^+$) or c-Kit$^+$ Lin$^-$ Sca1$^+$ Flt3$^-$ (KLSF). To determine donor-derived chimerism in transplantation-based assays, peripheral blood cells of transplant recipients were obtained by the submandibular bleeding method and prepared for analysis as previously described(Ito et al. 2010). All antibodies were purchased from BD Pharmigen, eBioscience or BioLegend. Apoptosis assays were performed by staining cells with Annexin-V and 7AAD (BD Pharmingen). Analysis of *in vivo* BrdU incorporation was performed using the FITC BrdU Flow Kit (BD Pharmingen) after a single intraperitoneal injection of BrdU (2 mg). Analysis and cell sorting were carried out on FACSVantage SE, FACStar, FACSCantoII, FACSDiva and FACSAria III machines (all from Becton Dickinson) and data were analyzed with FlowJo software (Tree Star Inc.).

2.3 Retro- and Lentiviral constructs and production

MIG-BCR-ABL was a gift from Warren Pear and Ann Marie Pendergast and was cloned into MSCV-IRES-YFP retroviral vector. MSCV-NUP98-HOXA9-IRES-YFP was a gift from Gary Gilliland and was cloned into the MSCV-IRES-GFP vector. MSCV-MLL-AF9-IRES-GFP was generously provided by Scott Armstrong. NRAS^{G12V} cDNA was a gift from Christopher Counter and was cloned into MSCV-IRES-YFP retroviral vector. pCXLIS1-RFP-IAP vector (Tanaka et al. 2004), encoding a full-length human LIS1 cDNA, was obtained from Joseph Gleeson and the protein coding region was cloned into MSCV-IRES-truncated hNGFR retroviral vector. *Numb* cDNA (p65 isoform, accession number BC033459, NCBI) was either cloned into the MSCV-IRES-GFP vector or fused to

CFP in the MSCV-CFP vector following the removal of IRES. H2B-GFP (pEGFPN1) vector (Kanda et al. 1998) was a gift from Geoffrey Wahl and the H2B-GFP chimeric gene was cloned into MSCV-IRES-GFP retroviral vector following the removal of IRES-GFP. mCherry-alpha-tubulin fusion construct (Day et al. 2009) was generously provided by John Chang and Sarah Russell.

Lentiviral short hairpin RNA (shRNA) constructs were cloned in FG12 as described previously (Qin et al. 2003). The target sequences are 5′-AGATGAACTAAATCGAGC-3′ for shLIS1-(592), 5′-TGTCTGCCTCAAGGGATA-3′ for shLIS1-(1191) and 5′-TGCGCTGCTGGTGCCAAC-3′ for luciferase as a negative control. LIS1 mutant cDNA resistant to shLIS1-(592) was constructed by inverse PCR strategy using a primer designed to include silent mutations (underlined) in the shLIS1-(592) target sequence: 5′ - AGACGAGCTTAACCGTGC -3′. The protein-coding region of mutated human LIS1 cDNA was cloned into MSCV-IRES-truncated hNGFR retroviral vector. Virus was produced in 293T cells transfected using the FuGENE®6 or X-tremeGENE HP (Roche) with viral constructs along with VSV-G and gag-pol. For lentivirus production Rev was also co-transfected. Viral supernatants were collected for three to five days followed by ultracentrifugal concentration at 50,000x g for 3h.

2.4 Cell culture and methylcellulose colony formation

For liquid culture, freshly isolated adult KLS ($cKit^+$ Lin^- $Sca\text{-}1^+$) bone marrow cells were plated into a 96-well U bottom plate in X-Vivo15 (with Gentamicin and Phenol

Red) (Lonza) supplemented with 50 μM 2-mercaptoethanol, 10% (vol/vol) fetal bovine serum, stem cell factor (SCF; 100 ng/ml, R&D Systems) and thrombopoietin (TPO; 20 ng/ml, R&D Systems). 4-OH tamoxifen (Sigma) was dissolved in ethanol at 1 mg/ml (1000X), and a 1X solution was made immediately before treatment. For certain immunofluorescence experiments, cells were treated for 24 hrs with either 10 μM Cytochalasin B (Sigma) or 10 nM Nocodazole (Sigma).

For fetal liver methylcellulose assays, individual fetal livers (FL) from embryonic day 12.5 (E12.5) embryos were dissected in cold phosphate-buffered saline, disaggregated and passed through a 74-μm nylon mesh (Corning) to generate single-cell suspensions. 5,000 FL cells were plated in triplicate in Iscove's modified medium-based methylcellulose medium (Methocult M3434, StemCell Technologies). Erythroid (BFU-E) hematopoietic progenitors were scored by morphological criteria on day 7 and myeloid (CFU-GM) and multilineage (CFU-GEMM) colonies were scored on day 10.

For yolk sac and placenta methylcellulose assays, sorted yolk sac or placenta cells were plated (300-500 cells/well) in triplicate in Methocult M3434. Colonies generated from yolk sac cells were counted on day 8 and colonies formed from placenta cells were scored on day 14. For methylcellulose assays performed with leukemia cells, 5,000 lineage-negative (Lin^-) bcCML cells ($BCR\text{-}ABL^+$, $NUP98\text{-}HOXA9^+$) were plated in triplicated and scored on day 8.

2.5 In vivo transplantation assays

For fetal liver transplants, 5,000 Lin^- $AA4.1^+$ fetal liver cells (derived from E14.5 embryos expressing CD45.2) or 3 x 10^5 whole fetal liver cells (derived from E12.5 embryos expressing CD45.2) along with 3 x10^5 competitive bone marrow cells derived from an unirradiated recipient mouse were transplanted by retro-orbital i.v. injections into lethally irradiated (9.5 Gy) congenic recipient mice (expressing CD45.1). Recipient mice received donor cells derived from one individual embryo of a given genotype. Peripheral blood of recipient mice was collected at 4, 8, 12 and 16 weeks after transplantation. Donor and recipient cells were distinguished by expression of CD45.1 (A20; eBioscience) and CD45.2 (104; eBioscience). For bone marrow transplants, 500 LT-HSCs ($cKit^+$ Lin^- $Sca\text{-}1^+$ $CD150^+$ $CD48^-$) isolated from bone marrow of mice expressing CD45.2 were transplanted into lethally irradiated (9.8 Gy) congenic recipient mice (expressing CD45.1) along with 3 x 10^5 Sca1-depleted bone marrow cells derived from an unirradiated recipient mouse. Peripheral blood of recipient mice was collected at 4, 8 and 28 weeks after transplantation. For Lis1 chimera bone marrow transplants, 3 x 10^5 whole bone marrow cells isolated from Lis1 chimera mice (expressing CD45.2) were transplanted into lethally irradiated (9.8 Gy) recipient mice (expressing CD45.1) along with 3 x 10^5 Sca1-depleted bone marrow cells derived from an unirradiated recipient mouse. Peripheral blood of recipient mice was collected at 16 weeks after transplantation.

2.6 Determining Numb inheritance

For experiments involving fixed cells, dividing cells in late telophase or undergoing cytokinesis were identified by pronounced cytoplasmic cleft by brightfield or visualized by staining cells for alpha-tubulin plus the presence of dual nuclei using DAPI. ImageJ 1.46r was used to determine fluorescence intensity of pixels following Numb staining. The fluorescence intensity of Numb was on average ~2.4-fold higher in the $Numb^{high}$ daughter cell relative to the $Numb^{low}$ daughter cell during an asymmetric division. Based on immunofluorescence data, Numb is ~1.8-fold higher in progenitors than in HSCs and thus, incipient daughters that expressed at least a 1.8-fold difference in Numb expression were scored as an asymmetric Numb inheritance.

For live imaging experiments, KLS cells isolated from *Lis1*$^{f/f}$; *Rosa26-creER/Rosa26-creER* and *Lis1*$^{+/+}$; *Rosa26-creER/Rosa26-creER* mice were co-infected with mCherry-α-tubulin and Numb-CFP fusion constructs and doubly-infected cells were subsequently plated in methylcellulose medium (Methocult M3434, StemCell Technologies) and treated with 4-OH tamoxifen (Sigma). Dividing cells identified in movie replay were visualized in spectrum color format (where red indicates pronounced α-tubulin expression and centrosome location) to readily identify the centrosomes. Using ImageJ 1.46r software, a line connecting the two centrosomes of a cell was drawn (Line 1; dotted). Subsequently, an additional line (Line 2; solid) was drawn perpendicular to Line 1, which marked the cleavage furrow and partitioned the mother cell into incipient

daughter cell 1 (D_1) and daughter cell 2 (D_2). Using the criteria described above and our immunofluorescence data, incipient daughters that expressed at least a 1.8-fold difference in Numb expression were scored as an asymmetric Numb inheritance.

2.7 Analysis of spindle orientation and mitotic events

Bone marrow KLS cells were isolated and sorted from age-gender matched *Lis1*$^{f/f}$; *Rosa26-creER*/*Rosa26-creER* and *Lis1*$^{+/+}$; *Rosa26-creER*/*Rosa26-creER* mice and cultured overnight in X-Vivo™15 media (Lonza) supplemented with 50 μM 2-mercaptoethanol, 10% (vol/vol) fetal bovine serum, SCF (100 ng/ml, R&D Systems) and thrombopoietin (20 ng/ml, R&D Systems). Cells were retrovirally-infected with MSCV-H2B-GFP and mCherry-*α*-tubulin, harvested 48 hrs after infection and re-sorted for GFP$^+$ mCherry$^+$ KLS cells. Sorted cells were either cultured in 96-well U-bottomed plates (BD Biosciences) for 48 hrs with 4-OH tamoxifen (Sigma) and subsequently placed on chambered coverglass slides (Lab-Tek II®, Thermo Scientific) coated with 0.1 μg/μl Retronectin® (Takara Bio Inc.) in the continual presence of 4-OH tamoxifen or plated in Iscove's modified medium-based methycellulose medium (Methocult M3434, StemCell Technologies) supplemented with 4-OH tamoxifen. Images were collected every 3-4 minutes with xyzt acquisition mode using an Axio Observer.Z1 microscope with the LSM 700 scanning module (Zeiss). Cultures were maintained at 37°C, 5% CO_2 using a Heating Insert P Lab-Tek S1 with an Incubator PM S1 (Zeiss). Mitotic cells were identified in movie replay. To measure spindle orientation, a concatenation of Z-stack

images of each cell at every measured time point from the start of metaphase to early telophase was generated and displayed orthogonally using Zen 2010 software. Subsequently, the angle formed between the substratum plane (Retronectin base) and the virtual line passing through spindle poles was measured using ImageJ 1.44. To quantify mitosis duration, the time between nuclear envelope breakdown and chromatin condensation until the beginning of telophase was determined. For chromosome counts, KLS cells were cultured in X-Vivo™15 media (Lonza) supplemented with 50 μM 2-mercaptoethanol, 10% (vol/vol) fetal bovine serum, SCF (100 ng/ml, R&D Systems) and TPO (20 ng/ml, R&D Systems) for 48 hrs, and then arrested in metaphase by a 2h incubation with 100 ng/ml colcemid (KaryoMAX solution, Gibco). Cells were treated with hypotonic solution (0.56% KCl) for 15 min at 37°C, then fixed with 3:1 methanol:glacial acetic acid and spread on a slide to prepare metaphase spreads. Karyotyping was performed by Cell Line Genetics, Inc. (www.clgenetics.com).

2.8 Generation and analysis of leukemic mice

Bone marrow KLS cells were isolated and sorted from age-gender matched *Lis1*$^{f/f}$*; Rosa26-creER/Rosa26-creER* and *Lis1*$^{+/+}$*; Rosa26-creER/Rosa26-creER* mice and cultured overnight in X-Vivo15 media (Lonza) supplemented with 50 μM 2-mercaptoethanol, 10% (vol/vol) fetal bovine serum, SCF (100 ng/ml, R&D Systems) and TPO (20 ng/ml, R&D Systems). Cells were retrovirally-infected with MSCV-BCR-ABL-IRES-YFP and MSCV-NUP98-HOXA9-IRES-GFP to generate myeloid blast crisis phase CML (bcCML)

or MSCV-MLL-AF9-IRES-GFP and MSCV-NRAS^{G12V}-IRES-YFP to generate *de novo* AML. Subsequently, cells were harvested 48 hours after infection. Doubly-infected cells (for bcCML experiments) or unsorted cells (for AML experiments) were transplanted retro-orbitally into cohorts of B6-CD45.1 mice. Before transplantation, for *de novo* AML transplants, infected cells regardless of donor genotype displayed similar infection efficiency. All recipients were sub-lethally (6-7 Gy) irradiated. For secondary bcCML transplantations, cells recovered from terminally ill primary recipients were sorted for lineage-negative (Lin-), MSCV-BCR-ABL-IRES-YFP and MSCV-NUP98-HOXA9-IRES-GFP and transplanted into secondary recipients. Analysis of diseased mice was conducted as previously described (Ito et al. 2010).

2.9 Human leukemia patient samples and cell lines

Patient samples were obtained from either Singapore General Hospital (Singapore), the Fred Hutchinson Cancer Research Center or from the Duke Adult Bone Marrow Transplant Clinic from Institutional Review Board-approved protocols with written informed consent in accordance with the Declaration of Helsinki. Primary bcCML cells were imatinib, nilotinib and dasatinib-resistant. Primary AML cells harbored the MLL-AF9 translocation. Leukemia cells were cultured in Iscove's modified Dulbecco medium (IMDM) with 10% fetal bovine serum (FBS), 100 IU/ml penicillin and 100 μg/ml streptomycin, 55 μM 2-mercaptoethanol and supplemented with SCF, IL-3, IL-6, Flt3L, and TPO. The human chronic myeloid leukemia cell line K562 was

maintained in Roswell Park Memorial Institute medium (RPMI-1640) with 10% FBS, 100 IU/ml penicillin and 100 μg/ml streptomycin. The human acute myeloid leukemia cell line MV4-11 was maintained in IMDM with 10% FBS, 100 IU ml^{-1} penicillin and 100 μg/ml streptomycin.

For colony forming assays, human cell lines or sorted $hCD34^+$ cells from primary patient samples were transduced with lentiviral shRNA (cloned in FG12-UbiC-GFP), and GFP-positive cells were sorted at 48 hrs and plated in complete methylcellulose medium (MethoCult Express, StemCell Technologies). For certain colony-forming experiments, K562 cells were co-transduced with lentiviral shRNA (FG12-UbiC-GFP) and retroviral constructs (MSCV-IRES-hNGFR) and doubly-infected cells were sorted and plated in methylcellulose. All knockdown experiments were conducted with the construct shRNA-LIS1-(592) except those involving human primary CML cells, which were instead transduced with an alternative shLIS1 construct: shRNA-LIS1-(1191). This construct represents an independent hairpin shRNA targeting LIS1 that more effectively knockdowns LIS1 in these cells. Colony numbers were counted 10-14 days after plating.

2.10 Gene expression microarray and data analysis

Control (*Lis1*$^{+/+}$*; Rosa-creER*) or *Lis1*$^{f/f}$*; Rosa-creER* mice were treated with tamoxifen for five consecutive days. Three days after the final tamoxifen administration, KLS bone marrow cells were FACS-sorted and total cellular RNAs were purified. RNAs were amplified, labeled, hybridized onto Affymetrix GeneChip Mouse Genome 430 2.0

Arrays and raw hybridization data were collected (Asuragen Inc., Austin, TX). Expression level data were normalized using a multiple-loess algorithm as previously described (Sasik et al. 2004). Probes whose expression level exceeds a threshold value in at least one sample were considered detected. The threshold value is found by inspection from the distribution plots of $\log_2$ expression levels. Detected probes were sorted according to their *q*-value, which is the smallest false discovery rate (FDR) (Benjamini and Hochberg 1995) at which the gene is called significant. An FDR value of α is the expected fraction of false positives among all genes with $q \leq \alpha$. FDR was evaluated using Significance Analysis of Microarrays and its implementation in the official statistical package *samr* (Tusher et al. 2001). To prevent unwarranted variances, the percentile of standard deviation values used for the exchangeability factor *s0* in the regularized *t*-statistic was set to 50.

The probe list, sorted by *q*-value in ascending order, was translated into Entrez gene ID's and parsed so that where several different probes represent the same gene, only the highest-ranking probe was kept for further analysis. The sorted list of genes was subjected to a non-parametric variant of the Gene Set Enrichment Analysis (GSEA) (Subramanian et al. 2005), in which the *p*-value of a gene set was defined as the minimal rank-order *p*-value of a gene in the gene set (Arnold et al. 1992) rather than the Kolmogorov-Smirnov statistic as in GSEA. Briefly, let r_k be the *k*-th highest rank among a gene set of size *N*. The rank-order *p*-value p_k of this gene is the probability that among *N*

randomly chosen ranks without replacement, the k-th highest rank will be at least r_k. The p-value of a gene set was defined as the smallest of all p_k. Finding the p-value of a gene set of size N requires calculation of N rank-order p-values; however, there is no need to adjust the p-values for the number of genes tested as the tests are highly statistically dependent. A Bonferroni adjustment of gene set p-values for the number of gene sets tested was performed. Gene sets with adjusted p-values ≤ 0.01 were reported. For the analysis of stem cell signature sets published (Eppert et al. 2011; Metzeler et al. 2008; Somervaille et al. 2009; Venezia et al. 2004; Wong et al. 2008; Yagi et al. 2003), all detected genes in the *Lis1*$^{-/-}$ (*Lis1*$^{f/f}$*creER* +tamoxifen) to control (*Lis1*$^{+/+}$*creER* +tamoxifen) comparison were sorted according to their q-values as above and gene set enrichment analysis for each signature gene set was performed. Each gene signature's p-value is Bonferroni-adjusted by a factor of 9 (number of signature gene sets tested). Heat maps were created using in-house hierarchical clustering software and the colors qualitatively correspond to fold changes. Microarray data reported have been deposited in the ArrayExpress Database (accession number E-MEXP-3855) (European Bioinformatics Institute 2013).

2.11 PCR genotyping and RT-PCR analysis

For genotyping by PCR, the reaction mixture contained MangoMix (Bioline), genomic DNA and 0.5 μM of each primer. PCR conditions for genotyping were as follows: 3 min at 94°C, followed by 35 cycles at 94°C for 30 s, 60°C for 1 min, and 72°C

for 1 min. To detect the wild-type, floxed, and deleted floxed mouse *Lis1* allele, the following primer sequences were used: *Lis1*-Common-R, 5′-GCTTGTTCATCAAGCTTGCAC-3′; *Lis1*-F_VI, 5′-GCTTCCTGTTCA GCAGATATG-3′; *Lis1*-F_II, 5′-GGCGATGATAACCACTGAGTC-3′. RNA was isolated using RNAqueous-Micro (Ambion) or RNeasy Mini kit (Qiagen). cDNA was prepared from equal amounts of RNAs using Superscript II reverse transcriptase (Invitrogen). The following primer sequences were used for standard RT-PCR reactions: *Lis1*-F, 5′-TGGATTCCCCGTCCACCTGA-3′; *Lis1*-R, 5′-TTGGCCGCACCATACGTACC-3′; *GAPDH*-F, 5′-CAATGACCCCTTCATTGACC-3′; *GAPDH*-R, 5′-TTGATTTTGGAGGGATCTCG-3′. Quantitative real-time PCRs were performed using iQ SYBR Green Supermix (Bio-Rad) on a CFX 96 C1000™ Thermal cycler (Bio-Rad). Results were normalized to the level of β2 microglobulin (*B2M*, human; *B2m*, mouse) or TATA-binding protein (*Tbp*, mouse). Primer sequences are as follows for mouse: *Numb*-F, 5′-ATGAGTTGCCTTCCACTATGCAG-3′; *Numb*-R, 5′-TGCTGAAGGCACTGGTGATCTGG-3′; *Tbp*-F, 5′-GTATCTACCGTGAATCTTGGCTG-3′; *Tbp*-R, 5′-AGTTGTCCGTGGCTCTCTTATTC-3′; *Socs3*-F, 5′-GGGTGGCAAAGAAAAGGAG-3′; *Socs3*-R, 5′-GTTGAGCGTCAAGACCCAGT-3′; *Brd4*-F, 5′-CCATGGACATGAGCACAATC-3′; *Brd4*-R, 5′-TGGAGAACATCAATCGGACA-3′; *Pml*-F, 5′-CCAGAGGAACCCTCCGAAGA-3′; *Pml*-R, 5′-GGCAGCGCAGAAACTGAAAT-3′; *Msi2*-F, 5′-TGCCATACACCATGGATGCGT-3′;

Msi2-R, 5′-GTAGCCTCTGCCATAGGTTGC-3′. *B2m*-F, 5′-ACCGGCCTGTATGCTATCCAGAA-3′; *B2m*-R, 5′-AATGTGAGGCGGGTGGAACTGT-3′. Mouse *Lis1* (Mm01253377_mH) gene levels were analyzed with TaqMan Gene Expression Assays. Primer sequences are as follows for human: *LIS1*-F, 5′-CATGAGCATGTGGTAGAATGC-3′; *LIS1*-R, 5′-GGCCCAGGTTTACCACTTTT-3′; *B2M*-F, 5′-ATGAGTATGCCTGCCGTGTGA-3′; *B2M*-R, 5′-GGCATCTTCAAACCTCCATG-3′.

2.12 Immunofluorescence staining

Cells were allowed to settle briefly on poly-L-lysine coated coverslips (BD Biosciences) at 37°C, fixed with 4% paraformaldehyde (USB Corporation) or methanol, permeabilized with 1X Dako wash buffer (Dako) and blocked with 20% normal goat serum (Invitrogen) or donkey serum (Abcam) in 1X Dako wash buffer. Bones were removed and fixed in 4% paraformaldehyde for 24 hrs at 4°C, saturated with 20% sucrose in 1X PBS overnight and embedded in O.C.T. Compound (Sakura). Bones were cut to sections using a Cyrojane Tape Transfer System and a Leica CM3050 S cryostat (Leica Microsystems). All bone sections were permeablized with 100% acetone for 5 min at -20°C. Primary antibody incubation was overnight at 4°C. The following primary antibodies were used: rabbit anti-Numb 1:50 or 1:100 (Abcam), goat anti-LIS1 1:500 (Santa Cruz Biotechnology), mouse anti-alpha-tubulin 1:200 (Abcam), rabbit anti-Sp7/Osterix 1:100 (Abcam), rat anti-α-tubulin 1:1000 (Abcam), mouse anti-α-tubulin conjugate FITC 1:200 (Sigma). Primary antibody incubation for Osterix was 3 hr at room

temperature. Secondary antibody incubation was performed for 1 hr at room temperature. DAPI (Molecular Probes) was used to detect DNA. Images were obtained with a Confocal Leica TCS SP5 II (Leica Microsystems) or an Axio Observer.Z1 microscope with the LSM 700 scanning module (Zeiss). ImageJ 1.46r was used to determine fluorescence intensity. For VE-cadherin analysis, Alexa Fluor 647 anti-mouse VE-Cadherin (50μg; BioLegend) was administered per mouse and imaged 30 minutes post-injection. Images were acquired using an upright Leica TCS SP5 II confocal system with a Leica DM 6000 CFS microscope and Leica LAS AF software (Leica Microsystems). Z-stack images were sequentially captured in 1024x1024 format with line averaging and max projection.

2.13 Western Blot

Cell lysates were prepared by lysing cells in NP-40 lysis buffer (Boston BioProducts) or RIPA lysis buffer (Sigma Aldrich) with protease inhibitor (Thermo Scientific), incubated for 15-30 min. on ice and centrifuged at 15,000 rpm for 10 minutes at 4°C. Before electrophoresis, lysates were diluted in sample buffer (10% glycerol, 1.5% SDS, 60 mM Tris/HCl, pH 6.8, 2.5% beta-mercaptoethanol, 0.0025% bromophenol blue) and heated at 95°C for 5 min. Proteins were separated by SDS-PAGE, transferred to either Immobilon polyvinylidene difluoride membranes (Millipore) or Hybond-ECL nitrocellulose membranes (GE Healthcare). Primary antibodies used: goat anti-LIS1 (1:100; Santa Cruz Biotechnology), rabbit anti-Numb (1:1000; Abcam), rabbit anti-beta

tubulin (1:2000; Abcam) and anti-alpha tubulin (1:5000; Abcam). Secondary antibodies used: IRDye 800CW anti-goat IgG (1:20000; LI-COR), IRDye 680RD anti-rabbit IgG (1:20000; LI-COR), IRDye 800CW anti-rabbit IgG (1:10000; LI-COR) and IRDye 680RD anti-mouse IgG (1:10000; LI-COR). Membranes were developed using the Odyssey CLx imaging system (LI-COR).

2.14 Statistical analysis

Statistical analyses were carried out using GraphPad Prism software version 5.0a or 5.0d (GraphPad software Inc.). Data are mean ± SEM. Chi-square test was used to determine deviation from Mendelian ratios. Two-tailed unpaired Student's *t*-tests with Welch's correction when appropriate were used to determine statistical significance (*$p<0.05$, **$p<0.01$, ***$p<0.001$, ****$p<0.0001$).

3. Lis1 is required for hematopoietic stem cell self-renewal activity during fetal development.

3.1 Introduction

During embryonic development, the hematopoietic stem cell (HSC) pool increases substantially to ensure a sufficient number of HSCs are produced for postnatal life and for the geometric expansion of differentiated blood cells that are imminently required for growth and development (Lessard et al. 2004). To accomplish this, HSCs modulate the balance between self-renewal and differentiation. Recently, it has been shown that HSCs have the ability to undergo both symmetric renewal division (generating two daughter stem cells) and asymmetric cell division (generating one daughter stem cell and one differentiating daughter cell) (Wu et al. 2007). Thus, one way HSCs may control the extent at which they either self-renewal or differentiate is by dynamically changing their mode of division (i.e. from an asymmetric mode of division to a symmetric mode of division). In this regard, during development, HSCs may predominately undergo symmetric renewal division to guarantee that the required number of HSCs are generated. Although it has been demonstrated that HSCs have the ability to undergo both modes of division, the intrinsic regulators of this process are largely unknown in the hematopoietic system. The dynein-binding protein Lis1 has previously been shown to play a role in the machinery control division pattern in the nervous system (Yingling et al. 2008), however, whether this molecule plays a role in the regulation of fetal HSC self-renewal was unknown.

3.2 Results

3.2.1 *Vav-Cre*-mediated deletion of *Lis1* permits evaluation of Lis1's role specifically in the hematopoietic system.

To enable assessment of Lis1's role in establishment of the hematopoietic system and self-renewal of fetal hematopoietic stem cells (HSCs), we took advantage of the Cre/loxP recombination system to genetically delete *Lis1* specifically in the hematopoietic system. Mice homozygous for the null *Lis1* allele die during embryogenesis before embryonic (E) day 9.5 (Hirotsune et al. 1998). Thus, to circumvent embryonic lethality and to spatially and temporally control the deletion of *Lis1*, we utilized a hypomorphic/conditional *Lis1* floxed allele, where a *loxP*-flanked *PGK-neo* gene was placed in the reverse transcriptional orientation relative to *Lis1* in intron 2 and another *loxP* site was placed in intron 6 of the *Lis1* gene (Hirotsune et al. 1998).

Conditional *Lis1* knockout mice were generated by crossing mice carrying the *Lis1* floxed allele to mice in which Cre recombinase is driven by vav regulatory elements (*Vav-Cre* mice). Vav is an adaptor protein expressed in all adult and fetal hematopoietic cell types, including HSCs derived from the fetal liver (Adams et al. 1999; Adams et al. 1992; Bustelo et al. 1993; Katzav et al. 1989; Ogilvy et al. 1999a; Ogilvy et al. 1999b). To confirm *Vav-Cre*-mediated recombination occurs within the fetal HSC population, we crossed *Vav-Cre* mice with Tomato reporter mice (*Rosa26-stop-tdTomato*). These fluorescent reporter mice harbor a *loxP*-flanked STOP cassette, which prevents transcription of the downstream fluorescent Tomato red protein. When crossed to *Vav-*

Cre mice, the STOP cassette is deleted only in *Vav-Cre*-expressing cells, resulting in expression of Tomato red. Using this strategy, we found that ~98.7% of E11.5 fetal liver HSCs (c-Kit$^+$ Lin$^-$ AA4.1$^+$) and ~99.4% of HSCs at E13.5 are Tomato positive, indicating that *Vav-Cre* is effectively expressed and functional in fetal HSCs (Figure 1).

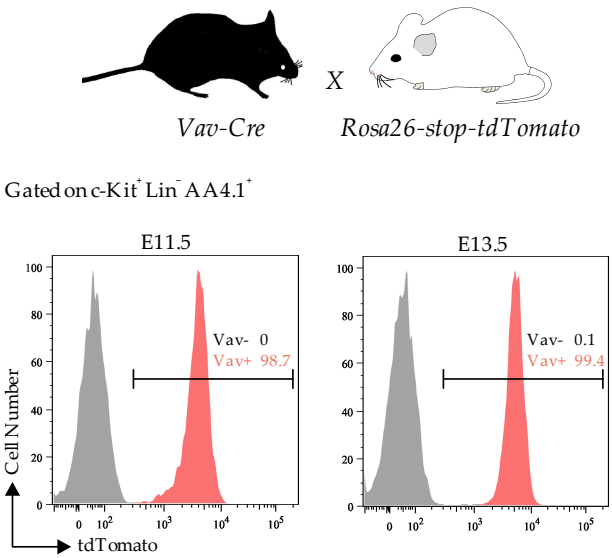

Figure 1: Efficiency of *Vav-Cre*-mediated recombination in fetal HSCs.

Figure 1: *Vav-Cre*-mediated recombination in fetal HSCs (c-Kit$^+$ Lin$^-$ AA4.1$^+$; KL AA4.1$^+$). *Vav-Cre* mice were crossed to *Rosa26-stop-tdTomato* reporter mice. Representative FACS histogram shows reporter activity (Tomato expression) in KL AA4.1$^+$ cells from control (*Tomato+; Vav-Cre-*) and *Tomato+; Vav-Cre+* littermates at E11.5 and E13.5; n=2-7 mice for each genotype for each gestational age.

Following the generation of blood-specific *Lis1* knockout mice, we performed genomic polymerase chain reaction (PCR) analysis of DNA extracted from CD45-positive fetal liver cells, which marks all hematopoietic cells, and confirmed loss of *Lis1*

expression in hematopoietic cells isolated from homozygous mutants (*Lis1$^{f/f}$; Vav-Cre;* hereafter referred to as *Lis1$^{-/-}$* mice) (Figure 2).

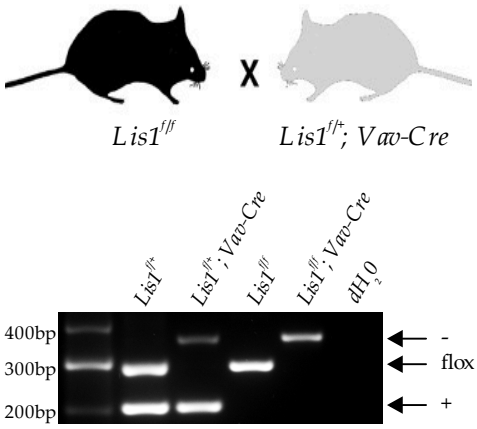

Figure 2: *Vav-Cre*-controlled deletion of *Lis1* in fetal hematopoietic cells.

Figure 2: The schematic indicates the strategy for deletion of *Lis1* in hematopoietic cells using mice homozygous for the floxed *Lis1* allele crossed to mice heterozygous for the floxed *Lis1* allele and carrying a transgene in which expression of the Cre recombinase is driven by the *Vav* promoter (top). Analysis of deletion efficiency by genomic PCR within CD45^{+} PI^{-} (Propidium iodide, live) fetal liver cells from E14.5 littermates (bottom).

3.2.2 Blood-specific deletion of *Lis1* leads to a significant reduction in fetal liver HSCs and a striking bloodless phenotype.

Using our *Vav-Cre*-based genetic approach, we found that out of a total of 344 viable progeny produced by breeding wild type mice homozygous for the *Lis1* floxed allele (*Lis1$^{f/f}$*) to Vav-positive heterozygotes (*Lis1$^{f/+}$; Vav-Cre*), 0 *Lis1$^{-/-}$* mice were born, where we expected 86 *Lis1$^{-/-}$* mice based on normal Mendelian ratios. Subsequently, the loss of *Lis1* led to lethality in late gestation between E15.5-E18.5 (Table 1).

Table 1: Genotype of offspring derived from the cross of *Lis1*$^{f/f}$ and *Lis1*$^{f/+}$; *Vav-Cre* mice.

Stage	Genotype				p-value
	Lis1$^{f/+}$	*Lis1*$^{f/f}$	*Lis1*$^{f/+}$; *Vav-Cre*	*Lis1*$^{f/f}$; *Vav-Cre*	
12.5 dpc	25	28	18	19	0.38
14.5 dpc	8	9	5	11	0.52
15.5 dpc	3	2	0	2	0.44
18.5 dpc	9	7	8	0	*0.04
Postnatal	140	94	110	0	***2.02x10^{-27}

In a retrospective analysis, we found that during gestation, loss of Lis1 led to a strikingly abnormal phenotype at E14.5 (Figure 3). Although grossly normal in form and size, *Lis1*$^{-/-}$ embryos are nevertheless quite pale in color, suggesting severe anemia.

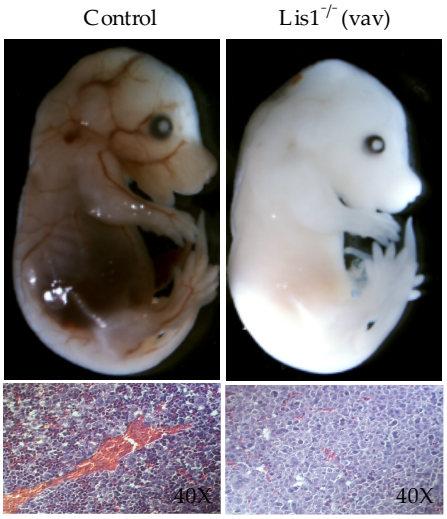

Figure 3: Blood-specific deletion of *Lis1* leads to a bloodless phenotype.

Figure 3: Representative image of Control (*Lis1*$^{f/+}$, upper left) and *Lis1*$^{-/-}$ (*Lis1*$^{f/f}$; *Vav-Cre*, upper right) littermates at E14.5. Representative hematoxylin and eosin (H&E) stain of fetal liver from Control (bottom left) and *Lis1*$^{-/-}$ (bottom right) littermates at E14.5. 40X.

Histologically, hematoxylin and eosin (H&E) stains of wild type and *Lis1*$^{-/-}$ fetal livers at E14.5 show a conspicuous loss of total hematopoietic cells within the fetal liver of *Lis1*$^{-/-}$ mice (Figure 3). Most noticeably, erythropoietic islands are numerous in wild type but not readily identifiable in *Lis1*$^{-/-}$ fetal livers. Interestingly, *Lis1* deletion led to a ~13.5 fold reduction in the frequency of HSCs (c-Kit^{+} Lin^{-} AA4.1^{+}) in the fetal liver at E14.5 (Figure 4a). Importantly, the 7-fold expansion of HSCs that occurs between E12.5-E15.5 and leads to the ultimate generation of a functional hematopoietic system failed to occur in the absence of Lis1 (Figure 4b). These data suggest that an underlying HSC defect may be responsible for the bloodless phenotype of *Lis1*$^{-/-}$ mice.

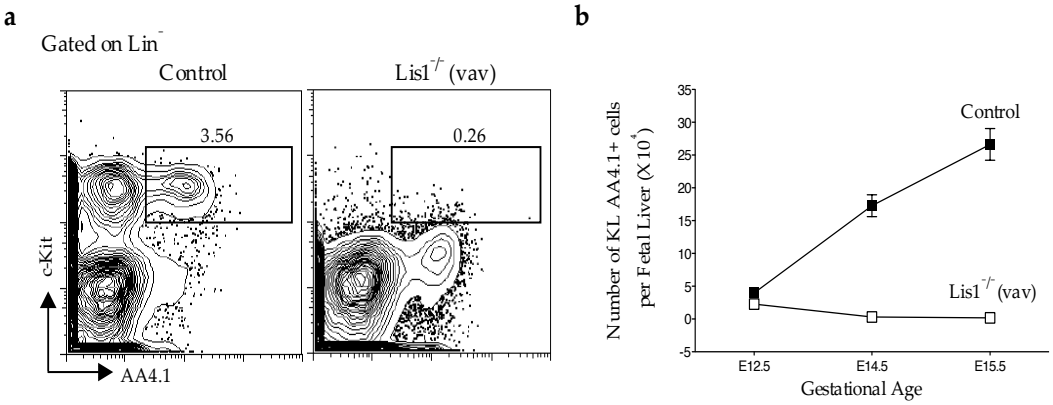

Figure 4: Failure of fetal HSC expansion in the absence of Lis1.

Figure 4: a, Fetal liver cells from Control (*Lis1*$^{f/+}$) and *Lis1*$^{-/-}$ mice were analyzed for frequency of fetal HSCs (cKit^{+} Lin^{-} AA4.1^{+}; KL AA4.1^{+}). Dot plots are shown for one representative Control (left) and *Lis1*$^{-/-}$ (right) E14.5 embryo. b, Absolute number of fetal HSCs (KL AA4.1^{+}) from Control (*Lis1*$^{f/+}$ or Lis1$^{f/f}$; solid squares) or *Lis1*$^{-/-}$ (squares) mice at different gestational ages; n=3-5 mice for each genotype for each gestational age.

3.2.3 Loss of Lis1 impairs fetal HSC self-renewal activity *in vitro* and *in vivo*.

To determine whether the failure of fetal HSC expansion *in vivo* was linked to functional defects in self-renewal we first assessed colony formation in methylcellulose cultures. An identical number of whole fetal liver cells from wild type or *Lis1*$^{-/-}$ littermates were cultured in methylcellulose to detect colony formation. Loss of *Lis1* led to a 3-fold reduction in total colony formation (Figure 5a). Importantly, the fact that the types of colonies formed (erythroid, BFU-E; myeloid, CFU-GM; multi-lineage, CFU-GEMM) were similar between wild type and *Lis1*-deficient cells indicated that differentiation capacity was unaffected in the absence of Lis1 (Figure 5b-d).

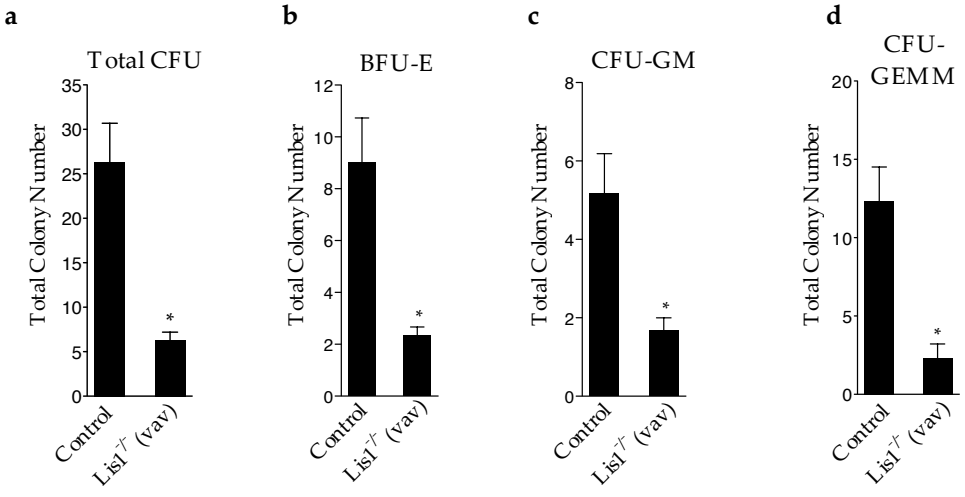

Figure 5: Impaired self-renewal capacity of *Lis1*-deficient fetal HSCs *in vitro*.

Figure 5: a, Total number of colonies generated from plating 5,000 whole fetal liver cells from Control (*Lis1*$^{f/+}$ *or Lis1*$^{f/f}$) and *Lis1*$^{-/-}$ embryos. b-d, Deconstruction of total number of colonies into the number of individual types of colonies generated: BFU-E (b), CFU-GM (c) and CFU-GEMM (d). Data are compiled from 3-6 embryos of each genotype. BFU-E was determined on Day 7 and

CFU-GM and CFU-GEMM were determined on Day 10 (*p=0.0194 for BFU-E, *p=0.0305 for CFU-GM, *p=0.0132 for CFU-GEMM). Error bars show the standard error of mean (SEM).

To test the self-renewal capacity of *Lis1*-deficient fetal HSCs *in vivo*, we transplanted HSC-enriched cells (Lin^- $AA4.1^+$) from either wild type or $Lis1^{-/-}$ E14.5 littermates into lethally irradiated congenic recipients. While transplantation of wild type HSC-enriched cells led to ~53% donor chimerism at 4 months post-transplant, no chimerism (0%) was detected in mice reconstituted with *Lis1*-deficient cells, suggesting that loss of *Lis1* affects fetal HSC self-renewal *in vivo* (Figure 6a, b).

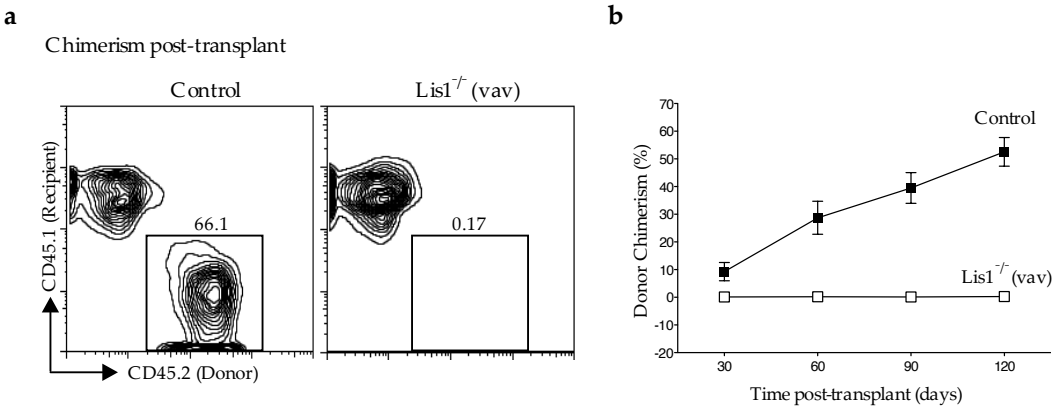

Figure 6: Loss of *Lis1* impairs self-renewal of fetal HSCs *in vivo*.

Figure 6: a, Representative FACS profile of donor chimerism (4 months) in $CD45.1^+$ recipients transplanted with 5,000 HSC-enriched cells (Lin^- $AA4.1^+$) from either Control ($Lis1^{f/+}$) or $Lis1^{-/-}$ E14.5 embryos. b, Average donor chimerism at different times post-transplantation (2-4 donor mice were used for each genotype and 4-6 recipient mice in each cohort). Control is shown with solid squares and $Lis1^{-/-}$ is shown with open squares. Error bars show the standard error of the mean (SEM).

In support of a requirement for Lis1 in HSC renewal activity *in vivo*, we also performed whole fetal liver transplants to test HSC function irrespective of phenotype.

While transplantation of wild type whole fetal liver cells led to ~70.4% donor chimerism, transplantation of *Lis1*-deficient whole fetal liver cells led to a chimerism of ~0.2%, indicating that the loss of Lis1 affected functional HSCs and is unlikely to have simply led to changes in phenotype (Figure 7).

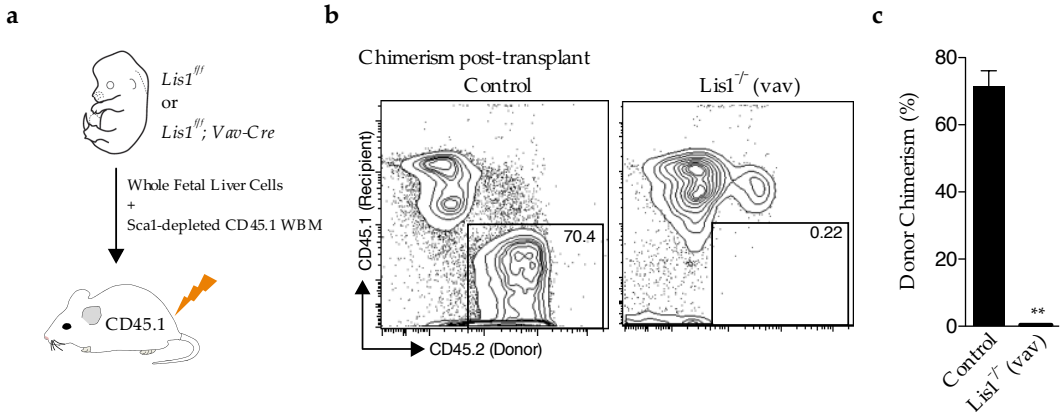

Figure 7: Repopulation ability of *Lis1*-deficient whole fetal liver cells.

Figure 7: a, Experimental scheme used to test repopulation ability of *Lis1*-deficient whole fetal liver cells. 300,000 whole fetal liver cells from control (*Lis1*$^{f/f}$) and *Lis1*$^{-/-}$ (*Lis1*$^{f/f}$*; Vav-Cre*) CD45.2^{+} littermates at E12.5 were transplanted along with 300,000 Sca1-depleted recipient-type (CD45.1^{+}) whole bone marrow cells into CD45.1^{+} recipient mice. b, Representative FACS plot shows donor chimerism (CD45.2^{+}) in recipients that received either control or *Lis1*$^{-/-}$ cells at 8 weeks post-transplantation. c, Average donor chimerism at 8 weeks post-transplantation (n=3-4 recipients per genotype; $^{**}p$=0.0041).

Collectively, these data demonstrate Lis1 plays an essential role in the maintenance of self-renewal ability of fetal liver HSCs.

3.2.4 Lis1 has a broad impact on HSC function at multiple sites during embryonic development.

Although HSCs primarily expand and differentiate within the fetal liver during embryonic development, HSCs emerge and are found in other anatomic sites including the placenta, which accrues a reservoir of HSCs during mid-gestation, and possibly the yolk sac (Alvarez-Silva et al. 2003; Ema and Nakauchi 2000; Gekas et al. 2005; Ottersbach and Dzierzak 2005). In this regard, we tested the impact of *Lis1* deletion on yolk sac and placental hematopoiesis. The *Vav-Cre*-driver led to a partial deletion of *Lis1* in $CD34^+$ stem/progenitor yolk sac cells at E11.5 (Figure 8a). Although we found no change in the frequency of $CD34^+$ cells (Figure 8b), this partial deletion of *Lis1* led to a ~11-fold reduction in total colony formation (Figure 8c).

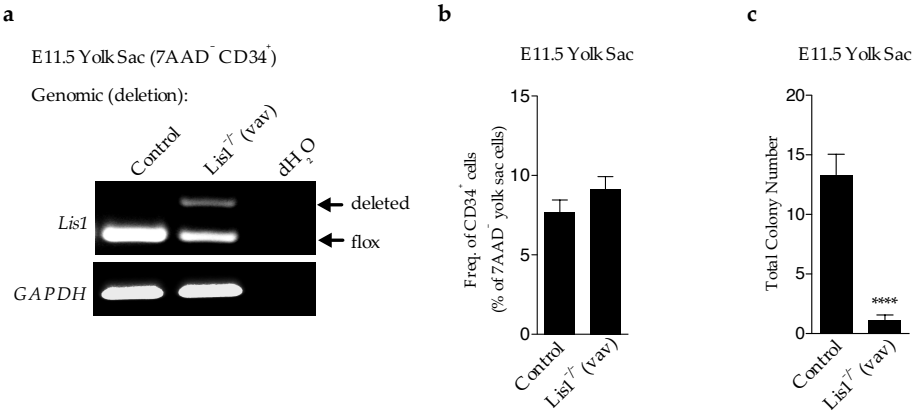

Figure 8: Analysis of colony-forming ability of HSCs/progenitors from yolk sac.

Figure 8: a-c, Impact of loss of Lis1 on colony-forming ability of stem/progenitor cells isolated from the yolk sac and placenta. a, Analysis of deletion efficiency in yolk sac. $7AAD^-$ $CD34^+$ yolk sac cells were isolated from control (*Lis1*$^{f/f}$) and *Lis1*$^{-/-}$ (*Lis1*$^{f/f}$; *Vav-Cre*) littermates at E11.5 and RT-PCR analysis performed to determine expression of *Lis1* mRNA (water was used as a negative control). b, Average frequency of $CD34^+$ stem/progenitor yolk sac cells from control (*Lis1*$^{f/f}$ or

Lis1$^{f/+}$) and *Lis1*$^{-/-}$ mice (n=2-4 mice for each cohort). c, Total number of colonies generated from plating 500 CD34$^+$ yolk sac cells from control (*Lis1*$^{f/f}$ or *Lis1*$^{f/+}$) and *Lis1*$^{-/-}$ embryos. Data are compiled from 2-4 embryos of each genotype in triplicate assay wells; ****p<0.0001. Error bars show the standard error or mean (SEM).

Likewise, we found that *Vav-Cre*-mediated deletion of *Lis1* led to a partial deletion of *Lis1* in c-Kit$^+$ CD34$^+$ stem/progenitor placenta cells at E12.5, which had no affect on the frequency of this population. However, c-Kit$^+$ CD34$^+$ placenta cells from homozygous mutants failed to form colonies *in vitro*. This data suggest Lis1 may have a significant impact on hematopoietic stem cell function at multiple sites during embryogenesis (Figure 9).

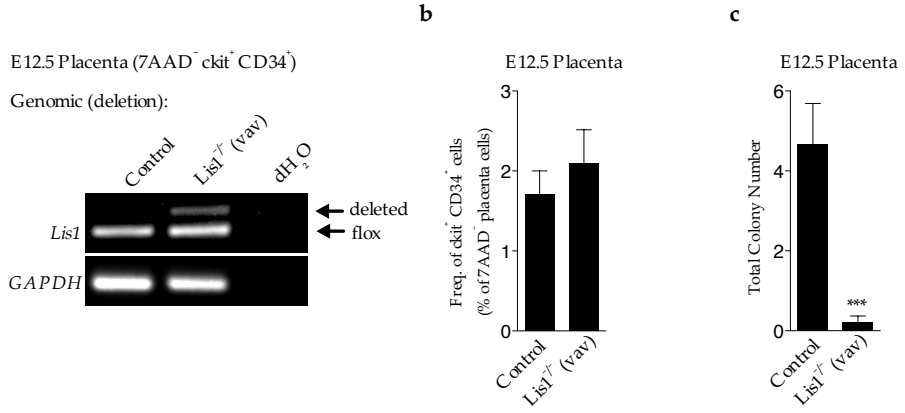

Figure 9: Analysis of colony-forming ability of HSCs/progenitors from placenta.

Figure 9: a-c, Impact of loss of *Lis1* on colony-forming ability of stem/progenitor cells isolated from the placenta. a, Analysis of deletion efficiency in placenta. 7AAD$^-$ c-Kit$^+$ CD34$^+$ placenta cells were isolated from control (*Lis1*$^{f/f}$) and *Lis1*$^{-/-}$ (*Lis1*$^{f/f}$; *Vav-Cre*) littermates at E12.5 and RT-PCR analysis performed to determine expression of *Lis1* mRNA (water was used as a negative control). b, Average frequency of c-Kit$^+$ CD34$^+$ stem/progenitor placenta cells from control (*Lis1*$^{f/f}$ or *Lis1*$^{f/+}$) and *Lis1*$^{-/-}$ mice (n=5-6 mice for each cohort). c, Total number of colonies generated from plating 300 c-Kit$^+$ CD34$^+$ placenta cells from control (*Lis1*$^{f/f}$ or *Lis1*$^{f/+}$) and *Lis1*$^{-/-}$ embryos. Data are compiled from 5-6 embryos of each genotype in triplicate assay wells; ***p=0.0001. Error bars show the standard error or mean (SEM).

3.3 Discussion

Self-renewing hematopoietic stem cells (HSC) are at the apex of the hematopoietic hierarchy on the basis of their ability to generate all cell types of the blood system (Orkin and Zon 2008). During embryogenesis, HSCs are generated *de novo* in numerous anatomical sites but primarily expand and differentiate within the fetal liver (Mikkola and Orkin 2006). The expansion of the HSC population within the fetal liver is essential to ensure that enough stem cells are generated to sustain postnatal life and to permit the geometric expansion of differentiated cells immediately required for embryonic growth and development. This period of HSC expansion during development depends on the ability of HSCs to self-renewal (divide and make more stem cells). Several intrinsic regulators of fetal HSC self-renewal have been identified including Sox17, Rae28, Meis1 and c-myb (Azcoitia et al. 2005; Hisa et al. 2004; Kim et al. 2007; Kim et al. 2004; Kirito et al. 2004; Mucenski et al. 1991; Ohta et al. 2002; Rebel et al. 2002; Sandberg et al. 2005). These intrinsic factors integrate with extrinsic cues to promote self-renewal divisions of fetal HSCs.

Here, we show that the dynein-binding protein, Lis1 plays a role in fetal hematopoiesis. Blood-specific deletion of *Lis1* leads to a strikingly bloodless phenotype that comparably mirrors the phenotypes observed following the genetic deletion of known HSC self-renewal regulators such as Aml-1/Runx1, Gata-2 and MLL (Okuda et al. 1996; Porcher et al. 1996; Tsai et al. 1994; Wang et al. 1996). The similarities in

phenotype suggest the intriguing possibility that events controlled by Lis1 activity may be integrated with the function of these transcription factors. Probing into Lis1's role in fetal hematopoiesis, we find Lis1 is critically required for fetal HSC self-renewal activity. Specifically, data from both *in vitro*-based experiments and transplantation-based *in vivo* assays convincingly show that the genetic deletion of *Lis1* leads to strong defects in fetal HSCs. Interestingly, the loss of Lis1 impairs the self-renewal ability of stem/progenitor cells from multiple sites of blood development including the yolk sac, placenta and the fetal liver. To date, while several regulators of self-renewal of fetal liver HSCs have been identified, the cell-intrinsic mediators of yolk sac and placental HSCs are largely unknown. Thus, the identification of Lis1 as an important regulator of HSC function in HSCs from non-fetal liver sites during development underscore the key requirement for Lis1 in HSC activity broadly during embryogenesis.

Interestingly, a role for Lis1 in stem cell self-renewal has also been shown in the mammalian nervous system. During neural development, neuroepithelial stem cells undergo rapid symmetric renewal divisions to expand and grow the neural tube, which is fundamental to the formation of the brain. Recently it was shown that Lis1 is critically required for the maintenance of proliferative neuroepithelial stem cells. In the absence of Lis1, neuroepithelial expansion of neuroepithelial stem cells fails to occur and instead neuroepithelial stem cells undergo apoptotic cell death (Yingling et al. 2008). Thus, these data implicating Lis1 in the self-renewal of neural stem cells along with our finding that

Lis1 is essential for blood stem cell renewal during development highlight the significance of Lis1 function to the regulation and maintenance of stem cell identity.

4. Critical requirement for Lis1 in the self renewal of adult HSCs

4.1 Introduction

Intrinsic regulators of hematopoietic stem cell (HSC) self-renewal might be distinct or shared between HSCs derived from the fetal liver and from that of the adult bone marrow. A number of genes including *Sox17* regulate the maintenance of fetal but not adult HSCs (Kim et al. 2007). In contrast, a number of genes including *Gfi-1, Tel*/*Etv6* and *Bmi-1* maintain adult but not fetal HSCs (Hock et al. 2004a; Hock et al. 2004b; Park et al. 2003). In addition to differences in transcriptional regulation, fetal and adult HSCs differ in terms of gene expression profile, surface marker expression, developmental potential and self-renewal capacity (Ikuta et al. 1990; Ivanova et al. 2002; Morrison et al. 1995; Phillips et al. 2000).

Although there are clear differences between fetal and adult HSCs, several genes appear to regulate the maintenance of HSCs throughout fetal and adult including *Rae28, Meis1* and *c-myb*, suggesting key players implicated in the regulation of fetal HSCs may have a conserved functional role in the adult system. (Azcoitia et al. 2005; Hisa et al. 2004; Kim et al. 2004; Kirito et al. 2004; Mucenski et al. 1991; Ohta et al. 2002; Rebel et al. 2002; Sandberg et al. 2005). Determining whether Lis1 plays a role in the adult blood system and in particular adult HSC self-renewal will provide further insight into the similarities and differences between fetal and adult HSCs.

4.2 Results

4.2.1 Use of a tamoxifen-inducible cre system leads to effective deletion of *Lis1* in adult HSCs.

To determine if Lis1 has a conserved functional role in the adult blood system, we took a genetic approach and crossed floxed *Lis1* mice to mice harboring a Cre-recombinase-O-estrogen-Receptor-T2 (Cre-ER^{T2}) allele targeted to the ubiquitously expressed ROSA26 locus (denoted hereafter as *Lis1$^{f/f}$; Rosa-creER* mice) (Ventura et al. 2007). In these mice, the ER^{T2} moiety fused to Cre retains the recombinase inactive in the cytosol until tamoxifen administration releases this inhibition. Thus, tamoxifen delivery allows effective temporal control over *Lis1* deletion.

To induce *Lis1* deletion in adult mice, both *Lis1$^{f/f}$; Rosa-creER and Lis1$^{+/+}$; Rosa-creER* control mice were administered tamoxifen daily for five consecutive days (Figure 10a). Three days post-tamoxifen treatment, we performed genomic polymerase chain reaction (PCR) analysis and showed that in tamoxifen-treated *Lis1$^{f/f}$; Rosa-creER* mice, the floxed allele was effectively deleted and the undeleted allele could no longer be detected in adult bone marrow HSC-enriched cells (c-Kit^{+} Lin^{-} Sca-1^{+} or KLS) (Figure 10b). Furthermore, real-time (RT)-PCR analysis indicated a clear reduction in *Lis1* mRNA expression in KLS cells (Figure 10b). In support of this, quantitative PCR showed a 92.4% reduction of *Lis1* mRNA expression in these cells (Figure 10c). To further confirm that our tamoxifen regiment effectively led to *Lis1* deletion, we immunostained highly enriched HSCs (KLS CD48^{-}) for Lis1 and found that Lis1 protein expression is markedly

reduced in HSCs after tamoxifen administration (Figure 10d,e). Collectively, these data demonstrate that we could effectively delete *Lis1* in adult HSCs using our tamoxifen-inducible cre system and that this model could be used to test the requirement of Lis1 in adult HSC renewal.

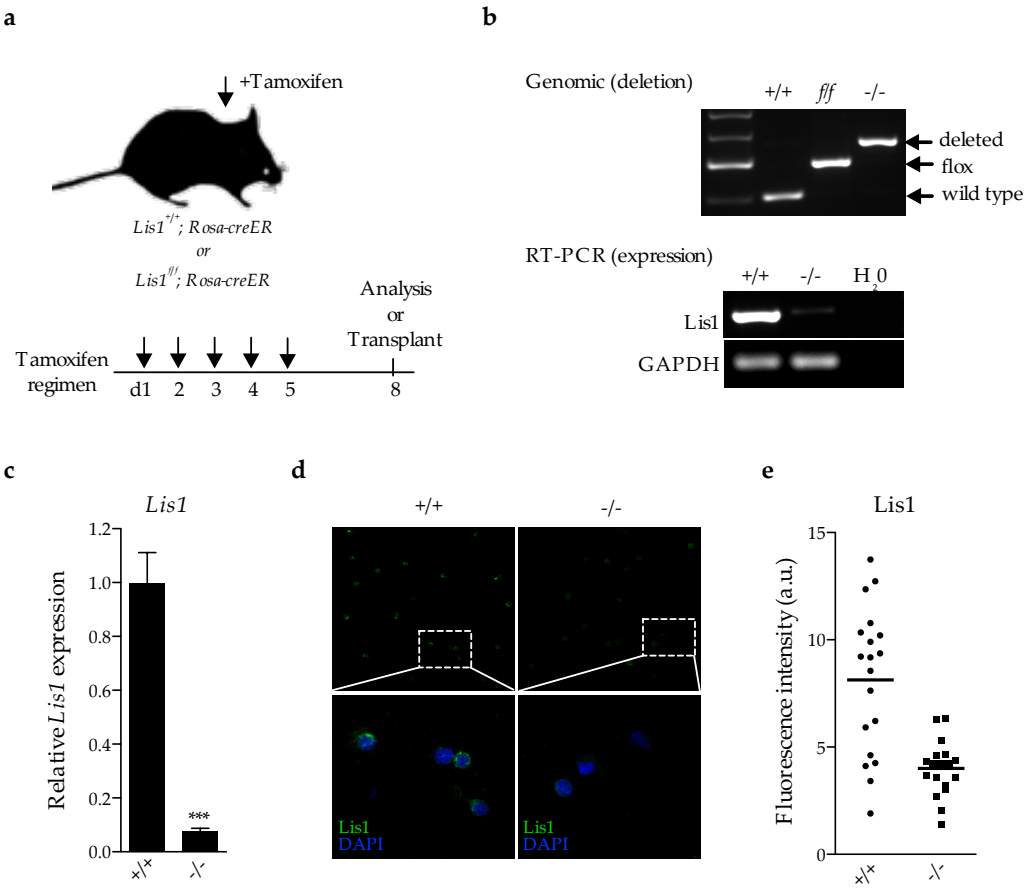

Figure 10: Tamoxifen-inducible cre activity effectively leads to *Lis1* deletion in adult hematopoietic stem cells.

Figure 10: a, Schematic shows strategy for deletion of *Lis1* in adult mice. Both control (*Lis1*$^{+/+}$; *Rosa26-creER/Rosa26-creER*, indicated as *Lis1*$^{+/+}$; *Rosa-creER*) and *Lis1*$^{f/f}$; *Rosa26-creER/Rosa26-creER* (indicated as *Lis1*$^{f/f}$; *Rosa-creER*) mice were administered tamoxifen daily for 5 days. Analyses and cell sorting were performed 3 days post-tamoxifen treatment. b, Analysis of deletion efficiency by

genomic PCR analysis (top) and RT-PCR (bottom). Genomic DNA from HSC-enriched cells (c-Kit$^+$ Lin$^-$ Sca1$^+$ or KLS) isolated from tamoxifen-treated control (*Lis1*$^{+/+}$; *Rosa-creER*, indicated as +/+), corn oil-treated control (*Lis1*$^{f/f}$; *Rosa-creER*, indicated as *f*/*f*) and tamoxifen-treated *Lis1*$^{f/f}$; *Rosa-creER* (indicated as -/-) mice. For RT-PCR analysis, KLS cells were isolated from control (+/+) and (-/-) mice and RT-PCR analysis was performed to determine expression of *Lis1* mRNA (water was used as a negative control). c, Analysis of *Lis1* deletion efficiency by quantitative PCR. For qPCR, KLS cells were isolated from control and *Lis1*$^{f/f}$; *Rosa-creER* mice and realtime PCR analysis performed to determine expression of *Lis1* mRNA (n=2; ***p=0.0004). Expression levels were normalized and displayed relative to the control TATA-binding protein (TBP). All error bars show the standard error of the mean (SEM). d, Analysis of *Lis1* deletion efficiency by immunofluorescence. HSCs (KLS CD48$^-$) isolated from control and *Lis1*$^{f/f}$; *Rosa-creER* mice 3 days post-tamoxifen treatment were immunostained with anti-Lis1 antibody (green) and 4′, 6-diamidino-2-phenylindole (DAPI, blue) and fluorescence intensity was quantified, ****p<0.0001. a.u., arbitrary units.

4.2.2 Adult *Lis1*-deficient HSCs have a cell-autonomous defect in self-renewal *in vivo*

Using our tamoxifen-inducible *Lis1* deletion strategy, we found that loss of Lis1 in adult mice led to a significant reduction in the frequency and absolute number of adult HSCs (c-Kit$^+$ Lin$^-$ Sca-1$^+$ Flt3$^-$) (Figure 11).

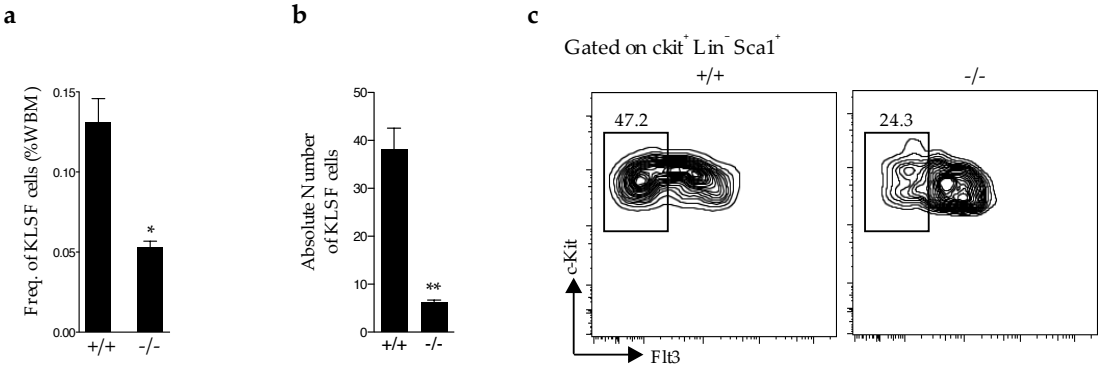

Figure 11: Reduction in the frequency and absolute number of adult HSCs in the absence of Lis1.

Figure 11: a, Average frequency of HSCs (KLS Flt3$^-$, KLSF) in whole bone marrow from control (+/+) and (-/-) mice; n=6 for control (+/+), n=5 for (-/-); *p=0.0268. b, Absolute number of HSCs in whole bone marrow from control (+/+) and (-/-) mice; n=6 for control (+/+), n=5 for (-/-); **$p=0.0085$. b, Representative FACS plots of HSCs (KLSF) from control (+/+) and (-/-) mice.

Functionally, self-renewal and reconstitution ability of adult HSCs was also affected by *Lis1* deletion *in vivo*. Specifically, while transplantation of HSCs (c-Kit$^+$ Lin$^-$ Sca-1$^+$ CD150$^+$ CD48$^-$) from tamoxifen-treated control (*Lis1*$^{+/+}$*; Rosa-creER*) mice led to increasing average donor chimerism from 39% to 51% over time, mice reconstituted with *Lis1*-deficents cells showed a gradual loss in donor chimerism from ~6.5% to 0% (Figure 12). These data suggest that, similar to Lis1's role in fetal development, Lis1 is also required for the self-renewal of HSCs during adulthood.

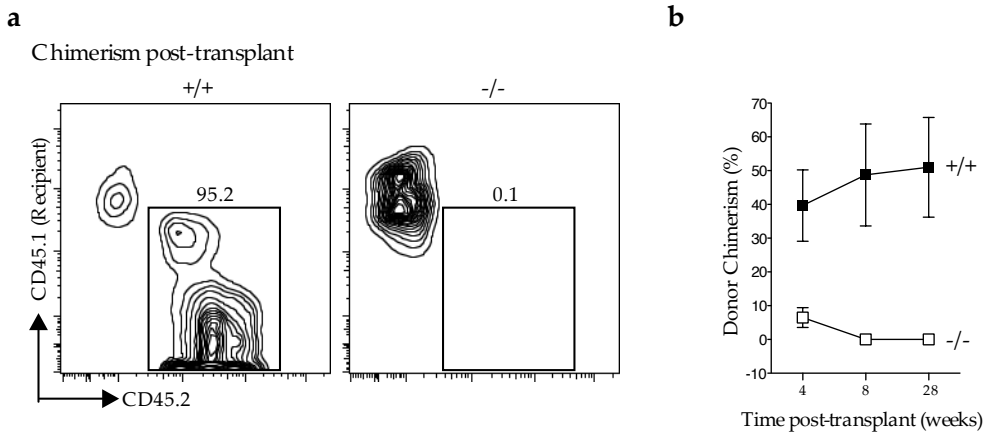

Figure 12: *Lis1*-deficient cells have impaired reconstitution ability *in vivo*.

Figure 12: a, Repopulation efficiency of *Lis1*$^{-/-}$ HSCs. Representative FACS plots shows donor chimerism (CD45.2$^+$ cells) in recipients transplanted with 500 HSCs (KLS CD150$^+$ CD48$^-$) from control (+/+) or (-/-) mice. FACS analysis was performed 28 weeks post-transplantation. b, Average donor chimerism at different times after transplantation (5-6 mice per cohort). Control (+/+) is shown with solid squares and (-/-) is shown with open squares.

To determine whether the reduced donor chimerism observed in recipients that received *Lis1*-deficient cells was due to a failure of *Lis1*-deficient HSCs to properly home to the bone marrow following transplantation, we transplanted whole bone marrow cells from either tamoxifen-treated control (*Lis1*$^{+/+}$; *Rosa-creER*) or *Lis1*$^{f/f}$; *Rosa-creER* mice into irradiated recipients. A short period after transplantation, mice that received *Lis1*-deficient cells displayed similar levels of donor chimerism compared to mice that received control cells, suggesting that the observed long-term renewal defects of *Lis1*-deficient HSCs were unlikely to be a consequence of impaired homing (Figure 13).

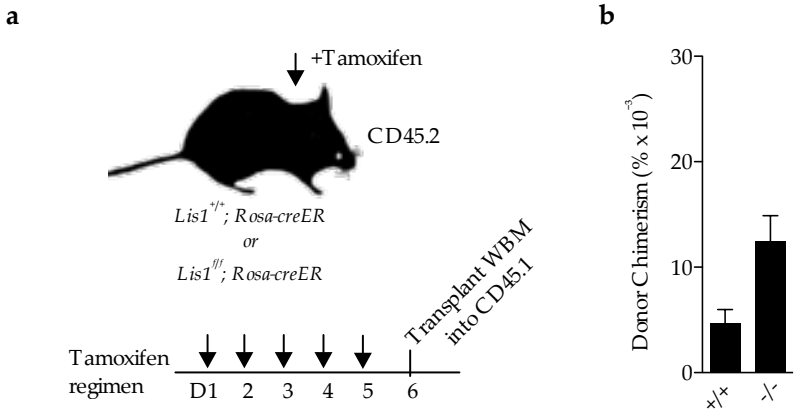

Figure 13: Loss of Lis1 does not affect homing ability of bone marrow cells.

Figure 13: a-b, Relative homing ability of control and *Lis1*$^{-/-}$ bone marrow cells. A total of 5 x 10^6 bone marrow cells from control (*Lis1*$^{+/+}$; *Rosa-creER*) and *Lis1*$^{f/f}$; *Rosa-creER* mice 1 day post-tamoxifen injections were transplanted into irradiated recipients (n=4-5 in each group), and the presence of donor-derived cells was analyzed by FACS 6 hr post transplant (b).

In our tamoxifen-inducible cre system, cre activation is under the control

of the ubiquitous Rosa26 promoter. Thus, following tamoxifen treatment, *Lis1* is deleted in non-hematopoietic tissues as well. In this regard, non-cell-autonomous defects may underlie the impaired self-renewal of HSCs following *Lis1* deletion. To address this, we initially tested whether the HSC bone marrow niche was affected by the loss of Lis1, and find that the frequency and extent of microenvironmental elements of the bone marrow such as VE-Cadherin^{+} blood vessels and Osterix^{+} osteoblasts are largely unaffected following *in vivo* deletion of *Lis1* (Figure 14).

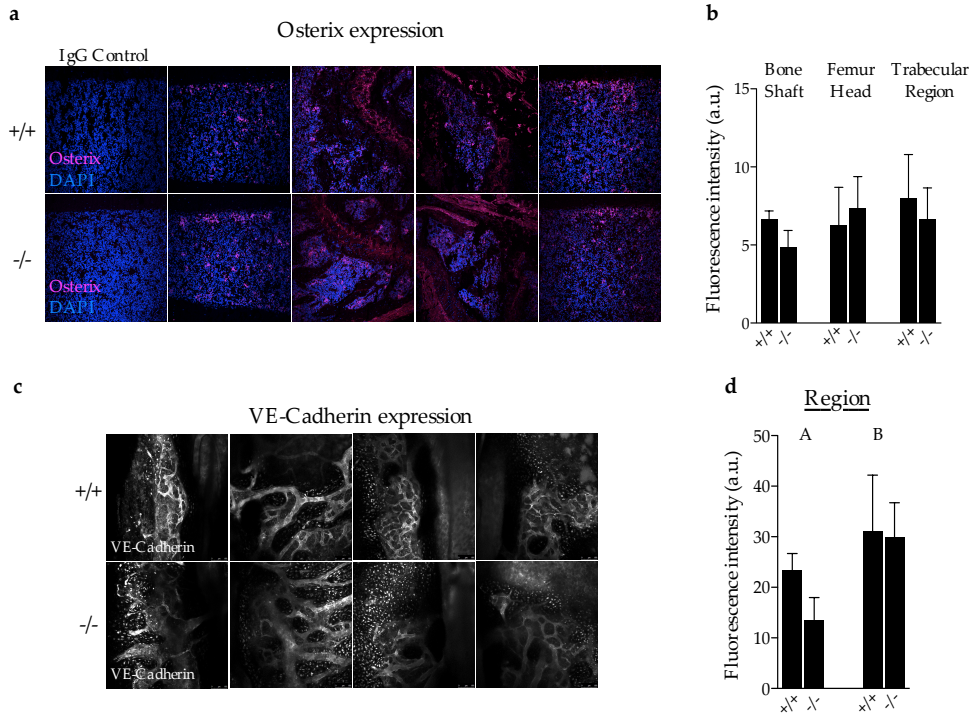

Figure 14: Frequency and extent of bone marrow microenvironmental elements are unaffected in the absence of Lis1.

Figure 14: a-d, Analysis of microenvironment of control (*Lis1*$^{+/+}$*; Rosa-creER*; +/+) and *Lis1*$^{f/f}$*; Rosa-creER* (-/-) mice that were administered tamoxifen daily for 4 days. a, Bone marrow sections from control (+/+) and (-/-) mice were immunostained for anti-Sp7/Osterix. (Osterix is shown in pink,

DAPI in blue). b, Average fluorescence intensity of Osterix in bone shaft, femur head, and trabecular bone regions of control (+/+) and (-/-) mice. Data are compiled from two independent experiments; n=2-3 mice per genotype. c, Representative images of VE-Cadherin (white) expression in different matched regions of the bone marrow in control (+/+) and (-/-) mice injected with anti-VE-Cadherin and imaged. d, Average fluorescence intensity of VE-Cadherin in two bone marrow regions in control (+/+) and (-/-) mice. Data are compiled from two independent experiments; n=2-3 mice per genotype.

However, to exclude the possibility that unidentified defects in the microenvironment may impact HSCs indirectly, we created chimeras in which only the hematopoietic system contained the *Lis1* floxed allele and the microenvironment remained wild type (Figure 15a). Thus, isolated HSCs from untreated control $Lis1^{+/+}$; *Rosa-creER* or $Lis1^{f/f}$; *Rosa-creER* mice were transplanted into lethally irradiated recipients. Eight weeks after transplantation, donor-derived HSCs successfully multi-lineage repopulated recipient mice (Figure 15b). Importantly, we achieved 80-90% donor chimerism regardless of the genotype of the donor cells. At this time, chimeric mice were treated with tamoxifen to delete *Lis1* specifically in the hematopoietic system. This led to a significant reduction in the frequency of donor-derived HSC-enriched cells (Figure 15c).

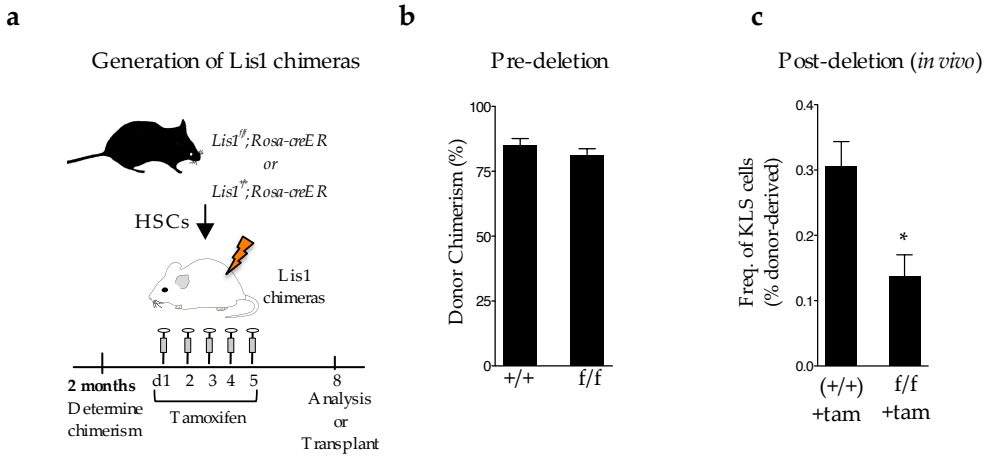

Figure 15: Significant reduction in the frequency of HSC-enriched cells in Lis1 chimeric mice.

Figure 15: a, Experimental scheme to generate chimeras with hematopoietic-specific *Lis1* deletion; 1,000 HSCs (KLS CD150$^+$ CD48$^-$) from control (*Lis1*$^{+/+}$; *Rosa-creER*) or *Lis1*$^{f/f}$; *Rosa-creER* (CD45.2$^+$) mice were transplanted into CD45.1$^+$ recipient mice. Two months post-transplantation, an average of ~80% donor-derived chimerism was observed. All recipient mice were administered tamoxifen daily for 5 days and analyses and cell sorting were performed 3 days post-tamoxifen treatment. b, Donor chimerism prior to tamoxifen (tam) treatment was assessed two months post-transplantation. (+/+) indicates control *Lis1*$^{+/+}$; *Rosa-creER* and (*f/f*) indicates *Lis1*$^{f/f}$; *Rosa-creER* transplanted mice (6 mice in each cohort). c, Frequency of donor-derived KLS cells in chimeric mice post-deletion. ((+/+) +tam) indicates mice that received donor cells from *Lis1*$^{+/+}$; *Rosa-creER* and ((*f/f*) +tam) indicates mice that received donor cells from *Lis1*$^{f/f}$; *Rosa-creER* mice; n=3 for each cohort, *p=0.0277.

To test cell autonomous stem cell function *in vivo*, donor-derived whole bone marrow cells from both control and *Lis1*-deficient chimeras were re-transplanted into recipient mice. While the average chimerism from control cells was 53.5%, chimerism from Lis1 null cells was nearly absent (0.3%), roughly recapitulating the phenotype of

non-chimeric *Lis1* null mice (Figure 16). These data suggest that adult *Lis1*-deficient HSCs have a cell-autonomous defect in self-renewal *in vivo*.

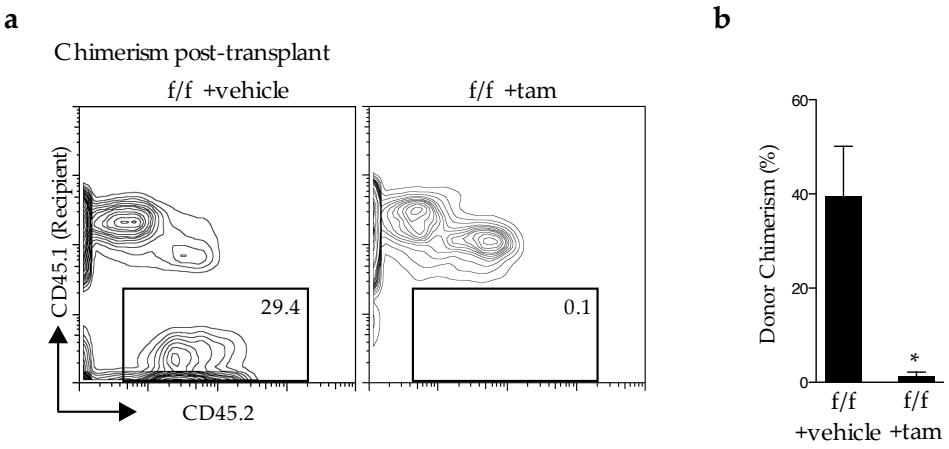

Figure 16: *Lis1*-deficient HSCs have a cell-autonomous defect in self-renewal *in vivo*.

Figure 16: a-b, Repopulation ability of whole bone marrow (WBM) cells isolated from Lis1 chimera mice. Lis1 chimeras that were generated by transplantation of HSCs derived from *Lis1$^{f/f}$; Rosa-creER* mice (CD45.2^{+}) were treated with corn oil (f/f +vehicle) or tamoxifen (f/f +tam) daily for 5 days. 3 days post-treatment 300,000 WBM cells were transplanted into recipient mice a, Representative FACS plots show donor chimerism (CD45.2^{+} cells) in recipients that received cells from either control (f/f +vehicle) or (f/f +tam) Lis1 chimeras. b, Average donor chimerism at 16 weeks post-transplantation (n=3-4 recipients per cohort; *$p=0.0369$).

4.3 Discussion

The hallmark of hematopoietic stem cells (HSC) is their dual abilities to self-renew and to differentiate into multiple blood cell lineages. Importantly, the remarkable ability of HSCs to balance self-renewal to maintain the HSC pool with differentiation to generate mature cells is why the mammalian hematopoietic system can generate 10^{11} blood cells everyday throughout an individual's lifetime (Morrison and Weissman 1994;

Orkin 2000). This balance is critical not only when the blood replaces cells to maintain homeostasis, but also after acute injury when an exponential rise in HSCs is required to quickly replenish the hematopoietic compartment. Importantly, improper control of this balance is intimately tied to the development of hematological malignancies. While a number of regulators and signaling pathways that are involved in the control of HSC self-renewal have been identified including Notch, Sonic hedgehog and Wnt, we are only beginning to understand the complex mechanisms and the interplay between cell-intrinsic and cell-extrinsic mechanisms that control this process (Reya 2003).

Here we show that Lis1, a facultative regulator of the minus-end directed motor protein dynein, is not only required for the self-renewal activity of fetal HSCs during development, but has a conserved functional role in the adult blood system. By using an inducible conditional knockout approach in adult mice, we demonstrate that *Lis1* deletion results in a loss of HSCs. Furthermore, specific deletion of *Lis1* within the hematopoietic system demonstrates a cell-autonomous requirement for Lis1 in adult HSC activity. Several genes, including *Rae28, Meis1* and *c-myb* have also been shown to control HSC maintenance in both fetal and adult HSCs and thus, events controlled by Lis1 activity may be integrated with the function of these genes. (Azcoitia et al. 2005; Hisa et al. 2004; Kim et al. 2004; Kirito et al. 2004; Mucenski et al. 1991; Ohta et al. 2002; Rebel et al. 2002; Sandberg et al. 2005).

During adulthood, HSCs reside in specialized microenvironments created by supporting bone marrow cells, primarily endothelial and osteoblastic cells, which produce factors and cytokines that influence HSC activity (Calvi et al. 2003; Kiel et al. 2005). Using a genetic system where *Lis1* presumably is deleted in non-hematopoietic tissues, we show that the loss of Lis1 does not significantly affect the integrity of VE-Cadherin+ blood vessels and Osterix+ osteoblasts, suggesting that Lis1 does not influence HSC activity in a non-cell-autonomous manner. However, further studies where Lis1 is deleted specifically in niche cell types will need to be done to convincing demonstrate whether Lis1 can act in a non-cell-autonomous manner to influence HSC function. Overall, we show that Lis1 is required for HSC self-renewal activity both during development and in adulthood, suggesting that certain critical mechanisms that control HSC self-renewal are not always development-stage specific.

5. Cellular and molecular basis of HSC defects that arise in the absence of Lis1

5.1 Introduction

Genetic deletion of *Lis1* both during development and in adult life results in a severe impairment of HSC self-renewal activity. In the absence of Lis1, fetal and adult HSCs exhibit impaired colony-forming ability *in vitro* and fail to effectively reconstitute the blood compartment of recipient mice in which endogenous hematopoiesis has been lethally ablated by radiation. Elucidating the cellular and molecular basis of the defects observed in the absence of Lis1 will aid in the determination of the mechanism(s) by which Lis1 exerts its biological influence on HSC function.

The ability of HSCs to maintain their numbers in homeostasis as well as to effectively respond to acute injury depends on tight regulation of quiescence/proliferation, self-renewal, survival and differentiation. Lis1 has previously been implicated in several of these events. In cell culture experiments, LIS1 overexpression or depletion by antibody injection supports a role for LIS1 in a myriad of dynein-dependent mitotic functions (Faulkner et al. 2000; Tai et al. 2002). Consistent with this, siRNA knockdown of *Lis1* in rat cortical slices results in defects in cell division (Tsai et al. 2005). A role for Lis1 in the control of self-renewal and differentiation has been demonstrated in spermatogenesis and in the *Drosophila* ovary (Chen et al. 2010; Nayernia et al. 2003).

Interestingly, a role for Lis1 in the regulation of stem cell division pattern has been shown in the mammalian nervous system. During development, neuroepithelial stem cells (NESC) extensively self-renew to grow the neural tube and thus, predominately undergo symmetric renewal divisions. However, loss of Lis1 in NESCs leads to spindle orientation defects that subsequently affect the ability of NESCs to control division pattern. As a result, the normal expansion of the stem cell compartment is profoundly disrupted (Yingling et al. 2008). In hematopoietic stem cell biology, an unresolved fundamental question is how self-renewal and cell fate determination may be influenced by mechanisms associated with asymmetric division. That Lis1 has been implicated in the machinery controlling division pattern in the nervous system strongly suggest that Lis1 may influences HSC function in this manner.

5.2 Results

5.2.1 Proliferative capacity of both fetal and adult HSCs is unaffected in the absence of Lis1.

In an effort to understand the basis of the hematopoietic stem cell (HSC) defects observed in the absence of Lis1, we first examined proliferation and apoptosis. To test whether *Lis1*-deficient HSCs have a reduced proliferative capacity we performed *in vivo* 5-bromo-2'-deoxyuridine (BrdU) incorporation assays combined with intracellular staining for DNA content (7AAD). In context of fetal HSCs, $Lis1^{f/f}$ mice were bred with $Lis1^{f/+}$; *Vav-Cre* mice and pregnant dams were administered BrdU via intraperitoneal injection. Following a 45-minute chase period, fetal liver cells were isolated from

individual embryos and analyzed for BrdU incorporation. As shown in Figure 17, BrdU incorporation rates were similar between control and *Lis1*$^{-/-}$ HSCs (c-Kit^{+} Lin^{-} AA4.1^{+}) from E12.5 fetal liver, suggesting proliferative capacity of fetal HSCs is largely unaffected in the absence of Lis1.

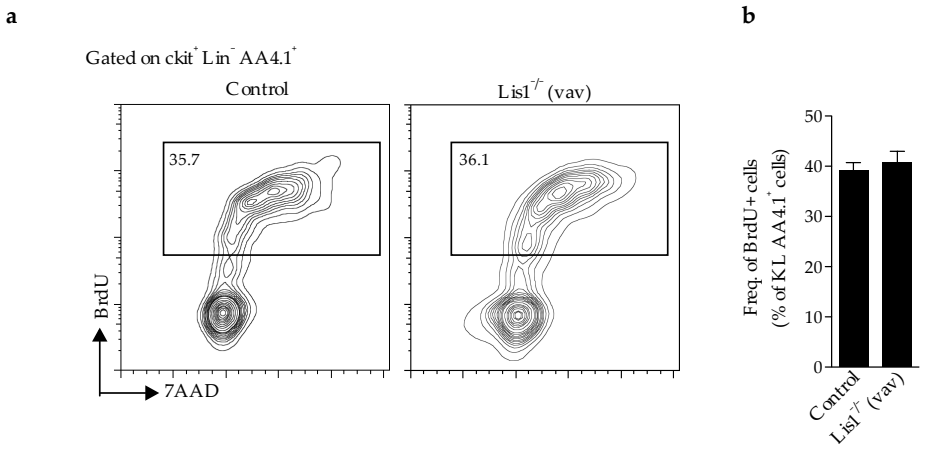

Figure 17: Proliferation of fetal HSCs is unaffected in the absence of Lis1.

Figure 17: a-b, Analysis of cell cycle of fetal HSCs. To test proliferation *in vivo*, pregnant females were administered BrdU and embryos analyzed 45 minutes post-BrdU injection. a, Representative BrdU/7AAD cell cycle plot of fetal HSCs (KL AA4.1^{+}) in E12.5. control (*Lis1*$^{f/f}$) and *Lis1*$^{-/-}$ (*Lis1*$^{f/f}$; *Vav-Cre*) littermates b, Average frequency of BrdU-positive KL AA4.1^{+} cells from control and *Lis1*$^{-/-}$ mice at E12.5. Data shown are from two independent experiments (n=4-9 per cohort).

To examine whether HSC defects in the adult blood system resulted from impaired proliferation of adult HSCs, control *Lis1*$^{+/+}$; *Rosa-creER* and *Lis1*$^{f/f}$; *Rosa-creER* mice were treated with tamoxifen daily for five days (D1-D5). On day 6 (D6), mice were administered BrdU and bone marrow cells were analyzed after an 18-hour chase period. As shown in Figure 18, purified *Lis1*-deficient HSCs (KLS CD150^{+} CD48^{-}), HSC-enriched

cells (KLS) and multipotent progenitors (KLS CD150$^-$ CD48$^+$) incorporated BrdU at a rate similar to control and displayed a normal cell cycle distribution (G_0/G_1, S and G_2/M). Collectively, these data suggest that in both the fetal and adult, HSC proliferation proceeds unabated following the loss of Lis1.

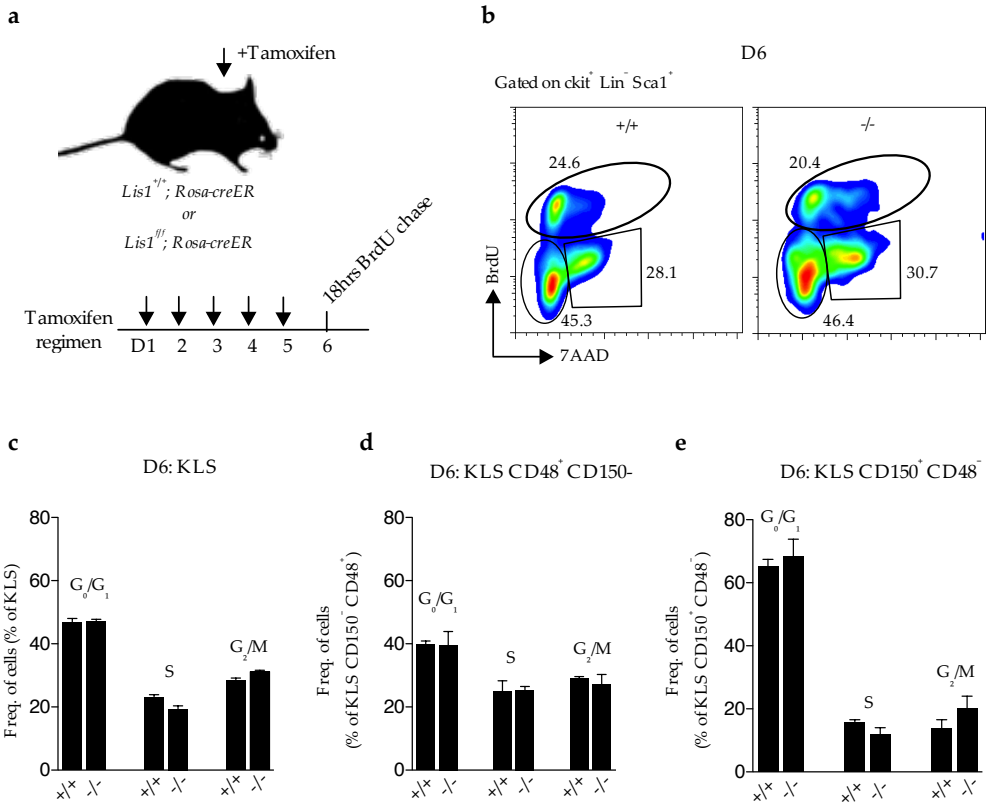

Figure 18: Proliferation of adult bone marrow HSCs is unaffected in the absence of Lis1.

Figure 18: Analysis of adult HSC cell cycle distribution. a, Schematic illustrates the strategy used to determine cell cycle status of hematopoietic cells following *Lis1* deletion. Control (*Lis1*$^{+/+}$*; Rosa-creER*) and *Lis1*$^{f/f}$*; Rosa-creER* mice were administered tamoxifen daily for 5 days (D1-D5). Mice were pulsed with 5-bromodeoxyuridine (BrdU) at 1 day post-injection (D6). After an 18 hr chase period, bone marrow cells were analyzed. b, Representative BrdU/7AAD plot showing cell cycle distribution of KLS (c-Kit$^+$ Lin$^-$ Sca1$^+$) cells in control (+/+) or (-/-) mice. c-e, Average frequency of

KLS (c) KLS CD48$^+$ CD150$^-$ (d) KLS CD150$^+$ CD48$^-$ (e) in G_0/G_1, S, and G_2/M cell cycle phases in control (+/+) and (-/-) mice. Data shown are from two independent experiments (n=2-3 per cohort). All error bars show the standard error of the mean (SEM).

5.2.2 Loss of Lis1 in both fetal and adult HSCs leads to necrotic/late stage apoptosis.

To determine whether the loss of Lis1 leads to cell death in fetal HSCs, we stained fetal liver cells from *Vav-Cre*-mediated conditional Lis1 knockout mice (*Lis1$^{f/f}$*; *Vav-Cre*) for AnnexinV and 7AAD and found that loss of Lis1 results in a slight increase in the frequency of AnnexinV$^+$ 7AAD$^+$ necrotic/late stage apoptotic fetal liver HSCs compared to controls (Figure 19).

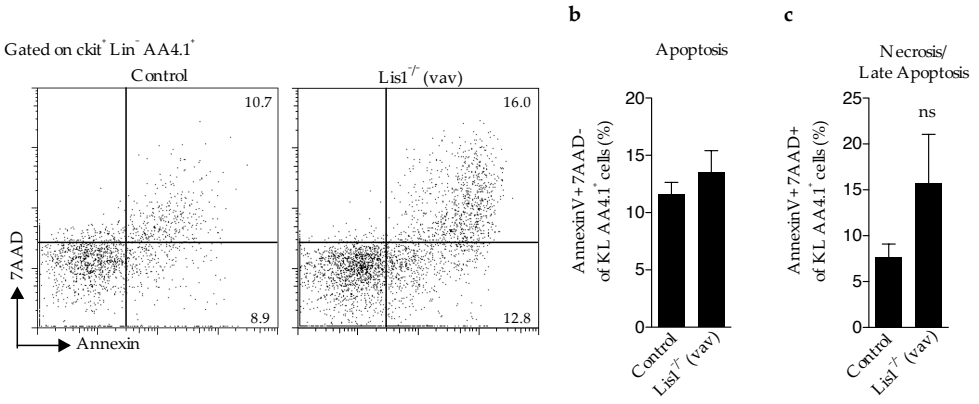

Figure 19: Loss of Lis1 leads to a marginal increase in necrotic/late apoptotic cells.

Figure 19: a-c, Cell death of fetal HSCs. a, Representative AnnexinV/7AAD profile of fetal HSCs (KL AA4.1$^+$) from control (*Lis1$^{f/f}$*) and *Lis1$^{-/-}$* (*Lis1$^{f/f}$; Vav-Cre*) littermates at E12.5. d-e, Frequency of KL AA4.1$^+$ cells undergoing apoptosis (AnnexinV$^+$ 7AAD$^-$) (b) or undergoing necrosis/late apoptosis (AnnexinV$^+$ 7AAD$^+$) (c) in control (*Lis1$^{f/f}$*) and *Lis1$^{-/-}$* (*Lis1$^{f/f}$; Vav-Cre*) littermates at E12.5. Data compiled from 3-5 embryos per genotype. All error bars show the standard error of the mean (SEM).

To examine whether HSC defects in the adult blood system resulted from increased cell death of adult HSCs, control *Lis1*$^{+/+}$*; Rosa-creER* and *Lis1*$^{f/f}$*; Rosa-creER* mice were treated with tamoxifen daily for five days (D1-D5). As shown in Figure 20, HSCs had equivalent frequencies of Annexin V$^+$ 7AAD$^-$ early apoptotic cells at several times points after *Lis1* deletion. However, an increase in Annexin V$^+$ 7AAD$^+$ necrotic/late stage apoptotic cells was detected at day 6 (D6) (Figure 20).

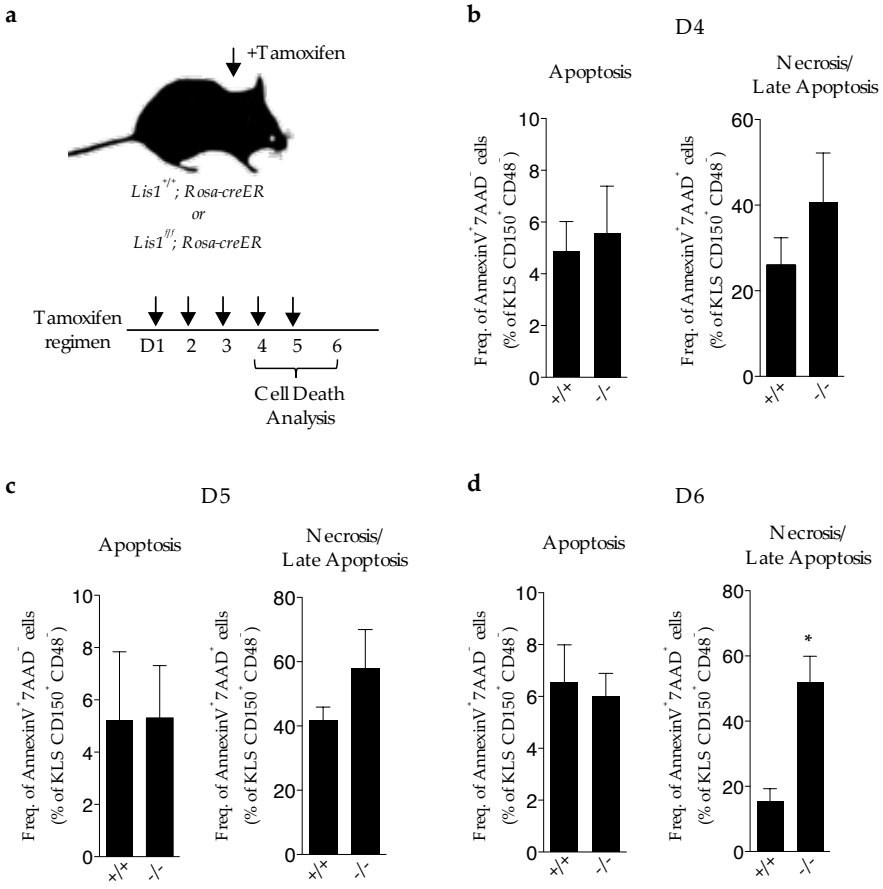

Figure 20: *Lis1* deletion results in an increase in late onset necrotic/late stage apoptotic adult HSCs.

Figure 20: Analysis of adult HSC cell death. a, Schematic illustrates the strategy used to analyze cell death of hematopoietic cells following Lis1 deletion. Control (Lis1+/+; Rosa-creER) and Lis1f/f; Rosa-creER mice were administered tamoxifen daily for 5 days (D1-D5). Cell death analysis was performed on D4, D5, during tamoxifen treatment and 1 day post-tamoxifen injections (D6). b-d, Percentage of HSCs (c-Kit+ Lin- Sca1+ CD150+ CD48-) undergoing apoptosis (AnnexinV+ 7AAD-) or undergoing necrosis/late apoptosis (AnnexinV+ 7AAD+) in control (+/+) and (-/-) mice on D4 (b), D5 (c) and D6 (d). Data shown are from two independent experiments (n=2-3 per cohort for each day analyzed; *p=0.0141). All error bars show the standard error of the mean (SEM).

Importantly, as shown in Figure 21, HSC depletion occurred as early as day 3 (D3) after *Lis1* deletion when no change in survival was observed. Thus, although it is possible that a late onset death contributes, in part, to the overall phenotype observed, the fact that it occurs later than when HSC defects are first observed suggest that Lis1 may influence hematopoietic stem cells through other mechanisms.

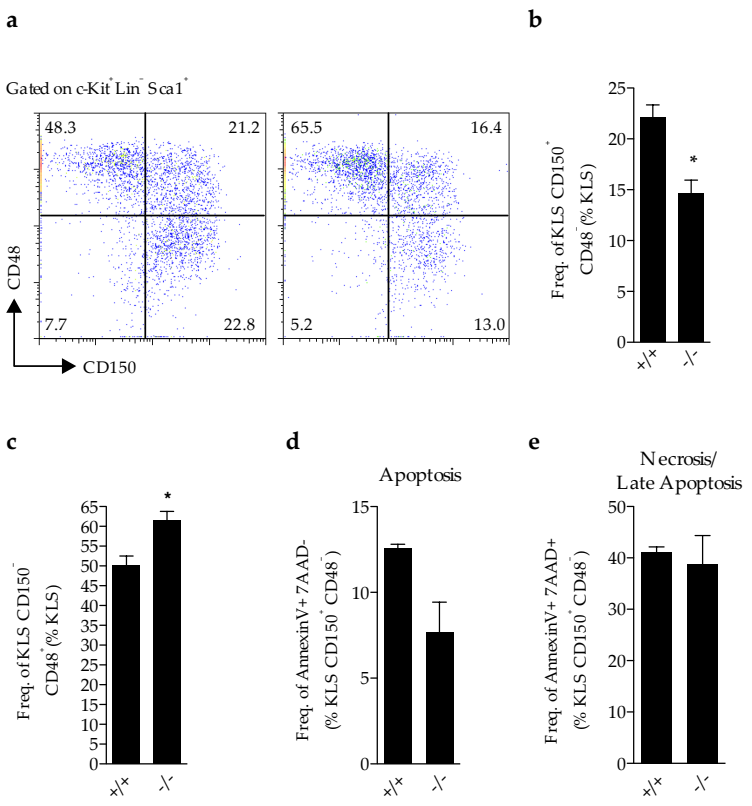

Figure 21: Early reduction in adult HSCs following the loss of Lis1.

Figure 21: a, Representative FACS profile of CD48/CD150 expression within the KLS compartment of control (+/+) and (-/-) mice. b-c, Average frequency of HSCs (KLS CD48$^-$ CD150$^+$) (b) and multipotent progenitors (MPPs; KLS CD48$^+$ CD150$^-$) (c) within the KLS population from control (+/+) and (-/-) mice; n=3 for control (+/+), n=4 for (-/-). *p=0.0103 for HSCs and *p=0.0211 for MPPs. d-e, Percentage of HSCs (KLS CD48$^-$ CD150$^+$) undergoing apoptosis (AnnexinV$^+$ 7AAD$^-$) (d) or undergoing necrosis/late apoptosis (Annexin V$^+$ 7AAD$^+$) (e) in control (+/+) and (-/-) bone marrow on day 3 of tamoxifen injections; n=3 for control (+/+), n=4 for (-/-).

5.2.3 Loss of Lis1 leads to accelerated differentiation of HSCs *in vitro* and *in vivo*.

The loss of the immature cell population *in vivo* following *Lis1* deletion suggested a potential defect in maintenance of the undifferentiated state; thus we tracked the

actual rate of differentiation of *Lis1*-deficient cells. To test this, identical number of HSC-enriched cells (c-Kit$^+$ Lin$^-$ Sca-1$^+$) isolated from either *Lis1$^{f/f}$; Rosa-creER* or control *Lis1$^{+/+}$; Rosa-creER* mice were plated *in vitro*, treated with 4-hydroxytamoxifen (4-OH tamoxifen) at t=0 and the generation of differentiated cells tracked following *Lis1* deletion, which was determined by genomic PCR analysis (Figure 22).

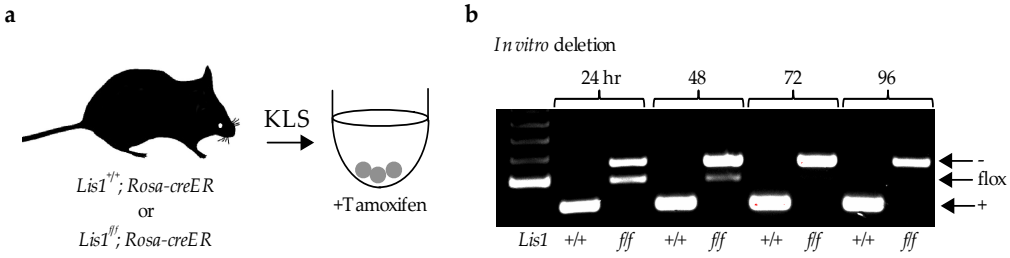

Figure 22: Approach and efficiency of *Lis1* deletion *in vitro*.

Figure 22: a, Schematic illustrates the approach used to delete *Lis1 in vitro.* Briefly, an HSC-enriched fraction of bone marrow cells (c-Kit$^+$ Lin$^-$ Sca1$^+$; KLS) was isolated from control (*Lis1$^{+/+}$; Rosa-creER*) and *Lis1$^{f/f}$; Rosa-creER* mice and treated with 4-OH-tamoxifen in liquid media. b, Analysis of deletion efficiency by genomic PCR analysis. Genomic DNA from cultured KLS cells at different time points after 4-OH-tamoxifen treatment.

By tracking the rate of cell differentiation, we found that over a period of 24 hours, ~23% of *Lis1$^{-/-}$* cells become positive for lineage markers (Lin$^+$) while in control cultures only ~9% of cells become positive for lineage markers (Lin$^+$) (Figure 23a,b). Importantly, as shown in Figure 23c, the observed increase in differentiated cells upon *Lis1* deletion was not due to a preferential death of immature cells (Lin$^-$).

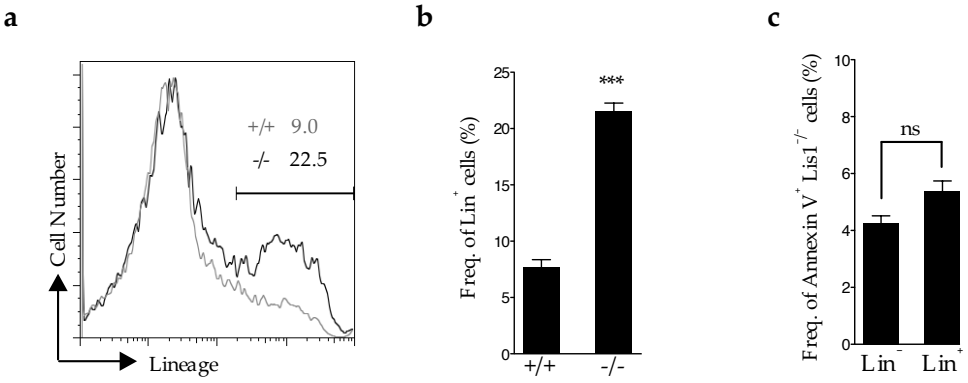

Figure 23: Loss of Lis1 leads to the accelerated differentiation of adult HSCs *in vitro*.

Figure 23: a-b, Analysis of rate of differentiation of *Lis1*$^{-/-}$ cells. Equal numbers of KLS cells were isolated from control (*Lis1*$^{+/+}$; *Rosa-creER*) and *Lis1*$^{f/f}$; *Rosa-creER* mice and treated with 4-OH-tamoxifen *in vitro*. a, Representative FACS plot shows frequency of cells expressing lineage markers in control (+/+; shown in gray) or *Lis1*-deficient (-/-; shown in black) populations 24 hours post-deletion. b, Average frequency of cells expressing lineage markers (Lin$^+$) cells in (+/+) and (-/-) cells. Data shown are from three independent experiments; ***p=0.0002. c, Analysis of apoptosis in Lin$^-$ and Lin$^+$ fraction of *Lis1*$^{-/-}$ cells. Percentage of Annexin V$^+$ cells is shown 24 hours post-deletion. Data shown are from two independent experiments. Error bars show the standard error of mean (SEM).

Looking in more detail, we tracked the specific types of differentiated cells generated following *Lis1* deletion. Using fluorescence-activated cell sorting (FACS) analysis, we find that of the mature lineage positive (Lin$^+$) *Lis1*-deficient cell population, 81.5% of the Lin$^+$ cells are Mac1$^+$ Gr1$^-$ cells (early myeloid) and 8.6% are Mac$^+$ Gr1$^+$ (granulocytic). In addition, 2.8% of cells are the B lineage (B220$^+$). Although 6.0% expressed CD4 and 0.3% expressed CD8 neither co-expressed CD3, suggesting either aberrant differentiation, or activated natural killer (NK) cell lineage (Figure 24).

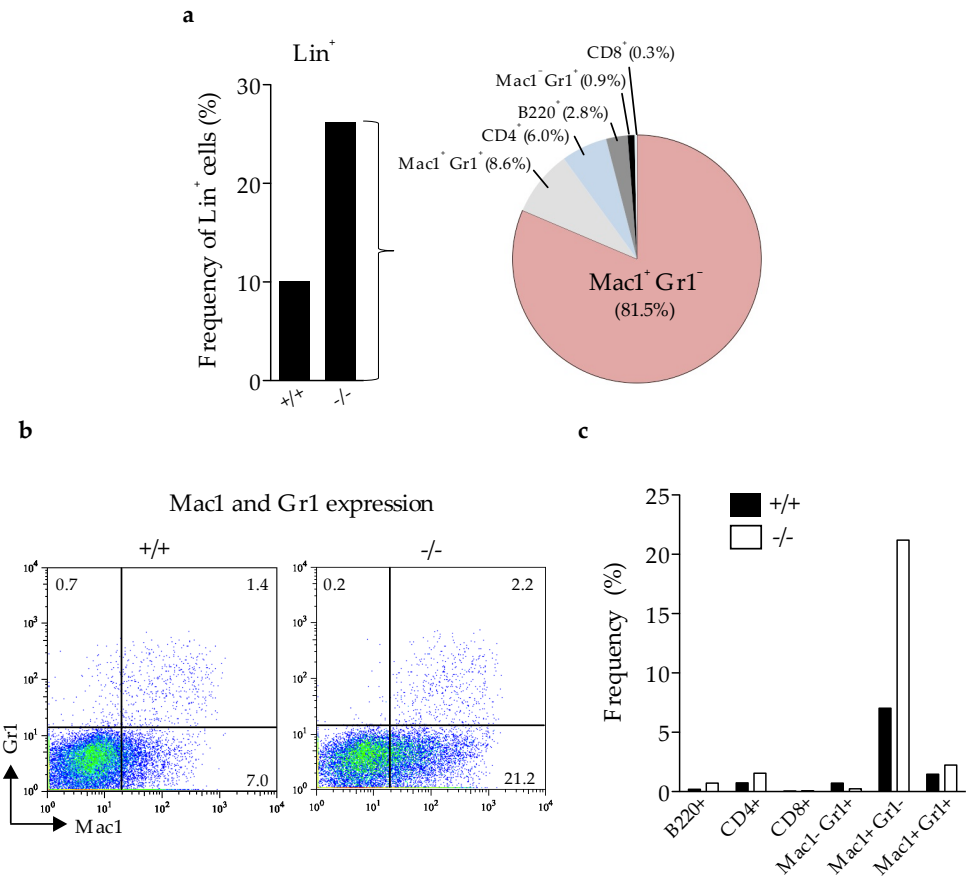

Figure 24: Accelerated differentiation of *Lis1* null HSCs into early myeloid cells.

Figure 24: a-c, Identical numbers of KLS cells were isolated from control (*Lis1*$^{+/+}$; *Rosa-creER*) and *Lis1*$^{f/f}$; *Rosa-creER* mice and treated with 4-OH-tamoxifen *in vitro*. a, Frequency of cells expressing lineage markers (Lin$^+$) cells in control (+/+) and (-/-) cells. Pie chart indicated composition of Lin$^+$ cells in (-/-) cells. b, Representative FACS plot of Mac1/Gr1 expression in (+/+) and (-/-) cells. c, Frequencies of mature cell populations in (+/+) and (-/-) cells. (+/+) is shown in black and (-/-) is shown in white.

Consistent with this, we analyzed the hematopoietic compartment *in vivo* for a wave of differentiation that may accompany the loss of HSCs. Following three days of tamoxifen treatment, we found that the loss of Lis1 promoted the differentiation of HSCs

(KLS CD150^{+} CD48^{-}) into multipotent progenitors (MPP; KLS CD150^{+} CD48^{+}). Specifically, tamoxifen treated *Lis1$^{f/f}$; Rosa-creER* mice had a 7.5% reduction in HSCs and a concomitant 11.3% rise in MPPs (Figure 21a-c). Collectively our *in vitro* and *in vivo* data suggest that the loss of Lis1 leads to the accelerated differentiation of HSCs.

5.2.4 Predominance of Numb asymmetry in the absence of Lis1 both *in vitro* and *in vivo*.

Because accelerated differentiation can be a consequence of defects in asymmetric division we examined whether the absence of Lis1 led to altered polarization of fate determinants within the mother cell or altered inheritance of these determinants by the daughter cells. Numb is an important fate determinant whose expression can mark differentiated cells. Specifically, we found by immunofluorescence that Numb is expressed 1.8-fold higher in progenitor cells (KLS CD48^{+}) than HSCs (KLS CD150^{+} CD48^{-}) (Figure 25a,b). In addition, PCR analysis revealed a 5.2-fold increase in *Numb* mRNA from immature lineage-negative (Lin-) cells to mature lineage-positive (Lin+) cells. Collectively, these data suggest that increased Numb expression increases with increased acquisition of the differentiated state (Figure 25b). Consistent with this, Numb was shown to be inherited at higher levels by daughter cells that become differentiated (Wu et al. 2007). We thus specifically tracked the polarization and inheritance of this fate determinant.

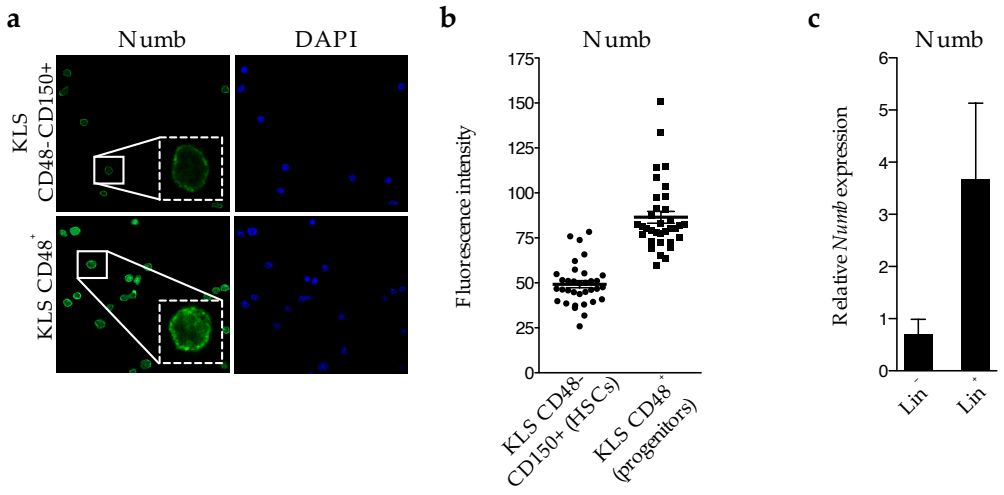

Figure 25: Expression of the cell fate determinant Numb can mark differentiated hematopoietic cells.

Figure 25: a, Expression of Numb in HSCs and progenitor cells. Representative image with zoomed inlay (dotted white box) shows HSCs (KLS CD48$^-$ CD150$^+$) and progenitor cells (KLS CD48$^+$) stained with anti-Numb antibody (green) and DAPI (blue), 63X. b, Average fluorescence intensity of Numb in individual HSCs and progenitor cells. c, Realtime RT-PCR analysis of *Numb* expression in Lin$^-$ and Lin$^+$ cells (n=2 each).

Distribution of Numb was first analyzed in HSC-enriched cells (c-Kit$^+$ Lin$^-$ Sca-1$^+$). To test this, KLS cells were isolated from either *Lis1$^{f/f}$; Rosa-creER* or *Lis1$^{+/+}$; Rosa-creER* control mice, treated with 4-OH tamoxifen *in vitro* to delete *Lis1* and fixed cells were stained for Numb. In 63% of cells Numb was distributed equally to both sides, and in 37% Numb was polarized on one side of the mother cell. As shown in Figure 26c, in the absence of Lis1, no change in the distribution of Numb was observed.

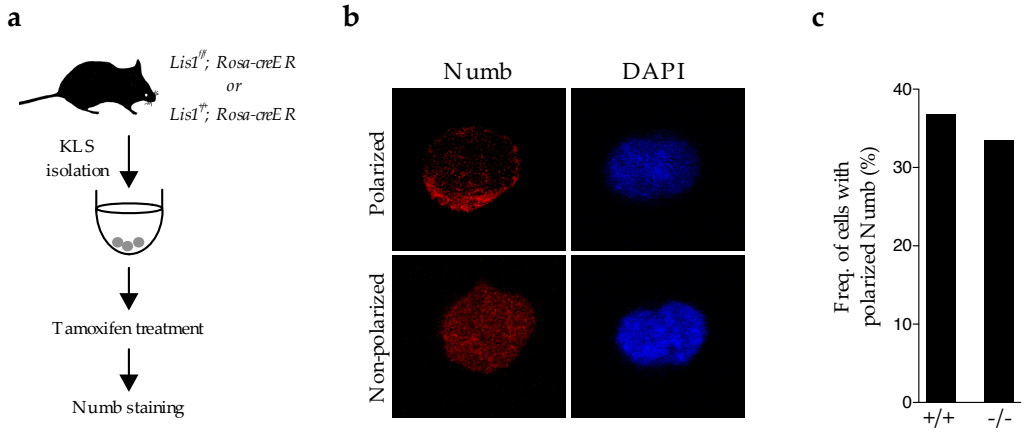

Figure 26: Polarization of Numb in HSCs is unaffected in the absence of Lis1

Figure 26: a, Experimental scheme used to determine Numb polarization and inheritance in HSC-enriched cells. KLS cells were isolated from control (*Lis1*$^{+/+}$; *Rosa-creER*) and *Lis1*$^{f/f}$; *Rosa-creER* mice, treated with 4OH-tamoxifen *in vitro* and analyzed 24 hours post-deletion. b, Representative images of individual cells with polarized or non-polarized Numb (Numb in red, DAPI in blue, zoomed 63x images). c, Frequency of control (+/+) or *Lis1*-deficient (-/-) cells with polarized Numb. Frequencies were determined out of 100 tracked cells for each genotype.

In cells in which the cell fate determinant Numb is polarized, the two daughters depending on the plane of division can inherit Numb equally or unequally (Figure 27a). To assess whether there were any changes in Numb inheritance, we used HSC-enriched cells in which Lis1 was deleted *in vitro.* HSC-enriched cells from control *Lis1*$^{+/+}$; *Rosa-creER* or *Lis1*$^{f/f}$; *Rosa-creER* mice were treated with 4-OH tamoxifen. Following *Lis1* deletion, the cells were stained for Numb and the ratio of symmetric and asymmetric cell divisions was determined. Only cells in late telophase or undergoing cytokinesis were tracked to assess Numb inheritance in incipient daughter cells. Cells either displayed equivalent distribution of low levels of Numb to both daughters (Figure 27b

top, symmetric), or unequal distribution, i.e. higher levels of Numb to one daughter and lower levels to the other (Figure 27b bottom, asymmetric). As shown in Figure 27c, control cells displayed two-fold more symmetric inheritance relative to asymmetric inheritance of Numb. In contrast, the absence of Lis1 led to a complete reversal in the pattern of inheritance with two-fold more cells undergoing asymmetric divisions where one daughter inherited higher levels of Numb. These data suggest HSC division pattern is significantly shifted in the absence of Lis1.

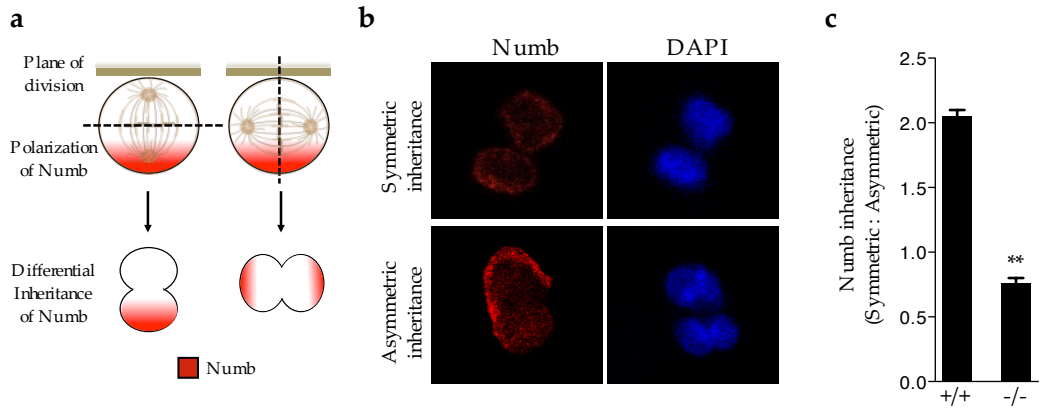

Figure 27: Absence of Lis1 leads to a complete reversal in the pattern of Numb inheritance *in vitro*

Figure 27: a, Model illustrates how two dividing cells may equivalently polarize Numb (shown in red) to one side of the cell, yet direct the cleavage plane in such a way to ensure either equal or unequal inheritance of Numb into the incipient daughter cells. b, Representative image of a tracked cell inheriting Numb symmetrically (top) or asymmetrically (bottom) into incipient daughter cells (Numb in red, DAPI in blue, zoomed 63x images). c, Relative ratios of symmetric:asymmetric division *in vitro*. Data shown are from two independent experiments; n=25-27 dividing cells were assessed for each experiment per cohort; ***p*=0.0022.

We next tested if this shift in division pattern occurred *in vivo*. To test this, we first generated *Lis1* chimeric mice (i.e. wild type microenvironment) by transplanting HSCs (c-Kit^{+} Lin^{-} Sca1^{+} CD150^{+} CD48^{-}) from either control *Lis1*$^{+/+}$; *Rosa-creER* or *Lis1*$^{f/f}$; *Rosa-creER* mice into lethally irradiated mice. Following successful donor repopulation, Lis1 chimeras were treated with tamoxifen to delete *Lis1* specifically in hematopoietic cells. Due to the limited number of telophase HSCs *in vivo* we targeted a less enriched but nonetheless immature lineage-negative (Lin^{-}) population. Thus, *Lis1* null or control Lineage negative (Lin^{-}) cells were isolated from chimeric mice and tracked to assess inheritance of the cell fate determinant Numb in incipient daughter cells (Figure 28a). Consistent with our *in vitro* data, we found that while control cells underwent 3.5 times more symmetric division, the loss of *Lis1* led to a predominance of asymmetry and only rare symmetric division. Remarkably, this shift in pattern led to a seven-fold difference in the ratio of symmetric:asymmetric division between wild type and *Lis1*-deficient cells (Figure 28b,c). Importantly, because the loss of *Lis1* affected the inheritance of Numb but not the polarization of Numb, these data cumulatively suggest that the absence of Lis1 affects inheritance by affecting the cleavage plane, and thus leads to a greater frequency of cells with increased Numb.

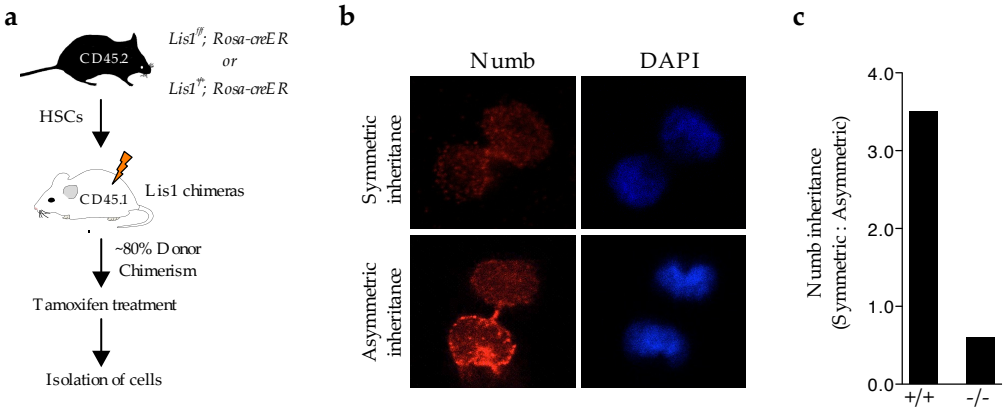

Figure 28: Predominance of Numb asymmetry in the absence of Lis1 *in vivo*.

Figure 28: a, Experimental scheme used to determine Numb inheritance *in vivo.* 1,000 HSCs (KLS CD48^{-} CD150^{+}) from untreated control (*Lis1*$^{+/+}$; *Rosa-creER*) and *Lis1*$^{f/f}$; *Rosa-creER* mice were transplanted into wild type recipients to generate chimeric mice with a wild type microenvironment. Following reconstitution, recipients were treated with tamoxifen and donor-derived lineage negative (Lin^{-}) cells were sorted, fixed and stained to determine Numb inheritance in cells undergoing telophase/cytokinesis. b, Representative image of symmetric (top) and asymmetric (bottom) inheritance of Numb by incipient daughter cells (Numb in red, DAPI in blue, zoomed 63x images). c, Relative ratio of symmetric:asymmetric division *in vivo* (nine dividing cells were assessed for the control (+/+) group; eight dividing cells were assessed for the *Lis1*-deficient (-/-) group. Data analyzed using three independent chimeric mice for each genotype).

5.2.5 Loss of Lis1 leads to spindle positioning defects in HSCs.

To directly test whether the loss of Lis1 led to differences in the plane of division and to define if this may be directed by defects in spindle orientation we developed a strategy to image spindle orientation during cell division in real time. This live imaging method was a modification of a method previously used to visualize the spindle using epithelial cell lines (Toyoshima and Nishida 2007). We first infected HeLa cells with the fusion construct H2B-GFP to mark histones and identify chromosomes during division

and mCherry-α-tubulin to mark the spindle during division and found that we could effectively visualize the spindle during progressive phases of cell division (Day et al. 2009; Kanda et al. 1998) (Figure 29a and Supplementary Movie 1). These cells were plated and imaged; 4 dimensional movies (x,y,z,t) of the dividing cells were visualized from the side to measure the spindle angle relative to the substrate (Figure 29b).

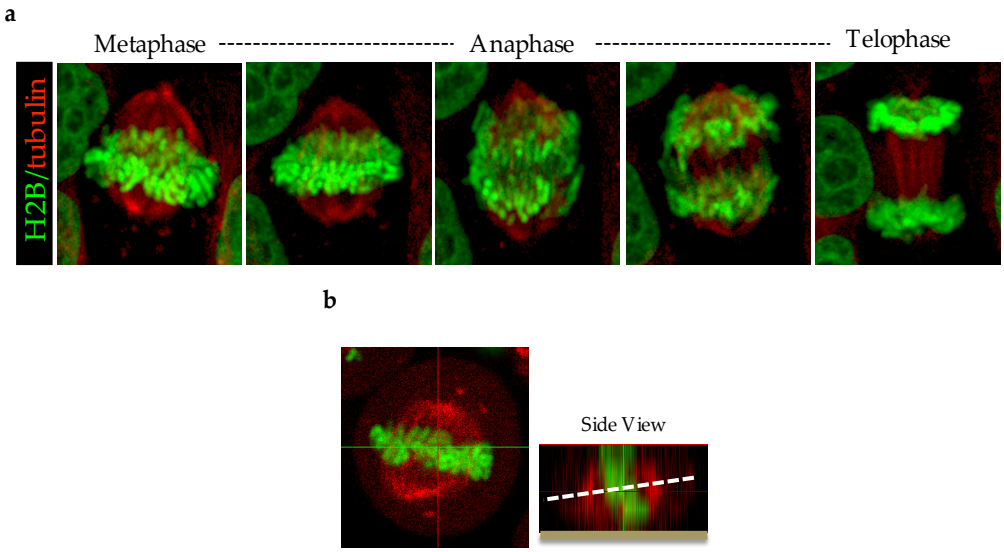

Figure 29: Imaging system permits visualization of mitotic spindle during progressive phases of cell division of HeLa cells

Figure 29: Visualization of a HeLa cell in progressive phases of mitosis in real-time. a, HeLa cells were retrovirally co-infected with H2B-GFP and mCherry-α-tubulin fusion constructs and individual cells tracked during division (corresponding movie shown in Supplementary Movie 1, which is described in Appendix A). b, Representative top view (left) and orthogonal view (right) of a GFP^+ $mCherry^+$ HeLa cell in metaphase. The spindle angle relative to the substrate can be measured by drawing a dotted line that bisects the cell's centrosomes.

Using this approach, we first assessed spindle orientation in the hematopoietic cell line M1. As shown in Figure 30a, these cells were infected with our fusion constructs

and plated on the adherence cue retronectin and their spindle angle relative to the retronectin base was measured over time. Although the cells had a range of spindle angles in metaphase, the spindle always positioned parallel (0-10°) to the substrate as the cells entered telophase, consistent with previous reports (Toyoshima and Nishida 2007) (Figure 30b).

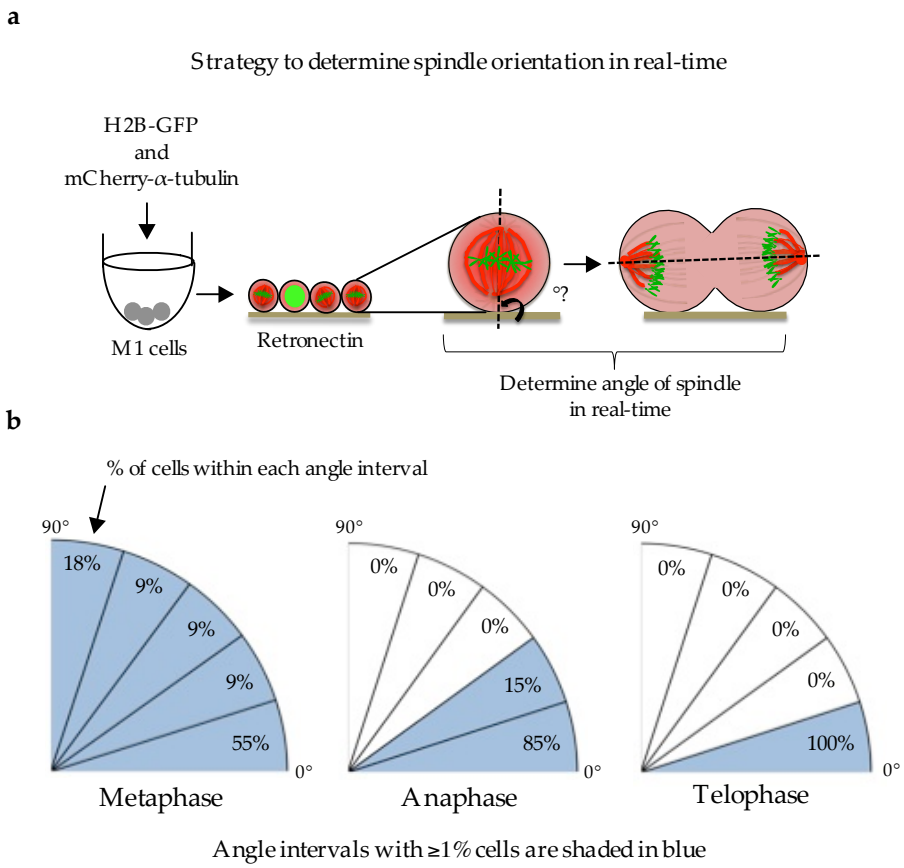

Figure 30: Retronectin directs re-positioning of the mitotic spindle of M1 cells.

Figure 30: a, Experimental scheme used to determine the orientation of the mitotic spindle in M1 cells. M1 cells were co-infected with H2B-GFP and mCherry-α-tubulin fusion constructs and plated on retronectin-coated slides and their spindle angle relative to the retronectin base was measured over time (corresponding movie shown in Supplementary Movie 1 and described in

Appendix A). b, Quantification of spindle orientation in M1 cells relative to the retronectin base. Values are expressed as a percentage of M1 cells within each angle interval. Angle intervals in which >1% cell are present are shaded in blue. Data are shown from three independent experiments; n=20 tracked cells.

The fact that retronectin directed re-positioning of the mitotic spindle allowed us to use this system to test the role of Lis1 in spindle orientation in primary hematopoietic cells. To test this, HSC-enriched cells (c-Kit^{+} Lin^{-} Sca-1^{+}) were isolated from either wild type control *Lis1*$^{+/+}$*; Rosa-creER* or *Lis1*$^{f/f}$*; Rosa-creER* mice and infected with H2B-GFP and mCherry-alpha-tubulin. Re-sorted HSC-enriched cells doubly infected for H2B-GFP and mCherry-alpha-tubulin were plated on retronectin and treated with 4-OH tamoxifen to delete *Lis1* (Figure 31a). Using this approach, we found that wild type HSC-enriched cells displayed a range of angles during metaphase but re-positioned their spindles by telophase (Figure 31b,c). Interestingly, in the absence of Lis1, cells were unable to correctly align their spindle in response to the substrate. These data suggest that loss of Lis1 leads to spindle positioning defects in HSC-enriched cells (Figure 31b,c).

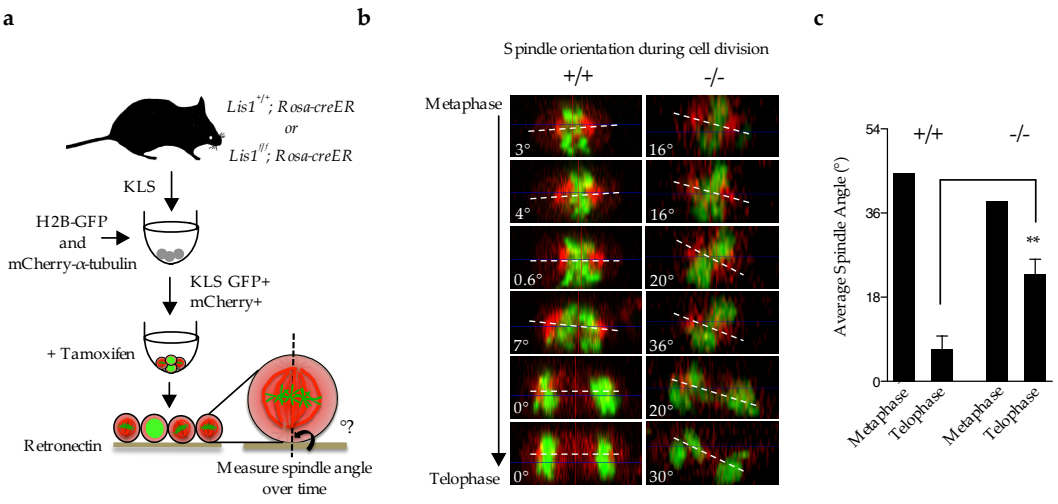

Figure 31: Loss of Lis1 leads to spindle positioning defects in HSC-enriched cells.

Figure 31: a, Experimental scheme used to determine spindle orientation in HSC-enriched cells in real-time. KLS cells were isolated from *Lis1*$^{+/+}$; *Rosa-creER* (control) and *Lis1*$^{f/f}$; *Rosa-creER* mice, infected with H2B-GFP and mCherry-α-tubulin, resorted and treated with 4OH-tamoxifen *in vitro*. Following *Lis1* deletion, cells were placed on retronectin-coated slides and imaged. b, Representative side view images of a control (+/+) and *Lis1*$^{-/-}$ (-/-) cell undergoing cell division and their spindle angles. c, Average metaphase and telophase spindle angles of control (+/+) and (-/-) cells relative to substrate; data shown are from three independent experiments; n=7 cells per genotype; ***p*=0.0054.

5.2.6 Spindle positioning defects drive the improper inheritance of Numb in the absence of Lis1.

To determine whether spindle orientation defects led to improper inheritance of Numb in the absence of Lis1, we tracked the orientation of the spindle coordinately with Numb inheritance in real time. To test this, HSC-enriched cells from either wild type control *Lis1*$^{+/+}$; *Rosa-creER* or *Lis1*$^{f/f}$; *Rosa-creER* mice were infected with mCherry-alpha-tubulin and Numb-CFP fusion vectors, re-sorted, plated in methylcellulose, treated with 4-OH tamoxifen to delete *Lis1* and Numb inheritance was tracked relative to the mitotic

spindle using time lapse microscopy. Of the cells we observed entering mitosis, we focused on those with polarized Numb since changes in the angle of the spindle could have a consequence of whether Numb is inherited asymmetrically or symmetrically only in those cells (i.e. non-polarized cells should invariably under undergo symmetric division regardless of spindle orientation).

An example of a cell with polarized Numb that subsequently aligns its spindle to facilitate a symmetric division, whereby Numb is inherited equally by the two daughter cells is shown in Figure 32. A corresponding time-lapse movie of this cell is shown in Supplementary Movie 2 and described in the Appendix. In addition, examples of cells with polarized Numb that subsequently positions their spindles in such a way to promote an asymmetric division, whereby Numb is inherited unequally by the two incipient daughter cells are shown in Figure 33 and Supplementary Movie 3 and 4 and described in the Appendix. Importantly, because it was extremely technically challenging to live image conditional mutant primary stem and progenitor cells infected with two fusion constructs, only a few cells could be tracked.

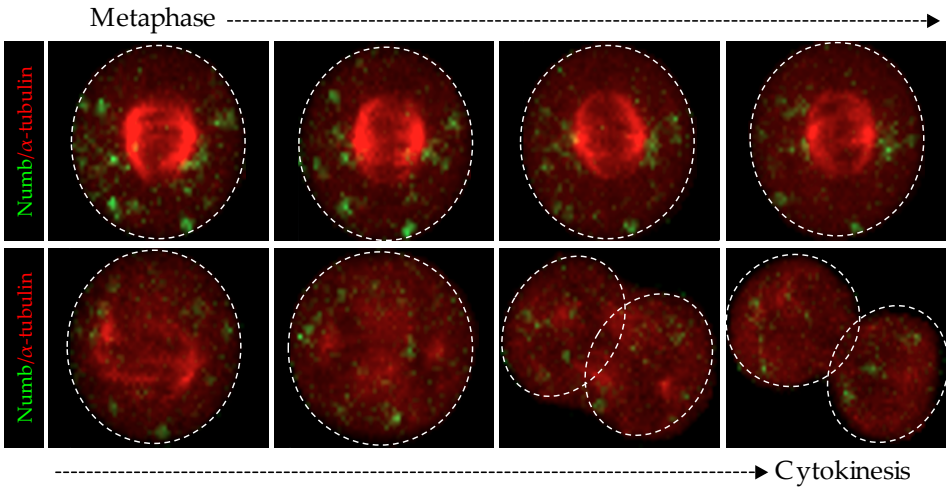

Figure 32: Real time imaging of a cell with polarized Numb subsequently undergoing a symmetric division.

Figure 32: Symmetric inheritance of Numb. HSC-enriched cells (KLS) were co-infected with Numb-CFP and mCherry-α-tubulin fusion construct and imaged overtime. (Numb is shown in green and α-tubulin is shown in red; corresponding movie is shown in Supplementary Movie 2 and described in the Appendix.

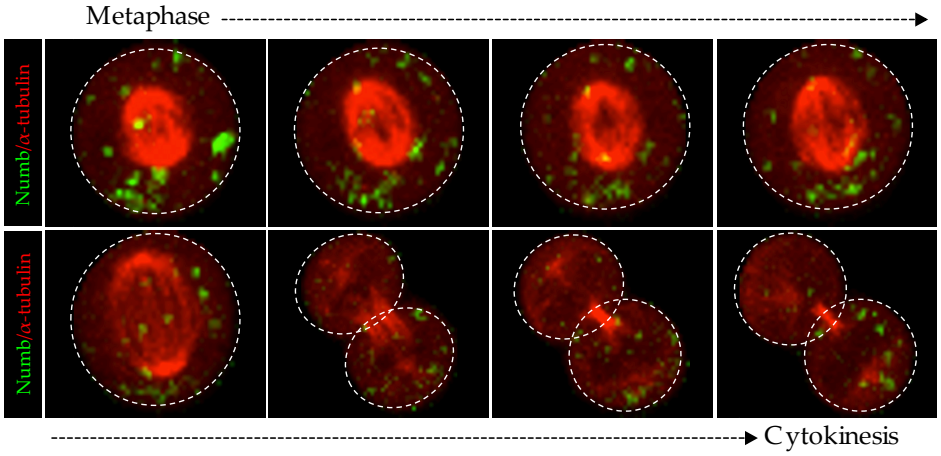

Figure 33: Real time imaging of a cell with polarized Numb subsequently undergoing an asymmetric division.

Figure 33: Asymmetric inheritance of Numb. HSC-enriched cells (KLS) were co-infected with Numb-CFP and mCherry-α-tubulin fusion construct and imaged overtime. (Numb is shown in

green and α-tubulin is shown in red; corresponding movie is shown in Supplementary Movie 3 and described in the Appendix.

Using our time-lapse imaging-based system, we found that the patterns observed were remarkably different between wild type and *Lis1*-deficient cells. While the mitotic spindle was positioned such that Numb was bisected asymmetrically in 56.5% of wild type cells, the mitotic spindle bisected Numb asymmetrically in 100% of Lis1 null cells (Figure 34).

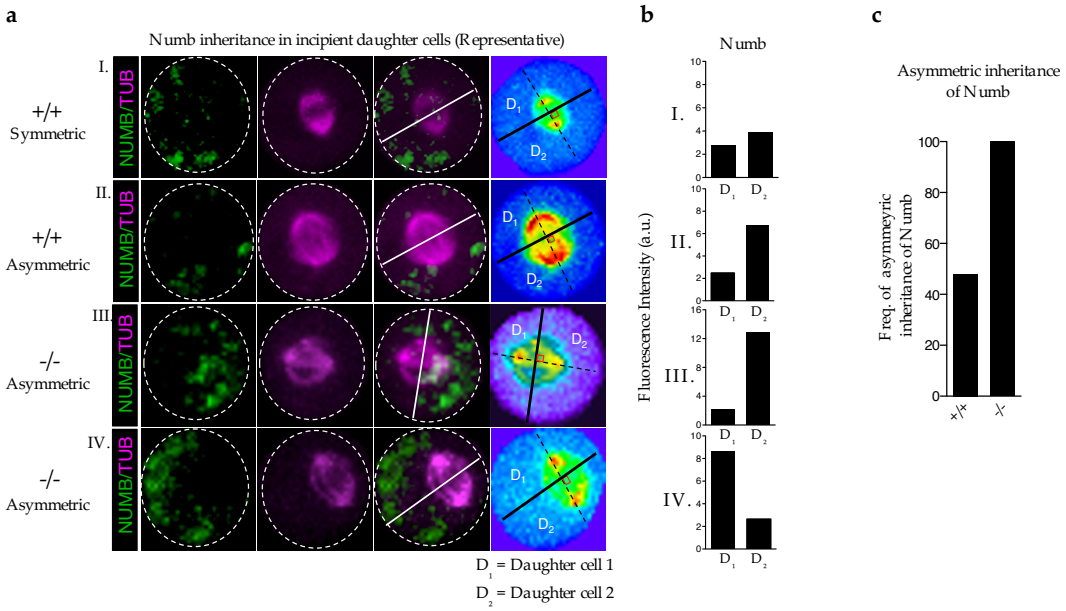

Figure 34: Defective spindle positioning drives increased asymmetric inheritance of Numb in the absence of Lis1.

Figure 34: a, Numb distribution in dividing HSC-enriched cells relative to mitotic spindle orientation. Representative images of control (+/+) cells (I and II) or *Lis1*$^{-/-}$ cells (-/-; III and IV) with examples of symmetric (I) or asymmetric (II, III, IV) inheritance of Numb by incipient daughter cells. Numb (green), α-tubulin (magenta). On far right panel, each cell is displayed in spectrum color format to facilitate accurate identification of spindle position (dotted black line connecting the two centrosomes highlighted in red) and the cleavage furrow (solid lines; white and black)

which partitions the dividing cell into incipient daughter 1 (D_1) and daughter 2 (D_2). b, Quantification of fluorescence intensity of Numb in D_1 and D_2 for each representative control (+/+; I and II) or *Lis1*$^{-/-}$ cell (-/-; III, IV) shown in (a). c, Frequency of cells undergoing asymmetric inheritance of Numb in control (+/+) or *Lis1*-deficient cells (-/-); data are shown for four independent experiments; n=23 for (+/+) and n=5 for (-/-). All error bars show the standard error of mean (SEM).

Thus, the set of *in vivo* and *in vitro* imaging experiments collectively suggest that defective spindle positioning drives the increased asymmetric inheritance of Numb in the absence of Lis1 and identifies a potential mechanism that may underlie, at least in part, the observed accelerated differentiation and subsequent depletion of HSCs.

5.2.7 Loss of Lis1 does not affect spindle morphology, nuclear envelope breakdown or mitotic duration of HSCs.

Although loss of Lis1 affects spindle positioning and orientation, it may also affect other aspects of stem cell function. Because Lis1 is linked to spindle assembly, we tested if *Lis1* deficiency affected bipolar spindle formation, spindle morphology and nuclear envelope breakdown. To determine whether spindle morphology was compromised in the absence of Lis1, we stained *Lis1*-deficient HSCs (c-Kit$^+$ Lin$^-$ Sca-1$^+$ CD48$^-$) for alpha-tubulin and found that bipolar spindle formation and spindle morphology was unaffected in the absence of Lis1 (Figure 35).

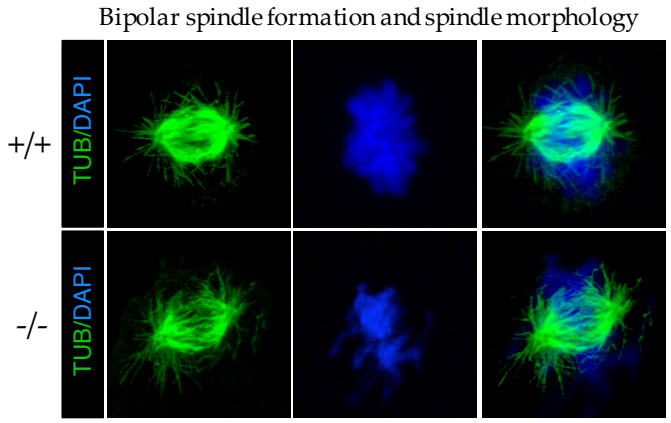

Figure 35: Formation of bipolar spindles and spindle morphology is unaffected in the absence of Lis1.

Figure 35: Bipolar spindle formation and spindle morphology of *Lis1*$^{-/-}$ cells. HSCs (KLS CD48^{-}) were isolated from control (*Lis1*$^{+/+}$*; Rosa-creER*) and *Lis1*$^{f/f}$*; Rosa-creER* mice and treated with 4-OH-tamoxifen *in vitro*. Representative images of control (+/+) and *Lis1*$^{-/-}$ (-/-) cells immunostained for anti-α-tubulin antibody (green) and 4′, 6-diamidino-2-phenylindole (DAPI, blue).

Further, we tracked mitotic events in HSC-enriched cells (c-Kit^{+} Lin^{-} Sca-1^{+}; KLS) through dynamic real time imaging. Specifically, KLS cells were isolated from either control *Lis1*$^{+/+}$*; Rosa-creER* or *Lis1*$^{f/f}$*; Rosa-creER* mice and co-infected with H2B-GFP and mCherry-alpha-tubulin. Sorted KLS GFP^{+} mCherry^{+} cells were treated with 4OH-tamoxifen to delete *Lis1* and subsequently tracked to determine if nuclear envelope disassembly was intact (Figure 36a). Using H2B-GFP to label chromatin, we found that in all *Lis1*-deficient cells tested, nuclear shrinking/chromosome condensation occurred normally (Figure 36b), which has previously been reported to coincide with and/or occur rapidly after nuclear envelope breakdown (NEBD) (Beaudouin et al. 2002), suggesting that NEBD is intact in the absence of Lis1.

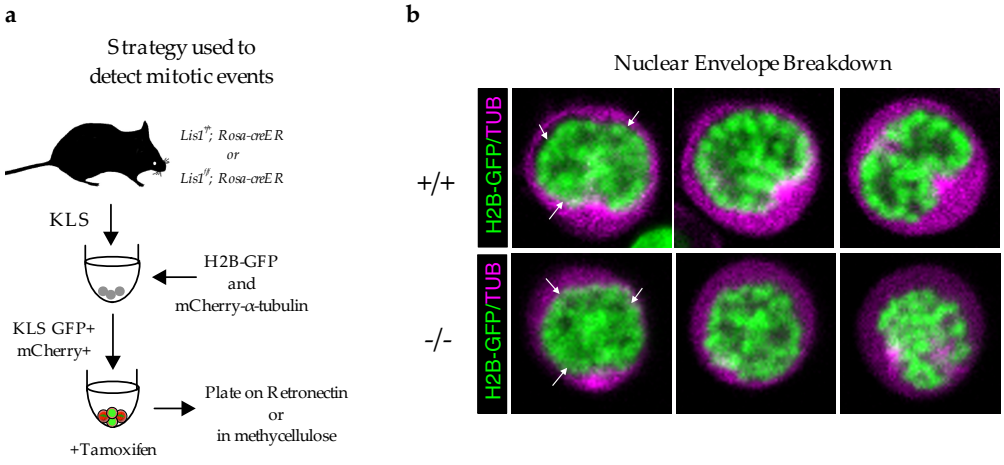

Figure 36: Nuclear envelope breakdown is intact in the absence of Lis1.

Figure 36: a, Schematic illustrates the strategy used to visualize cell division in real-time. KLS cells were isolated from *Lis1*$^{+/+}$*; Rosa-creER* (control) and *Lis1*$^{f/f}$*; Rosa-creER* mice, retrovirally infected with H2B-GFP and mCherry-α-tubulin, resorted and treated with 4-OH-tamoxifen *in vitro*. Following *Lis1* deletion, cells were placed on retronectin-coated slides or in methylcellulose and imaged. b, Representative images of a control (+/+) and *Lis1*$^{-/-}$ (-/-) cell undergoing nuclear envelope breakdown/chromosome condensation. H2B (green), α-tubulin (magenta). White arrows indicate NEB; n=18 for +/+ and n=14 for -/-.

To determine whether loss of Lis1 affected the length of mitosis, we quantified mitotic duration of dividing cells identified in movie replay by measuring the average time spent between NEBD and chromosome condensation until the beginning of telophase and found that duration of mitosis was relatively similar between *Lis1*-deficient cells and wild type control cells. However, there was a marginal rise in mitosis length in the *Lis1* null cells, but this was not significant (Figure 37).

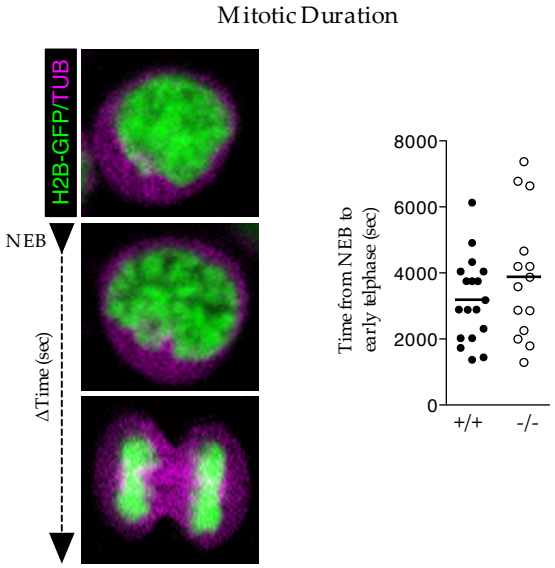

Figure 37: Loss of Lis1 does not affect the mitotic length of HSCs.

Figure 37: Duration of mitosis of *Lis1*$^{-/-}$ cells. Representative images of a *Lis1*$^{-/-}$ cell at the onset of NEB and at early telophase. H2B (green) and α-tubulin (magenta). Graph on right shows quantification of duration of mitosis (time in seconds from NEB to early telophase); n=18 tracked control (+/+) cells and n=14 tracked *Lis1*$^{-/-}$ (-/-) cells.

5.2.8 Marginal increases in the frequency of polyploidy and cells undergoing abnormal mitosis in the absence of Lis1.

To determine whether the loss of Lis1 leads to abnormal mitoses, we scored the frequency of cells that underwent an incomplete mitosis, defined by a cell that compacted its chromatin but failed to complete division, and found that over an initial 48 hour period, ~3% (2/66) of wild type cells and ~1.5% (1/67) of *Lis1*-deficient cells underwent incomplete mitosis, and during the next 24 hours, 8.7% (2/23) of *Lis1*-deficient cells underwent incomplete mitosis (Figure 38). Multipolar cell division (defined by the segregation of chromosomes to three poles during anaphase and the

subsequent generation of three aneuploid daughter cells) were also scored: while no apparent multipolar cell divisions were observed in control, ~3% (2/67) and 8.7% (2/23) of *Lis1*-deficient cells underwent multipolar cell division at 48 and 72 hours respectfully (Figure 38).

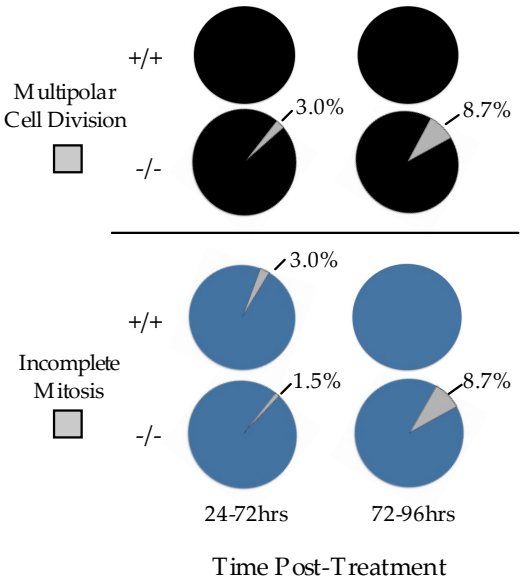

Figure 38: Loss of Lis1 in HSCs leads to a rise in the number of cells with abnormal mitosis.

Figure 38: Percentage of control (+/+) and *Lis1*$^{-/-}$ (-/-) cells that underwent a multipolar cell division or an incomplete mitosis. (n=67 cells per genotype tracked between 24-72 hrs and n=23 cells per genotype tracked between 72-96 hrs).

We also carried out a cytogenetic analysis on G-banded HSC-enriched (c-Kit^{+} Lin^{-} Sca-1^{+}) metaphase cells after *in vitro* deletion of *Lis1* and found that *Lis1*-deficient cells demonstrated an apparent normal karyotype. However, whereas ~6% (3/50) of wild type cells were polyploid, 14% (7/50) of *Lis1*-deficient cells were polyploid (Figure 39).

Collectively, these data suggest that a potential consequence of loss of Lis1 in cultured HSCs may be the acquisition of polyploidy or aneuploidy Although compared to wild type control cells, *Lis1*-deficient cells display more mitotic defects, these events are not very dominant. However, they could cumulatively be compounding the differentiation/spindle orientation defects and thus, contribute to the overall blood phenotype observed.

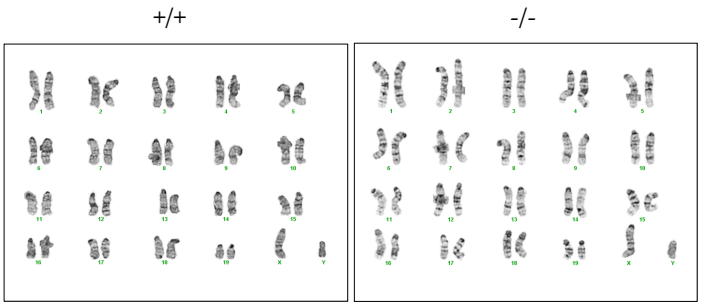

	Normal Karyotype (40, XY)	Freq. of Polyploidy
+/+	100% (14/14)	6% (3/50)
-/-	100% (16/16)	14% (7/50)

Figure 39: Elevated frequency of polyploidy in HSCs in the absence of Lis1.

Figure 39: Karyotype of *Lis1*$^{-/-}$ cells. Representative G-banded karyogram of a control (+/+) and *Lis1*$^{-/-}$ (-/-) cell (top) and table showing the percent of (+/+) and (-/-) cells with normal karyotypes and the frequency of polyploidy (bottom).

5.2.9 Loss of the "stem cell signature" is a key downstream consequence of *Lis1* deletion.

To provide molecular insight into how Lis1 operates and in particular to examine genes that have been identified to affect HSC self-renewal, we carried out a genome wide expression analysis on wild type and *Lis1*-deficient HSC-enriched cells.

Specifically, wild type control *Lis1*$^{+/+}$; *Rosa-creER* and *Lis1*$^{f/f}$; *Rosa-creER* mice were administered tamoxifen daily for five consecutive days and three days post-tamoxifen treatment, HSC-enriched cells (c-kit+ Lin- Sca-1^{+}) were FACS-sorted and total cellular RNA were purified. Comparison of transcriptional profiles of the wild type and *Lis1*-deficient cells led to the identification of 746 down-regulated and 622 up-regulated gene sets at significance level (false discovery rate) of 0.01 as affected by the loss of Lis1 (Figure 40a). While some stem cell-related genes such as *Runx1*, *Msi2* and *Bmi1* do not appear to be changed significantly other genes known to play important regulatory roles in hematopoietic stem/progenitor cell maintenance and differentiation such as *Pim1*, *Socs3*, *Trib2* and *Pml* are altered and may mediate downstream effects of Lis1 (Figure 38e).

Interestingly, the differentially expressed gene sets that were affected by the loss of Lis1 revealed significant enrichment of multiple stem-associated gene expression profiles identified (Figure 40b-d) (Wong et al. 2008) (Venezia et al. 2004) (Eppert et al. 2011). That loss of the stem cell signature is a key downstream consequence of *Lis1* deletion confirms, through an independent molecular strategy, that Lis1 is critical to maintaining the stem cell fate.

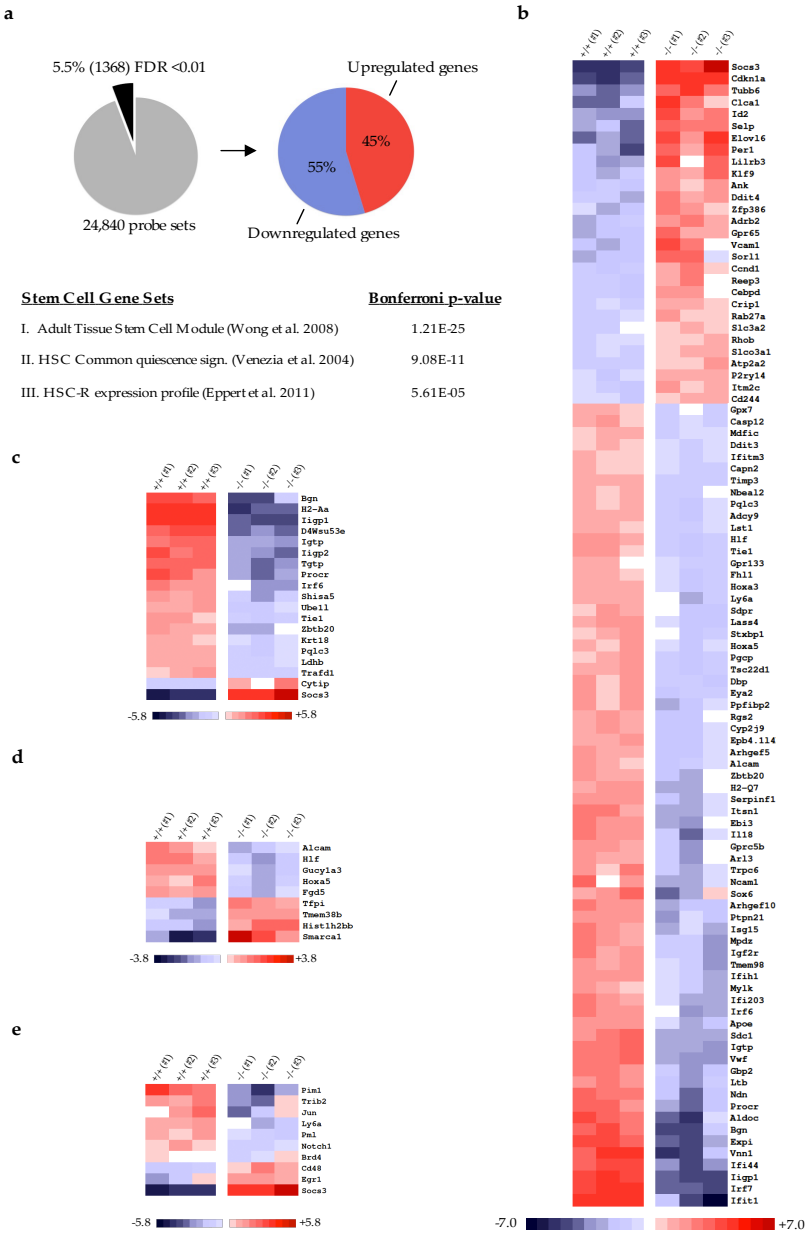

Figure 40: Loss of the "stem cell gene signature" is a key consequence of *Lis1* deletion.

Figure 40: a-e, Genome wide expression analysis of *Lis1*-deficient HSC-enriched cells. Control (*Lis1*$^{+/+}$; *Rosa-creER*) and *Lis1*$^{f/f}$; *Rosa-creER* mice were treated with tamoxifen daily for 5 days. KLS cells were isolated from control and Lis1 null mice 3 days post-tamoxifen treatment and microarray analysis was performed (3 independent RNA samples were used for each genotype, each sample was prepared from cells isolated from 2-3 mice, total of 12-18 mice analyzed). a,

Comparative gene set enrichment analysis identified 5.5% of genes as changed with a false discovery rate of <0.01; 746 probe sets were down-regulated and 622 probe sets were up-regulated. b-d, Significant differential expression of mRNAs identified previously as part of a stem cell-associated gene signature. Heat map showing expression changes in mRNAs highly enriched in (b), Adult Tissue Stem Cell Module (FDR <-0.01) (Wong et al. 2008); Bonferroni *p*-value=1.25E-25, (c), HSC-Common quiescence signature (Venezia et al. 2004); Bonferroni *p*-value=9.08E-11, (d), HSC-R expression profile (Eppert et al. 2011); Bonferroni *p*-value=5.61E-05 in the *Lis1*-deficient HSC-enriched cells. e, Heat map of known regulators of stem cell and progenitor cell activity significantly affected by the loss of *Lis1*.

5.3 Discussion

Using two independent strategies to direct the genetic deletion of *Lis1* in the hematopoietic system, we showed that the dynein-binding protein Lis1 not only has a broad impact on HSC function at multiple sites during embryogenesis, but also has a conserved functional role in the adult blood system. We report here that the basis of the HSC defects (i.e. HSC depletion and impaired self-renewal ability *in vitro* and *in vivo*) that arise following *Lis1* deletion is largely due to a loss of cell fate control. Specifically, by tracking the rate of differentiation *in vitro*, we found that *Lis1*-deficient HSCs fail to maintain the undifferentiated state and prematurely differentiate predominantly into early myeloid progenitor cells. This accelerated differentiation phenotype was also apparent *in vivo*, where we found that the loss of Lis1 initially leads to a drop in HSCs with a concomitant rise in multipotent progenitor cells. Importantly, we show that the loss of HSCs that occurs immediately following *Lis1* deletion was not due to elevated apoptosis or alterations in cell cycle. Although at later time points we did find some

increase in AnnexinV$^+$ 7AAD$^+$ necrotic/late stage apoptotic cells, it is difficult to know if this may be a consequence of increased differentiation, or an independent event.

Interestingly, we found that the inability of *Lis1*-deficient HSCs to maintain the undifferentiated state is due to an underlying defect in the regulation of HSC division pattern. In previous studies where we used transgenic notch reporter mice and time-lapse microscopy to trace cell division, we showed that HSCs have the ability to undergo both symmetric and asymmetric cell division (Wu et al. 2007). Importantly, we found that during an asymmetric division, the cell fate determinant Numb is selectively partitioned into the differentiated hematopoietic daughter cell and thus, the pattern of Numb inheritance could be used to code a division as either symmetric or asymmetric.

With this approach, we found that HSCs preferentially undergo symmetric renewal division. Although it is more commonly thought that under homeostatic conditions, HSCs predominantly undergo asymmetric division; a division mode that favors maintenance over expansion, the observation that HSCs underwent more symmetric renewal divisions suggest that experimental conditions (i.e. culturing conditions) could have unintentionally shifted the balance. Interestingly, we found that both *in vitro* and *in vivo* loss of Lis1 leads to a predominance of asymmetry and only rare symmetric renewal divisions. Since perpetual asymmetric divisions compared to either a balance of asymmetric and symmetric division or perpetual symmetric renewal divisions would generate more differentiated cells overtime, the increase in asymmetric

division observed following the loss of Lis1 provides a possible explanation for the accelerated differentiation of HSCs that occurs in the absence of Lis1.

Previous studies demonstrated that the cell fate determinant Numb induces differentiation by inhibiting Notch signaling, most likely by controlling the intracellular trafficking of Notch intermediates (Berdnik et al. 2002). Interestingly, we found that changes in Numb inheritance following *Lis1* deletion affected Notch signaling. Specifically, genome wide expression and gene set enrichment analysis on RNA samples isolated from wild type or *Lis1*-deficient HSC-enriched cells indicated a marked downregulation of the Notch receptor *Notch1* and the Notch1 target gene *Trib2*, suggesting potential repression of Notch signaling in the absence of Lis1. In addition to changes in Trib2 expression, the promyelocytic leukemia gene *Pml* was also significantly downregulated following *Lis1* deletion. Loss of both of these genes have been linked to increased differentiation and may be part of the downstream mechanisms that sets into motion the accelerated differentiation we observe (Ito et al. 2012; Keeshan et al. 2006).

In *Drosophila* neuroblasts, vertebrate skin progenitor cells and mammalian neuroepithelial stem cells, it has been documented that precise positioning of the mitotic spindle is one of several mechanisms, which concur to facilitate the regulation of cell fate (reviewed in (Morin and Bellaiche 2011)). The fact that upon *Lis1* deletion, Numb inheritance is altered and not polarization, suggest that the spindle-directed cleavage plane is affected in the absence of Lis1. Using a sophisticated real time imaging system,

we were able to visualize the mitotic spindle in HSCs during progressive phases of cell division and show that in the absence of Lis1, HSCs fail to undergo rectronectin-directed spindle positioning, suggesting an inability of *Lis1*-deficient HSCs to properly regulate spindle orientation in response to either cell-extrinsic or cell-intrinsic cues. In the hematopoietic system, and in several other systems, whether spindle orientation has a direct instructive role on cell fate specification is still unclear, because none of the reports in which spindle orientation is misoriented has adequately addressed the distribution of fate determinants. In this study, using a live imaging approach, we were able to track spindle orientation coordinately with Numb inheritance and show that changes in spindle orientation triggered by Lis1 loss ultimately affected how the pool of polarized Numb was fractioned and subsequently inherited by the incipient daughter cells. These data convincingly demonstrate Lis1 influences HSC function by regulating HSC division pattern at the level of controlling spindle orientation.

A role for Lis1 in spindle orientation and positioning has been demonstrated in the budding yeast *Saccharomyces cerevisiae* (Lee et al. 2003), *C. elegans* (Cockell et al. 2004), *Drosophila* neuroblasts (Siller and Doe 2008a), in cultured epithelial cells (Faulkner et al. 2000) and in the mammalian neuroepithelium (Yingling et al. 2008). Studies primarily in invertebrate systems have elucidated a model in which a cascade of protein interactions involving heterotrimeric G proteins, Pins/AGS3 and Mud/NuMA establish a docking site for astral microtubules to orient the mitotic spindle. The Lis1/dynein complex

facilitates the interaction between proteins concentrated at the cell cortex and astral microtubules (reviewed in (Knoblich 2008). Future work will need to be done to determine whether this established framework on how spindle orientation is regulated is conserved in the mammalian hematopoietic system.

6. Lis1 is a key regulator of malignant hematopoietic development.

6.1 Introduction

While properly controlled self-renewal is a key feature of normal stem cell maintenance, aberrant and uncontrolled self-renewal can be a hallmark of oncogenesis. One important question that remains unaddressed is whether regulators of spindle orientation and division plane can drive aberrant self-renewal in cancer. This may be particular relevant for understanding cancers that become increasingly undifferentiated during progression, since division can shift towards symmetric renewal in order to generate immature daughters, and contribute to the failure of differentiation.

In the hematopoietic system, acute phase myeloid leukemias such as blast crisis chronic myelogenous leukemia (bcCML) and *de novo* acute myelogenous leukemia (AML) display a severe differentiation blockade. In context of bCML progression, recently we showed that *NUP98-HOXA9*, a chromosomal translocation product implicated in bcCML and *de novo* AML, promotes leukemia by shifting the normal balance of asymmetric and symmetric cell division towards more symmetric renewal divisions. Since Lis1 may control normal HSC activity by regulating division pattern, the ability of *NUP98-HOXA9* to subvert the normal balance of asymmetric and symmetric division may depend on Lis1 function. Thus using bcCML and AML as models we tested if Lis1 plays a role in cancer.

6.2 Results

6.2.1 Lis1 is required for the establishment, maintenance and propagation of blast crisis chronic myelogenous leukemia (bcCML).

To determine if Lis1 plays a role in bcCML, we modeled the disease in the mouse by employing a "2-hit" retroviral-based system. Previous studies showed that the delivery of the translocation product *NUP98-HOXA9* together with *BCR-ABL* leads to the development of a disease characterized by arrested differentiation and accumulation of immature myeloid cells and thus, faithfully recapitulates human bcCML (Dash et al. 2002; Mayotte et al. 2002; Neering et al. 2007). Thus, to generate bcCML, HSC-enriched cells (c-Kit$^+$ Lin$^-$ Sca-1$^+$) from *Lis1*$^{+/+}$*; Rosa-creER* or *Lis1*$^{f/f}$; *Rosa-creER* mice were co-infected with *BCR-ABL* and *NUP98-HOXA9* and transplanted into sub-lethally irradiated mice. Three days post-transplantation, recipients were given tamoxifen or corn oil daily for 5 days to delete *Lis1* specifically in the cells driving leukemia development *in vivo*. Whereas tamoxifen-treated mice transplanted with control *BCR-ABL*/*NUP98-HOXA9*-infeced cells all succumbed to bcCML, only 22% of the tamoxifen treated mice transplanted with *Lis1*$^{f/f}$*; Rosa-creER BCR-ABL*/*NUP98-HOXA9*-infected cells developed leukemia. (Figure 41). These data suggest that Lis1 is required for the propagation of bcCML *in vivo*.

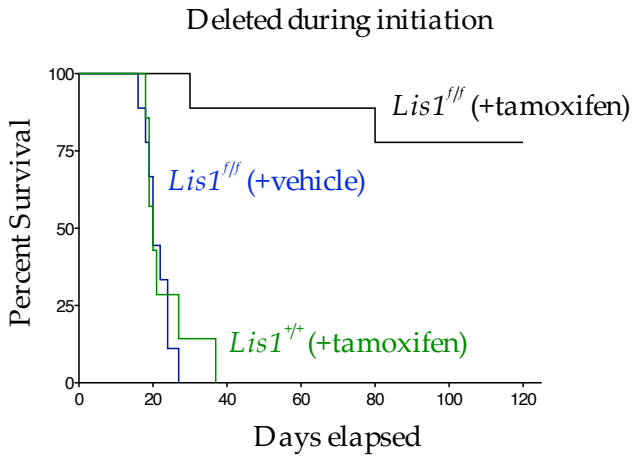

Figure 41: Lis1 is required for the propagation of bcCML *in vivo*.

Figure 41: Impact of loss of Lis1 on bcCML initiation. KLS cells were isolated from control (*Lis1*$^{+/+}$*; Rosa-creER*) and *Lis1*$^{f/f}$*; Rosa-creER* mice and co-transduced with BCR-ABL-YFP and NUP98-HOXA9-GFP; 500 double positive cells transplanted into recipients. Three days post-transplantation, recipients were administered tamoxifen or vehicle (corn oil) daily for 5 days and survival monitored. Data shown are from three independent experiments (n=10 for *Lis1*$^{f/f}$ +tamoxifen (black), n=9 for *Lis1*$^{f/f}$ +vehicle (corn oil) (blue) and n=7 for *Lis1*$^{+/+}$ +tamoxifen (green)).

The ability to temporally control *Lis1* deletion allowed us to delete *Lis1* after disease establishment and thus test whether Lis1 is required for the continual maintenance of bcCML. We first tested whether colony-forming ability of established leukemia cells was impaired in the absence of Lis1. To do this, established bcCML cells negative for lineage markers (bcCML-propagating cells) and harboring a *Lis1*$^{f/f}$ allele were plated in methylcellulose and treated with 4OH-tamoxifen to delete *Lis1.* Whereas control cells successfully formed colonies, deletion of *Lis1* lead to a 5.5 fold reduction in colony formation (Figure 42a).

To determine whether the loss of Lis1 affects the propagation and maintenance of bcCML *in vivo*, established bcCML-propagating cells with a *Lis1*$^{f/f}$ allele were transplanted into sub-lethally irradiated mice. Seven days post-transplantation, recipient mice were treated with tamoxifen. Whereas all the mice transplanted with control leukemia-propagating cells succumbed to leukemia, none of the mice transplanted with floxed *Lis1* cells developed leukemia (Figure 42b).

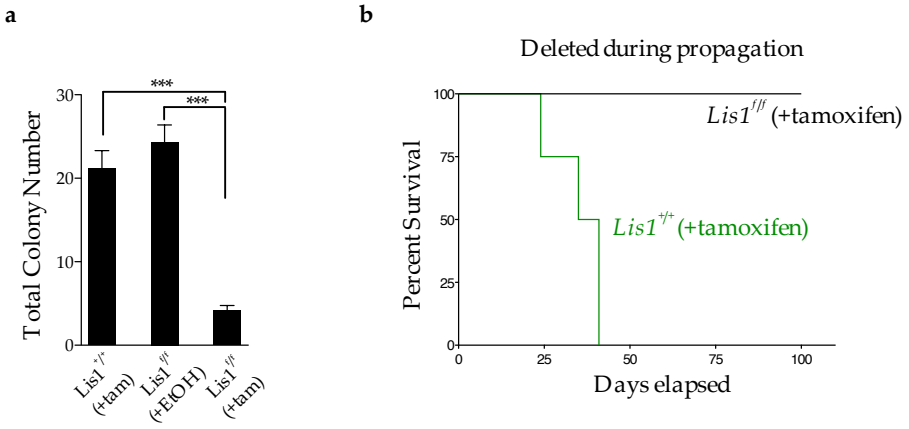

Figure 42: Lis1 is important for the maintenance and propagation of bcCML.

Figure 42: a, Impact of loss of *Lis1* on colony-forming ability of established bcCML cells. 3-5,000 lineage-negative (Lin$^-$) cells from control *Lis1*$^{+/+}$*; Rosa-creER* or *Lis1*$^{f/f}$*; Rosa-creER* bcCML were plated in methylcellulose and treated with either 4-OH-tamoxifen or ethanol (EtOH) *in vitro* and total colonies generated were scored, ***p<0.001. b, Impact of loss of *Lis1* on propagation of established bcCML. 1,000 Lin-negative cells from established control *Lis1*$^{+/+}$*creER* or *Lis1*$^{f/f}$*creER* bcCML were transplanted into secondary recipients. Seven days post-transplantation, recipients were administered tamoxifen daily for 5 days and survival monitored (n=4 for *Lis1*$^{+/+}$, green and n=3 for Lis1$^{f/f}$, black).

Interestingly, detailed tracking of tumor growth *in vivo* indicated that deletion of *Lis1* well after the tumor burden had begun to climb allowed complete reversion to normal cell counts. Specifically, whereas tumor burden on average increased 4.7-fold in control mice, tumor burden in mice that received *Lis1* floxed leukemia cells decreased 3.4-fold during a 10 day period following the start of tamoxifen injections (Figure 43a). Important, this reversion to normal cell counts was accompanied by a resolution of splenomegaly (Figure 43b).

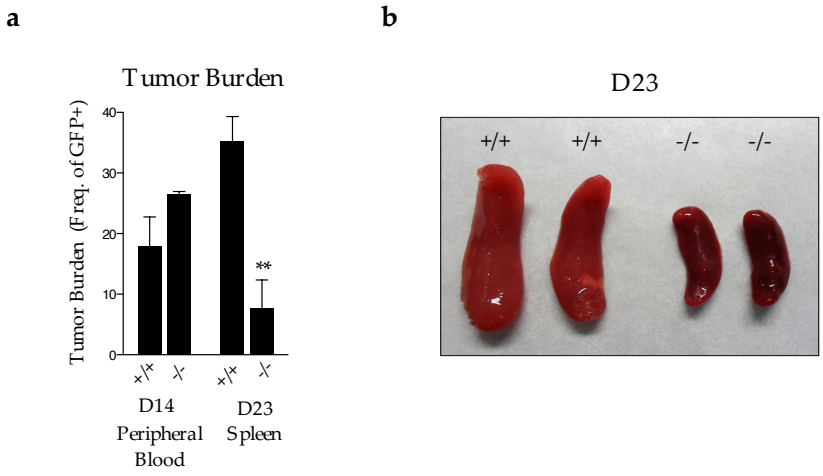

Figure 43: Resolution of disease following *Lis1* deletion.

Figure 43: a, Average tumor burden was tracked before and after tamoxifen delivery. 40,000 lineage-negative (Lin^-) cells from control *Lis1*$^{+/+}$*; Rosa-creER* or *Lis1*$^{f/f}$*; Rosa-creER* established bcCML were transplanted into secondary recipients. Tumor burden was assessed in the peripheral blood at day 14 (D14) post-transplantation before the start of tamoxifen injections (daily for 5 days; D14 to D18) and again 5 days post-tamoxifen injections on day 23 (D23) in the spleen of mice that received wild type control bcCML (+/+) or *Lis1*$^{f/f}$ bcCML (-/-); n=4 for control (+/+) and n=3 for (-/-) mice; $^{**}p$=0.0065. b, Representative image shows control (+/+) and (-/-) spleens 5 days post-tamoxifen treatment.

Collectively, these data strongly indicate that Lis1 is critically important not only for the establishment but also for the continual maintenance and propagation of bcCML *in vivo*.

6.2.2 Lis1 is required for the establishment of *de novo* acute myelogenous leukemia (AML) *in vivo*.

Both blast crisis phase CML and the majority of *de novo* AML share similar disease characteristics such as an aggressive growth of immature cells and reduced differentiation. Therefore, it is possible that *de novo* AML also depends on Lis1 function. To determine whether Lis1 is required for the development of AML, we took advantage of a previously established mouse model of AML induced by co-expression of human mixed-lineage leukemia fusion gene (MLL-AF9; also known as MLLT3) and constitutively active NRAS ($NRAS^{G12V}$) (Zuber et al. 2009). HSC-enriched cells isolated from either untreated *Lis1$^{f/f}$; Rosa-creER* or *Lis1$^{+/+}$; Rosa-creER* control mice were retrovirally co-infected with MLL-AF9 and $NRAS^{G12V}$ and subsequently transplanted into sub-lethally irradiated recipients. Seven days post-transplantation, recipient mice were administered tamoxifen or corn oil daily for 5 days. While all control mice died of leukemia within 3 weeks, only ~40% of mice transplanted with floxed *Lis1* cells developed AML, and those that did exhibited a longer disease latency (Figure 44). These data show that Lis1 is important for the establishment of MLL-AF9-induced AML *in vivo*.

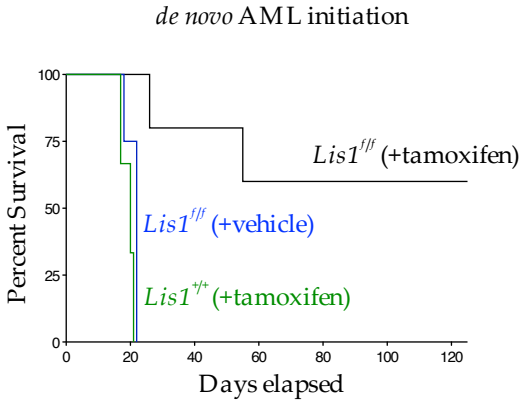

Figure 44: Loss of Lis1 impairs establishment of *de novo* AML *in vivo*.

Figure 44: Impact of loss of *Lis1* on *de novo* AML. KLS cells were isolated from control (*Lis1*$^{+/+}$; *Rosa-creER*) and *Lis1*$^{f/f}$; *Rosa-creER* mice and co-transduced with MLL-AF9-GFP and NRAS^{G12V}-YFP and 120,000 cells were transplanted into recipients. Seven days post-transplantation, recipients were administered either tamoxifen or corn oil daily for 5 days and survival was monitored. Data shown are from two experiments (n=5 for *Lis1*$^{f/f}$ +tamoxifen (black), n=4 for *Lis1*$^{f/f}$ +vehicle (corn oil) (blue) and n=3 for *Lis1*$^{+/+}$ +tamoxifen (green)).

6.2.3 Lis1 plays a critical role in maintaining the undifferentiated state of leukemia cells.

To understand the cellular and molecular impact of *Lis1* deletion on leukemogenesis, we used the bcCML model and specifically determined if the *in vivo* loss of Lis1 leads to accelerated differentiation, impairs proliferation and/or triggers cell death of leukemia cells. To test this, established bcCML cells with *Lis1*$^{f/f}$ alleles were transplanted into secondary recipients. Fourteen days post-transplantation, recipient mice were given tamoxifen daily for 5 days. Interestingly, one day post-tamoxifen treatment, the most notable and immediate impact of *Lis1* deletion was a 5-fold increase in differentiated leukemic cells (Figure 45a,b). This accelerated differentiation of

leukemia cells following *Lis1* deletion was accompanied by a rise in Numb levels (Figure 45c,d). Thus, similar to Lis1's role in normal HSC activity, Lis1 plays a critical role in maintaining the undifferentiated state of leukemia cells.

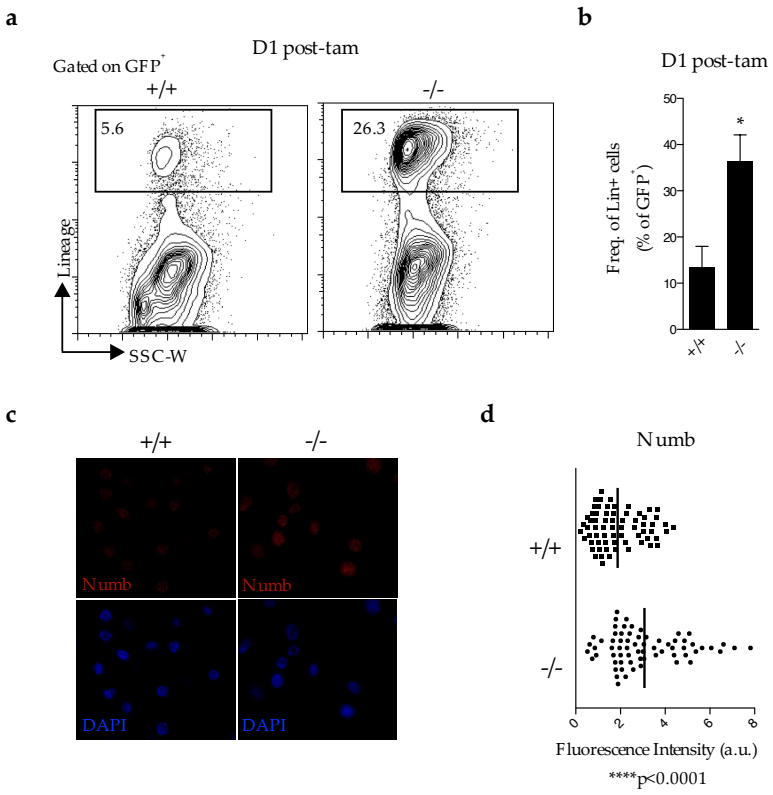

Figure 45: Accelerated differentiation of leukemia cells and enhanced Numb levels following *Lis1* deletion.

Figure 45: a, Representative FACS plots show frequency of bcCML cells expressing lineage markers in control (+/+) or *Lis1*-deficient (-/-) populations 1 day post-tamoxifen treatment. b, Average frequency of bcCML cells expressing lineage markers (Lin^+). Data shown are from two independent experiments (n=4 for +/+ and n=6 for -/-, **p*=0.0204). c, Representative image shows control (+/+) and (-/-) leukemia cells stained with anti-Numb antibody (red) and DAPI (blue), 63X. d, Average fluorescence intensity of Numb in individual bcCML cells (n=67 cells each, ****p*<0.0001).

6.2.4 Impaired proliferation and late onset death of *Lis1*-deficient leukemia cells.

To determine whether *Lis1*-deficient leukemia cells not only prematurely differentiate but also have an impaired proliferative ability, we performed *in vivo* BrdU incorporation assays. Specifically, established bcCML cells carrying *Lis1* floxed alleles were transplanted into recipient mice. Fourteen days post-transplantation, recipient mice were given tamoxifen daily for 5 days. On the last day of tamoxifen treatment, mice were administered BrdU and following an 18-hour chase period leukemia cells were analyzed. No difference in proliferation was observed between the immature (lineage negative; Lin^-) and mature (lineage positive; Lin^+) compartments (Figure 46b-d). These data suggest that the increase in differentiated leukemia cells observed following *Lis1* deletion is not due to a preferential proliferation defect of immature cells. However, as shown in Figure 46a-c, Lis1 loss led to a slight 1.5-fold reduction in proliferation in both cell compartments; thus the differentiation and proliferation defect may act in concert to lead to the deep defects observed in leukemogenesis.

To determine whether the loss of Lis1 in bCML cells resulted in an increase in cell death we stained cells for AnnexinV and found that consistent with what was observed in normal hematopoiesis, the loss of Lis1 did not lead to any significant defects in apoptosis at early time points (Figure 46e). However, the loss of Lis1 did lead to a two-fold increase in apoptosis in conjugation with a more pronounced impairment of

proliferation at later time points. Specifically, when cell death and BrdU incorporation assays were conducted 5 days post-tamoxifen, we found that *Lis1*-deficient bcCML lineage negative cells display an ~3-fold reduction in BrdU incorporation and a concomitant ~2-fold increase in the percentage of cells positive for AnnexinV (Figure 46f-h). Collectively, these data suggest that the loss of Lis1 prevents bcCML-propagating cells from establishing and maintaining the disease state initially by triggering their premature differentiation and subsequently halting their robust proliferative capacity and inducing their late-onset death.

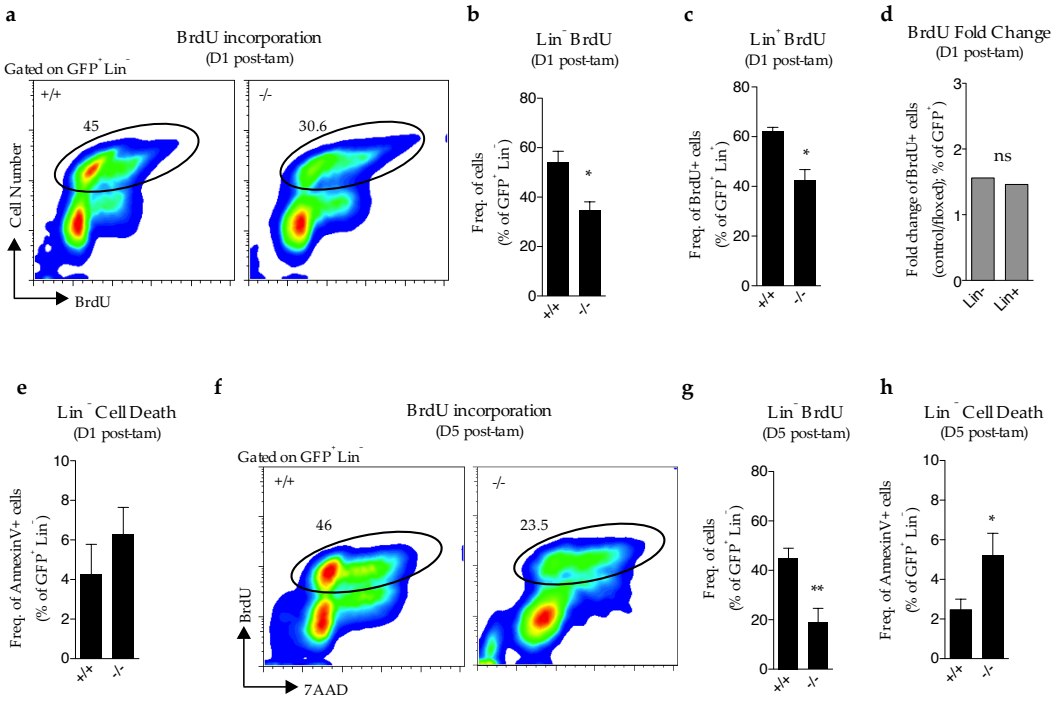

Figure 46: Impaired proliferation and late onset death of leukemia cells in the absence of Lis1.

Figure 46: Impact of loss of *Lis1* on the growth and survival of bcCML cells. 40,000 lineage-negative (Lin^-) cells from established control $Lis1^{+/+}$; *Rosa-creER* or $Lis1^{f/f}$; *Rosa-creER* bcCML were transplanted into secondary recipients. Fourteen days post-transplantation, recipients were administered tamoxifen daily for 5 days. On the last day of treatment or 5 days post-tamoxifen, mice were pulsed with 5-bromodeoxyuridine (BrdU). After an 18 hr chase period, bcCML cells were analyzed. a, Representative BrdU/7AAD plot showing cell cycle distribution of lineage-negative (Lin^-) bcCML cells 1 day post-tamoxifen treatment. b, Average frequency of BrdU+ lineage-negative (Lin^-) bcCML cells 1 day post-tamoxifen treatment (n=3 for +/+ and n=6 for -/-, **p*=0.0154). c, Average frequency of BrdU+ lineage-positive (Lin+) bcCML cells 1 day post-tamoxifen treatment (n=3 for +/+ and n=6 for -/-, **p*=0.0171). d, The relative fold change ((+/+)/(-/-)) of the percentage of BrdU+ cells from lineage-negative (Lin-) or lineage-positive (Lin+) bcCML cells 1 day post-tamoxifen treatment. e, Average frequency of AnnexinV+ lineage-negative (Lin^-) bcCML cells 1 day post-tamoxifen treatment (n=4 for +/+ and n=6 for -/-). f, Representative BrdU/7AAD plot showing cell cycle status of lineage-negative (Lin^-) bcCML cells 5 days post-tamoxifen treatment. g, Percentage of BrdU+ lineage-negative (Lin^-) bcCML cells 5 day post-tamoxifen treatment (n=7 for +/+ and n=4 for -/-, ***p*=0.0040). h, Percentage of AnnexinV+ lineage-negative (Lin^-) bcCML cells 5 days post-tamoxifen treatment (n=7 for +/+ and n=4 for -/-, **p*=0.0309). Error bars represent the standard error of mean (SEM).

6.2.5 Loss of Lis1 alters the expression of genes implicated in regulating leukemic development.

To gain molecular insight into how Lis1 loss may lead to defects in leukemia formation we focused on genes that were altered in the normal stem cell-enriched fraction but have also been implicated in regulating leukemogenesis. Of these, *Pml* and *Msi2* were significantly downregulated, and *Socs3* was upregulated based on quantitative PCR analysis (Figure 47). These data suggest that these downstream players may in part, mediate the defects observed.

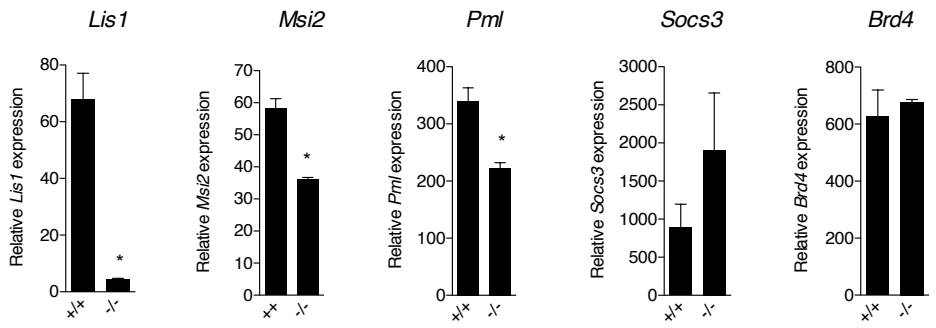

Figure 47: Loss of Lis1 leads to altered expression of genes implicated in leukemia maintenance and propagation.

Figure 47: Gene expression changes in *Lis1*-deficient established blast crisis CML cells. 40,000 lineage-negative (Lin$^-$) cells from established control *Lis1$^{+/+}$; Rosa-creER* or *Lis1$^{f/f}$; Rosa-creER* bcCML were transplanted into recipient mice. Fourteen days post-transplantation, recipients were administered tamoxifen daily for 5 days and 5 days post-tamoxifen treatment, RNA samples were isolated from lineage-negative (Lin$^-$) leukemia cells of recipient mice. Lis1, Msi2, Pml, and Socs3 expression in Lin$^-$ control (+/+) and (-/-) leukemia cells; n=2, *$p=0.020$ for *Lis1,* *$p=0.205$ for *Msi2* and *$p=0.0415$ for *Pml.* For realtime PCR, expression levels were normalized to the level of beta-2 microglobulin and displayed relative to the control. Error bars represent the standard error of the mean (SEM).

6.2.6 LIS1 plays a critical role in sustaining human leukemic growth.

To test whether Lis1 was also required for human myeloid leukemia, we deleted *Lis1* in both cell lines and primary patient samples. Both K562, a bcCML cell line, and MV411, a *de novo* AML cell line, were infected with shRNA targeting *LIS1* and colony-forming ability was measured. As shown in Figure 48, we confirmed effective knockdown of *LIS1* both by quantitative PCR and by western blot analysis.

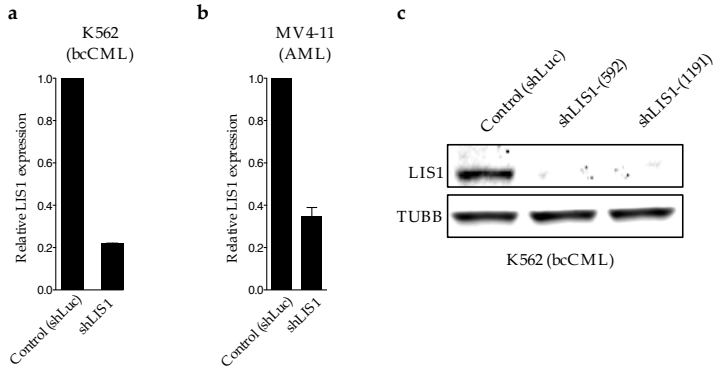

Figure 48: Efficient shRNA knockdown of *LIS1* in human leukemia cell lines.

Figure 48: a-b, Realtime RT-PCR analysis of *LIS1* mRNA expression in a, K562 blast crisis CML cells b, MV4-11 AML cells following transduction with either firefly luciferase shRNA as a control (shLuc) or *LIS1* shRNA (shLIS1). Expression levels were normalized to beta-2-microglobulin and displayed relative to the control arbitrarily set at 1. Error bars represent standard error of the mean (SEM) of triplicate PCRs. c, Resorted K562 blast crisis CML cells were analyzed by western blot; shLIS1-(592) and shLIS1-(1191) represent two independent hairpin shRNA targeting LIS1.

Effective knockdown of *LIS1* lead to a significant reduction in colony-forming ability of both cell lines (Figure 49).

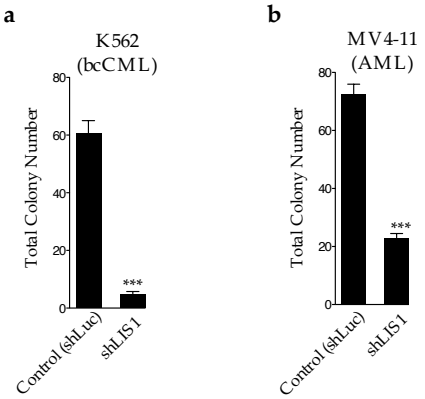

Figure 49: shRNA-mediated knockdown of *LIS1* impairs colony-forming ability of leukemia cell lines.

Figure 49: Influence of Lis1 on human leukemia growth. Human leukemia cells were infected with either control (shLuc) or lentiviral shRNA targeting human *LIS1* (shLIS1). Subsequently infected cells were sorted and plated in methylcellulose. Colony formation was assessed in K562 blast crisis CML cells (a), MV4-11 AML cells (b); *$p<0.05$, **$p<0.01$, ***$p<0.001$. Error bars represent standard error of the mean (SEM).

To demonstrate that the observed effects of the shLIS1 are not the result of off-target effects, we used an independent LIS1 shRNA and show a similar response (Figure 50a-d). In addition, shLIS1-mediated reduction in colony formation was completely rescued by introducing a shRNA-resistant mutant LIS1, further suggesting the observed effects of the shLIS1 were not the result of off-target effects (Figure 50e,f).

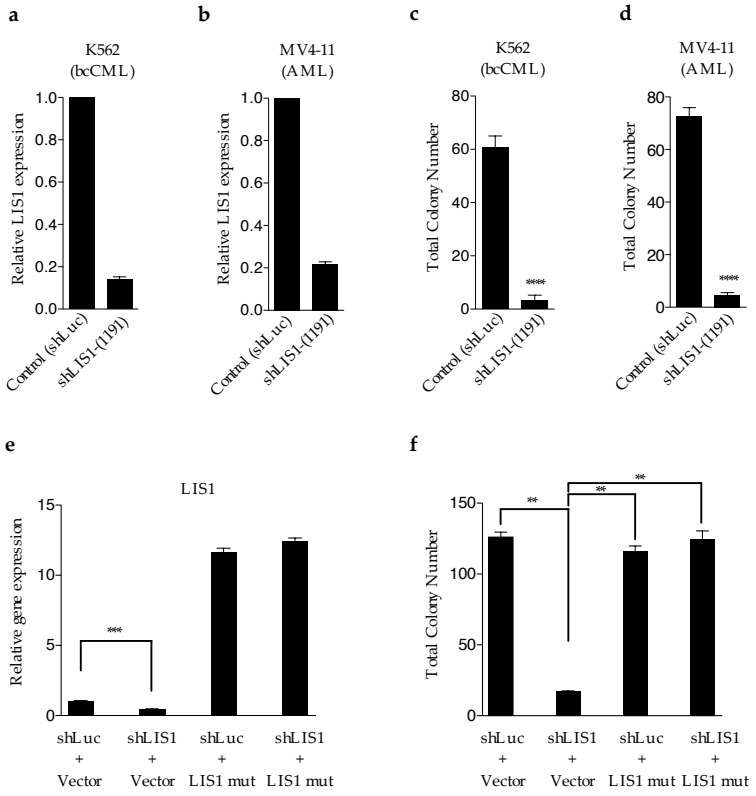

Figure 50: LIS1 inhibition via an independent shRNA construct.

Figure 50: a-d, Human leukemia cells were infected with either control (shLuc) or lentiviral shRNA targeting human *LIS1* (shLIS1): shLIS1-(1191) represent an independent hairpin shRNA targeting LIS1. a-b, Resorted K562 blast crisis CML cells (a) and MV4-11 AML cells (b) were analyzed by realtime RT-PCR for LIS1 expression. Error bars represent the standard error of the mean (SEM) of triplicate PCRs. c-d, Reduction of colony formation of K562 cells (c) and MV4-11 (d) by shLIS1-(1191) (n=2 for each cell type; ****p<0.0001. e, LIS1 expression levels in samples expressing the indicated constructs. LIS1 mut: shLIS1-resistant LIS1 mutant cDNA. Error bars represent SEM of triplicate PCRs. ***p=0.0002. f, Rescue of shLIS1-mediated reduction of colony-forming ability with expression of shLIS1-resistant LIS1 mutant cDNA. K562 blast crisis CML cells were transduced retrovirally with either Vector control or LIS1 mutant together with the indicated shRNA constructs, sorted and plated in methylcellulose media for colony formation. **p<0.01.

To test if LIS1 function may be relevant for primary human leukemia growth, primary patient-derived CD34⁺ bcCML cells that were triple resistant to the tyrosine kinase inhibitors imatinib, nilotinib and dasatinib as we as primary CD34⁺ AML patient cells harboring the frequently therapy-resistant MLL-AF9 translocation were infected with shLIS1, and colony-forming ability was assessed. As shown in Figure 51, inhibition of *LIS1* expression led to a significant blockade of colony-forming ability suggesting that LIS1 plays a critical role in sustaining human leukemic growth.

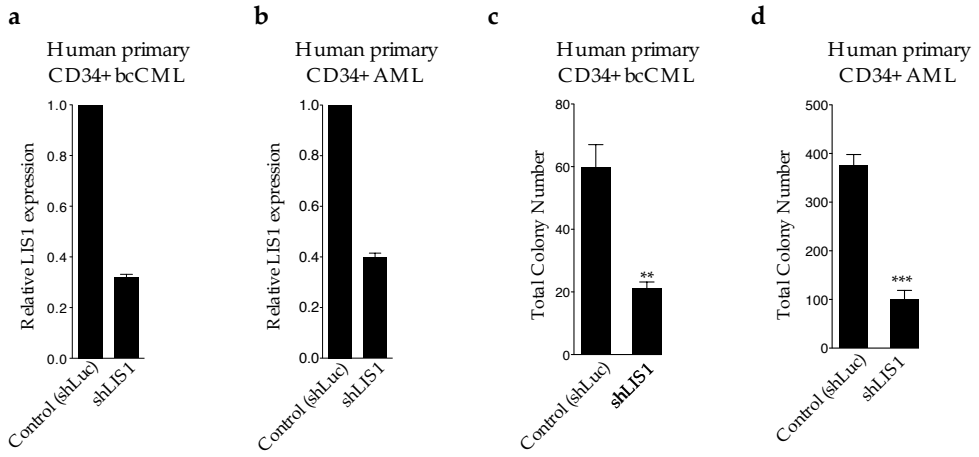

Figure 51: Impaired colony-forming ability of primary human leukemia cells in the absence of LIS1.

Figure 51: a-b, Efficiency of shRNA knockdown of *LIS1* in primary human leukemia. a-b, Realtime RT-PCR analysis of *LIS1* mRNA expression in a, human primary CD34⁺ bcCML and b, human primary CD34⁺ AML following transduction with either firefly luciferase shRNA as a control (shLuc) or *LIS1* shRNA (shLIS1). Expression levels were normalized to beta-2-microglobulin and displayed relative to the control arbitrarily set at 1. c-d, Influence of LIS1 on human leukemia growth. Colony formation was assessed in Imatinib, Nilotinib and Dastinib-resistant human primary CD34⁺ bcCML (c) and human primary CD34⁺ AML (d); *p<0.05, **p<0.01, ***p<0.001. Error bars represent standard error of the mean (SEM).

6.3 Discussion

We report here that the asymmetric division regulator Lis1 is critical for the aberrant cell growth that occurs in myeloid leukemia. Using a mouse model of blast-crisis CML (bcCML), we show that deletion of *Lis1* prevents disease initiation and progression. In the context of bcCML, it has been shown that only the immature fraction (cells bereft of mature lineage markers; Lin^- cells) of the leukemia cell population can successfully establish and propagate the disease in secondary recipients (Dash et al. 2002; Mayotte et al. 2002; Neering et al. 2007). Interestingly, *Lis1*-deficient bcCML-propagating cells (Lin^-) fail to establish and propagate the disease in secondary recipients; even deletion of *Lis1* at later stages of myeloid leukemia, when tumor burden is at ~25% of the peripheral blood population, results in complete reversion to normal cell counts and resolution of disease. Since in the clinical setting, most cancers are discovered only when the tumor is either palpable or at a size amendable to detection, treatments are usually initiated at a time when the disease is already well advanced. The finding that Lis1 loss even at later stages of the disease nearly eradicates the cancer, underscores Lis1 as an attractive therapeutic target.

The essential requirement for Lis1 in disease initiation extends to *de novo* AMLs as well. Cells transformed with MLL-AF9 and constitutively active NRAS give rise to an aggressive AML-like disease state (Zuber et al. 2009), which fails to occur in the absence

of Lis1. These data suggest that Lis1 is broadly required for the development of aggressive undifferentiated myeloid leukemias.

Both blast crisis phase CML and the majority of *de novo* AML share similar disease characteristics such as an aggressive growth of immature cells and reduced differentiation. Progression and continually propagation of the disease, therefore, may require maintenance of the undifferentiated state. Indeed, the most notable and immediate impact of *Lis1* deletion is a significant increase in differentiated leukemia cells. These data suggest that the forced differentiation of leukemic cells following the loss of Lis1 may be the underlying reason the disease fails to establish or propagate in the absence of Lis1. In addition to differentiation defects, we found that loss of Lis1 also lead to reduced proliferative capacity and an increase in cell death of leukemia cells, suggesting that the differentiation, proliferation and death defects may act in concert to lead to the deep defects observed in leukemogenesis.

Importantly, a role for Lis1 in leukemia is not limited to our mouse model systems. We found that inhibition of *LIS1* expression lead to a significant blockade of colony-forming ability of both human leukemia cell lines and primary, therapy-resistant human patient samples, suggesting that LIS1 plays an important role in sustaining human leukemic growth.

Signals that are important in development are often critical in cancer. This has been demonstrated for genes such as *PML* and *Foxo3a* (Ito et al. 2008; Miyamoto et al.

2007; Naka et al. 2010). Here we show that, in addition to a requirement of Lis1 in normal hematopoietic stem cell self-renewal, Lis1 is also required for aberrant self-renewal in cancer.

7. Conclusions and perspectives

7.1 Lis1 plays a critical role in blood development and in HSC self-renewal in both fetal and adult life by regulating asymmetric cell division.

During embryonic development, hematopoietic stem cells (HSCs) are generated *de novo* in numerous anatomical sites including the yolk sac and placenta but primarily self-renewal and differentiate within the fetal liver. Late in development, hematopoietic activity moves to the bone marrow, where HSCs reside in specialized microenvironments (Mikkola and Orkin 2006). During embryogenesis and adult life, an elaborate interplay of extrinsic and intrinsic mechanisms controls the balance between HSC self-renewal and differentiation. Proper control of this balance is critical during development to ensure that enough stem cells are generated for postnatal life and for the production of differentiated cells immediately required for growth and development. Furthermore, in adult life, tight regulation of this balance is important not only when the body replaces cells to maintain homeostasis, but also after hematopoietic insult when a precipitous rise in HSCs is required for effective regeneration.

Here we show that the cell fate regulator Lis1 plays an important role in blood development and in HSC self-renewal in both fetal and adult life. Genetic deletion of *Lis1* causes a significant suppression of fetal HSC expansion and thus leads to a near bloodless embryo and lethality before birth. Such an impact on fetal hematopoiesis has been previously reported mainly for key transcription factors such Runx1/Aml1, Scl/Tal-

1 and Gata2 (Okuda et al. 1996; Porcher et al. 1996; Tsai et al. 1994; Wang et al. 1996). The similarities in phenotype suggest the possibility that cellular and molecular events controlled by Lis1 activity may be integrated with the function of these transcription factors. It is also important to note that the drastic impact to the fetal HSC compartment following *Lis1* deletion is consistent with the phenotype previously reported in neuronal development, where following neural-specific deletion of *Lis1*, there is a profound disruption of stem cell expansion, resulting in a catastrophic phenotype (Yingling et al. 2008). That loss of Lis1 has such an affect on the stem cell compartments in a variety of tissues, suggest that Lis1 may have a broad role in stem cell renewal during development.

The identification of numerous developmental-stage specific regulators of HSC self-renewal, such as Sox17, Meis1 and Rae28 suggest that self-renewal mechanisms employed by HSCs might be distinct or shared between HSCs derived from the fetal liver and from that of the adult bone marrow (Kim et al. 2007). While an understanding of how HSC self-renewal is regulated during development is important, the identification of regulators and mechanisms that specifically control (or also control) adult HSC self-renewal may be more relevant and critical for the development of novel regenerative therapies and treatments aimed at reigning in leukemia stem cells.

Using a tamoxifen-inducible cre system, we deleted *Lis1* in the adult blood system and found that loss of Lis1 in adult life led to a significant reduction in the

frequency and absolute number of HSCs. In addition, in a transplantation-based assay, *Lis1*-deficient adult HSCs failed to effectively repopulate the blood compartment of lethally irradiated recipient mice, suggesting a critical role for Lis1 in adult HSC self-renewal activity *in vivo*. To determine whether Lis1 was cell-autonomously required for adult HSC function, we generated *Lis1* chimera mice (i.e. wild-type microenvironment) and found that blood-specific deletion of *Lis1* led to a significant reduction in HSC-enriched cells, suggesting Lis1 plays a role in HSC self-renewal activity in a cell-autonomous manner. Collectively, these data underscores Lis1's critical role in HSC activity in both fetal and adult life.

What is the mechanism by which Lis1 influences HSC self-renewal? A well-characterized functional role of Lis1 is being a facultative regulator of the minus-end directed motor protein dynein (Lee et al. 2003; Lei and Warrior 2000). In this context, Lis1 has been linked to several cell division events that require dynein function. In a variety of cell types including neural progenitor cells and cultured epithelial cells, perturbations in Lis1 expression results in mitotic defects and impaired cell cycle progression that in some instances subsequently leads to increased apoptotic death (Faulkner et al. 2000; Tsai et al. 2005; Yingling et al. 2008). Here we show that cell cycle status and survival of HSCs are largely unaffected in the absence of Lis1. However, we do see an increase in the frequency of late apoptotic/necrotic cells in the absence of Lis1. Furthermore, we find that loss of Lis1 in cultured HSCs results in a slight increase in the

frequencies of aneuploid and polyploid cells. These data suggest that both elevated HSC death and increased acquisition of polyploidy and/or aneuploidy may contribute to the deep phenotype that manifest following *Lis1* deletion.

The profound loss of the immature cell population in both fetal and adult blood, suggested a potential defect in maintenance of the undifferentiated state. Intriguingly, by tracking the actual rate of differentiation of cultured HSCs, we found that loss of Lis1 led to accelerated differentiation of these cells *in vitro*. In support of this, a wave of premature HSC differentiation accompanied the loss of Lis1 *in vivo*. These data suggest that mechanisms that control HSC self-renewal and maintain the stem cell state may be dysfunctional or ineffective in the absence of Lis1. Interestingly, genome wide expression analysis of wild type and *Lis1*-deficient HSC-enriched cells demonstrated a significant loss of core genes that form the stem cell signature, as well as elevated levels of pro-differentiation genes such as *Socs3* and *CD48*. These data further confirm, through an independent molecular approach, that Lis1 function is important to maintain the stem cell state.

In other stem cell systems, including those of *Caenorhabditis elegan* and *Drosophila melanogaster*, asymmetric cell division represents one of the critical mechanisms of self-renewal regulation. Intriguingly, Lis1 has been implicated in the machinery controlling division pattern in these systems (Siller and Doe 2009). Whether HSCs undergo asymmetric division to facilitate the balance between self-renewal and differentiation

has been difficult to address largely due to the absence of a marker that unambiguously distinguishes HSCs from differentiating daughter cells. Recently, using a transgenic reporter-based system, where GFP marks stem cells and is lost as cells differentiate, we showed that HSCs have the capacity to undergo both asymmetric and symmetric division (Wu et al. 2007). These data suggest that, similar to other stem cell systems, asymmetric division may serve as an important mechanism of self-renewal regulation in the hematopoietic system.

Because accelerated differentiation can be a consequence of defects in asymmetric division, we tested whether the loss of Lis1 had an impact on this specific renewal mechanism. Previously, we found that differential cell fate of paired daughter cells correlated with the asymmetric acquisition of the Numb protein, a known asymmetric cell fate determinant in other cell types (Wu et al. 2007). We thus specifically tracked the polarization and inheritance of Numb and found that while the polarization of Numb was unaffected in the absence of Lis1, the loss of Lis1 led to a complete reversal of the pattern of Numb inheritance both *in vitro* and *in vivo*. In contrast to wild type cells, which preferentially undergo symmetric renewal division, *Lis1*-deficient cells predominately undergo asymmetric cell division, and only rarely symmetrically divide. Since an increase in asymmetric division would generate more differentiated cells over time, the predominance of asymmetry in the absence of Lis1 may explain the observed accelerated differentiation defect.

As a potential mechanism that may underlie the increased inheritance of Numb and a marked imbalance of asymmetric and symmetric divisions, we show that loss of Lis1 leads to defective spindle positioning during HSC division. Specifically, while wild type cells effectively direct the position of their spindles in such a way to facilitate equal inheritance of Numb by the two incipient daughter cells, *Lis1*-deficient cells ineffectively direct the position of their spindles, thus causing changes in the cleavage plane. These changes in cleavage plane undoubtedly increases the likelihood that Numb will be differentially inherited by the two daughter cells. Collectively, these data suggest that the premature differentiation and HSC loss observed in the absence of Lis1 is primarily due to spindle orientation defects that drive increased asymmetric inheritance of Numb. In this context, our findings identify Lis1 as a key component of the molecular machinery that directs asymmetric division in hematopoietic stem cells and provides the first genetic proof for the requirement of a proper balance of asymmetric division and its regulators for hematopoiesis *in vivo*. These data raise the possibility that the position and orientation of the immature hematopoietic cells within its microenvironment may be critically important in directing self-renewal and differentiation and indicates that environmental cues may specify the plane of division of hematopoietic cells through Lis1.

7.2 The asymmetric division regulator Lis1 is critically required for malignant hematopoietic development.

Elucidating the basis of maintenance of the undifferentiated state in normal HSCs is important because it may allow an understanding of mechanisms that underlie the blockade of differentiation, a hallmark of many cancers such as glioblastoma, breast cancer and leukemias (Calabretta and Perrotti 2004; Maher et al. 2001; Stingl and Caldas 2007). Under normal conditions, the ability of HSCs to undergo different modes of division (symmetric or asymmetric cell division) allows for effective modulation of the balance between HSC self-renewal and differentiation. Thus, asymmetric cell division represents one of the critical mechanisms of self-renewal regulation in normal HSCs. Interestingly, in the context of oncogenesis, we recently showed that certain oncogenes promote leukemia development by subverting the normal balance of asymmetric and symmetric division. Specifically, whereas *BCR-ABL,* the hallmark genetic abnormality in CML, cannot affect the choice between asymmetric and symmetric division, *NUP98-HOXA9*, an oncogene associated with aggressive, undifferentiated blast crisis CML, shifts the normal balance of asymmetric and symmetric division towards symmetric renewal divisions (Wu et al. 2007). These data suggest that dysregulation of HSC division pattern may, in part, be responsible for the failure of differentiation that occurs during disease progression

Intriguingly, emerging studies indicate that the presence and dysregulated expression of fate determinants and asymmetric division regulators may be important

elements of the induction and/or propagation of cancers that become increasingly undifferentiated during progression. In the context of leukemia, the cell fate determinants Musashi (Msi2) and Numb have been implicated in CML disease progression (Ito et al. 2010; Kharas et al. 2010), Prox1 (*Drosophila* Prospero) mutations have been reported in several primary leukemia samples and cell lines (Nagai et al. 2003), and repression of the polarity protein Llgl1 has been shown to be associated with human leukemia development (Heidel et al. 2013).

We now show, using mouse models of blast crisis CML and *de novo* AML, that the asymmetric division regulator Lis1 is critically required for the initiation and maintenance of these hematopoietic malignancies. For both diseases, only ~30% of mice (compared to 100% in control groups) developed leukemia when Lis1 was deleted during initiation. Importantly, those that did succumb to leukemia exhibited longer disease latency. Remarkably, deletion of *Lis1* at late stages of blast crisis CML results in complete reversion to normal blood cell counts and resolution of disease. These data strongly imply that Lis1 inhibitors may be attractive candidates for a novel molecular target therapy in hematological malignancies. In support of this, inhibition of *LIS1* expression in primary human leukemias that are resistant to current and conventional therapy led to a significant blockade of colony-forming ability, highlighting a critical requirement for LIS1 in the growth of human leukemias.

Similar to the basis of the defects observed in normal HSCs in the absence of Lis1, we find that the immediate impact of loss of Lis1 in leukemia is increased differentiation of immature lineage negative cells, a population that harbors leukemia stem cells (Neering et al. 2007). This increase in differentiation is not due to changes in viability or proliferation within the immature population. However, overtime, the loss of Lis1 does lead to defects in proliferation and apoptosis. Thus, these late-onset defects in conjunction with increases in differentiation may act together to lead to the deep defect observed in leukemogenesis. Importantly though, the increased propensity for *Lis1*-deficient leukemia stem cells to differentiate is suggestive that the observed defects in disease propagation and sustainability may be due, at least in part, to a shift toward pro-differentiation divisions, as opposed to perpetual self-renewal divisions.

Fate determinants, such as Numb and Msi2 have recently been shown to play a role in the onset and or/propagation of several cancers, including leukemia (Ito et al. 2010; Pece et al. 2004). Our work now shows that regulatory mechanisms that direct the inheritance of these determinants are equally important for the establishment and continued propagation of malignancies. Previous studies have shown that loss of asymmetric division proteins including Brat, Prospero and Numb can trigger tumor formation in *Drosophila* neuroblasts (Bello et al. 2006; Betschinger et al. 2006; Caussinus and Gonzalez 2005; Lee et al. 2006a; Lee et al. 2006b; Wang et al. 2006). Using mouse models and patient samples of leukemias that are resistant to therapy in the clinic, our

data is the first to link Lis1 and the machinery regulating determinant inheritance with mammalian oncogenesis and thus provide an important complement to studies in *Drosophila*. This raises the possibility that modulators of determinant inheritance could serve as a powerful new class of regulators of cancer growth and that further work in this area may define new approaches to therapy.

Appendix

Supplementary Movie 1: Imaging Cell Division in Real Time. Cells were co-infected with H2B-GFP and mCherry-α-tubulin fusion constructs and imaged over time. Representative movies showing A. HeLa cell, B. M1 Cell, and C. Primary Hematopoietic Stem & Progenitor Cells undergoing cell division (H2B-GFP is shown in green and α-tubulin is shown in magenta).

Supplementary Movie 2: Symmetric inheritance of Numb

HSC-enriched cells (KLS) were co-infected with Numb-CFP and mCherry-α-tubulin fusion constructs and imaged overtime. Representative movie showing a KLS cell undergoing a symmetric division (Numb is shown in green and α-tubulin is shown in red).

Supplementary Movie 3: Asymmetric inheritance of Numb

HSC-enriched cells (KLS) were co-infected with Numb-CFP and mCherry-α-tubulin fusion constructs and imaged overtime. Representative movie showing a KLS cell undergoing an asymmetric division (Numb is shown in green and α-tubulin is shown in red).

Supplementary Movie 4: Asymmetric inheritance of Numb

HSC-enriched cells (KLS) were co-infected with Numb-YFP and mCherry-α-tubulin fusion constructs and imaged overtime. Representative movie showing a KLS cell undergoing an asymmetric division (Numb is shown in green and α-tubulin is shown in red).

References

Adams, J.M., Harris, A.W., Strasser, A., Ogilvy, S., and Cory, S. (1999). "Transgenic models of lymphoid neoplasia and development of a pan-hematopoietic vector." Oncogene 18(38): 5268-5277.

Adams, J.M., Houston, H., Allen, J., Lints, T., and Harvey, R. (1992). "The hematopoietically expressed vav proto-oncogene shares homology with the dbl GDP-GTP exchange factor, the bcr gene and a yeast gene (CDC24) involved in cytoskeletal organization." Oncogene 7(4): 611-618.

Alvarez-Silva, M., Belo-Diabangouaya, P., Salaun, J., and Dieterlen-Lievre, F. (2003). "Mouse placenta is a major hematopoietic organ." Development 130(22): 5437-5444.

Arnold, B.C., Balakrishnan, N., and Nagaraja, H.N. (1992). A First Course in Order Statistics (Wiley Series in Probability and Statistics) (New York).

Aumais, J.P., Tunstead, J.R., McNeil, R.S., Schaar, B.T., McConnell, S.K., Lin, S.H., *et al.* (2001). "NudC associates with Lis1 and the dynein motor at the leading pole of neurons." J Neurosci 21(24): RC187.

Azcoitia, V., Aracil, M., Martinez, A.C., and Torres, M. (2005). "The homeodomain protein Meis1 is essential for definitive hematopoiesis and vascular patterning in the mouse embryo." Dev Biol 280(2): 307-320.

Beaudouin, J., Gerlich, D., Daigle, N., Eils, R., and Ellenberg, J. (2002). "Nuclear envelope breakdown proceeds by microtubule-induced tearing of the lamina." Cell 108(1): 83-96.

Beekman, R., Valkhof, M.G., Sanders, M.A., van Strien, P.M., Haanstra, J.R., Broeders, L., *et al.* (2012). "Sequential gain of mutations in severe congenital neutropenia progressing to acute myeloid leukemia." Blood 119(22): 5071-5077.

Bello, B., Reichert, H., and Hirth, F. (2006). "The brain tumor gene negatively regulates neural progenitor cell proliferation in the larval central brain of Drosophila." Development 133(14): 2639-2648.

Benjamini, Y., and Hochberg, Y. (1995). "Controlling the false discovery rate: A practical and powerful approach to multiple testing." J R Stat Soc Ser B 57(289–300.

Berdnik, D., Torok, T., Gonzalez-Gaitan, M., and Knoblich, J.A. (2002). "The endocytic protein alpha-Adaptin is required for numb-mediated asymmetric cell division in Drosophila." Dev Cell 3(2): 221-231.

Betschinger, J., and Knoblich, J.A. (2004). "Dare to be different: asymmetric cell division in Drosophila, C. elegans and vertebrates." Curr Biol 14(16): R674-685.

Betschinger, J., Mechtler, K., and Knoblich, J.A. (2006). "Asymmetric segregation of the tumor suppressor brat regulates self-renewal in Drosophila neural stem cells." Cell 124(6): 1241-1253.

Bonnet, D., and Dick, J.E. (1997). "Human acute myeloid leukemia is organized as a hierarchy that originates from a primitive hematopoietic cell." Nat Med 3(7): 730-737.

Bustelo, X.R., Rubin, S.D., Suen, K.L., Carrasco, D., and Barbacid, M. (1993). "Developmental expression of the vav protooncogene." Cell Growth Differ 4(4): 297-308.

Cahana, A., Escamez, T., Nowakowski, R.S., Hayes, N.L., Giacobini, M., von Holst, A., *et al.* (2001). "Targeted mutagenesis of Lis1 disrupts cortical development and LIS1 homodimerization." Proc Natl Acad Sci U S A 98(11): 6429-6434.

Calabretta, B., and Perrotti, D. (2004). "The biology of CML blast crisis." Blood 103(11): 4010-4022.

Calvi, L.M., Adams, G.B., Weibrecht, K.W., Weber, J.M., Olson, D.P., Knight, M.C., *et al.* (2003). "Osteoblastic cells regulate the haematopoietic stem cell niche." Nature 425(6960): 841-846.

Caspi, M., Atlas, R., Kantor, A., Sapir, T., and Reiner, O. (2000). "Interaction between LIS1 and doublecortin, two lissencephaly gene products." Hum Mol Genet 9(15): 2205-2213.

Caussinus, E., and Gonzalez, C. (2005). "Induction of tumor growth by altered stem-cell asymmetric division in Drosophila melanogaster." Nature Genet 37(10): 1125-1129.

Chang, J.T., Palanivel, V.R., Kinjyo, I., Schambach, F., Intlekofer, A.M., Banerjee, A., *et al.* (2007). "Asymmetric T lymphocyte division in the initiation of adaptive immune responses." Science 315(5819): 1687-1691.

Chen, S., Kaneko, S., Ma, X., Chen, X., Ip, Y.T., Xu, L., *et al.* (2010). "Lissencephaly-1 controls germline stem cell self-renewal through modulating bone morphogenetic protein signaling and niche adhesion." Proc Natl Acad Sci U S A 107(46): 19939-19944.

Choksi, S.P., Southall, T.D., Bossing, T., Edoff, K., de Wit, E., Fischer, B.E., *et al.* (2006). "Prospero acts as a binary switch between self-renewal and differentiation in Drosophila neural stem cells." Dev Cell 11(6): 775-789.

Cicalese, A., Bonizzi, G., Pasi, C.E., Faretta, M., Ronzoni, S., Giulini, B., *et al.* (2009). "The tumor suppressor p53 regulates polarity of self-renewing divisions in mammary stem cells." Cell 138(6): 1083-1095.

Clarke, M.F., and Fuller, M. (2006). "Stem cells and cancer: two faces of eve." Cell 124(6): 1111-1115.

Cockell, M.M., Baumer, K., and Gonczy, P. (2004). "lis-1 is required for dynein-dependent cell division processes in C. elegans embryos." J Cell Sci 117(Pt 19): 4571-4582.

Congdon, K.L., and Reya, T. (2008). "Divide and conquer: how asymmetric division shapes cell fate in the hematopoietic system." Curr Opin Immunol 20(3): 302-307.

Coquelle, F.M., Caspi, M., Cordelieres, F.P., Dompierre, J.P., Dujardin, D.L., Koifman, C., *et al.* (2002). "LIS1, CLIP-170's key to the dynein/dynactin pathway." Mol Cell Biol 22(9): 3089-3102.

Cumano, A., Dieterlen-Lievre, F., and Godin, I. (1996). "Lymphoid potential, probed before circulation in mouse, is restricted to caudal intraembryonic splanchnopleura." Cell 86(6): 907-916.

Dash, A.B., Williams, I.R., Kutok, J.L., Tomasson, M.H., Anastasiadou, E., Lindahl, K., *et al.* (2002). "A murine model of CML blast crisis induced by cooperation between BCR/ABL and NUP98/HOXA9." Proc Natl Acad Sci U S A 99(11): 7622-7627.

Day, D., Pham, K., Ludford-Menting, M.J., Oliaro, J., Izon, D., Russell, S.M., *et al.* (2009). "A method for prolonged imaging of motile lymphocytes." Immunol Cell Biol 87(2): 154-158.

de Andres-Aguayo, L., Varas, F., Kallin, E.M., Infante, J.F., Wurst, W., Floss, T., *et al.* (2011). "Musashi 2 is a regulator of the HSC compartment identified by a retroviral insertion screen and knockout mice." Blood 118(3): 554-564.

de Boer, J., Williams, A., Skavdis, G., Harker, N., Coles, M., Tolaini, M., *et al.* (2003). "Transgenic mice with hematopoietic and lymphoid specific expression of Cre." Eur J Immunol 33(2): 314-325.

de Bruijn, M.F., Speck, N.A., Peeters, M.C., and Dzierzak, E. (2000). "Definitive hematopoietic stem cells first develop within the major arterial regions of the mouse embryo." Embo J 19(11): 2465-2474.

Dobyns, W.B., Reiner, O., Carrozzo, R., and Ledbetter, D.H. (1993). "Lissencephaly. A human brain malformation associated with deletion of the LIS1 gene located at chromosome 17p13." Jama 270(23): 2838-2842.

Domen, J., Cheshier, S.H., and Weissman, I.L. (2000). "The role of apoptosis in the regulation of hematopoietic stem cells: Overexpression of Bcl-2 increases both their number and repopulation potential." J Exp Med 191(2): 253-264.

Duncan, A.W., Rattis, F.M., DiMascio, L.N., Congdon, K.L., Pazianos, G., Zhao, C., *et al.* (2005). "Integration of Notch and Wnt signaling in hematopoietic stem cell maintenance." Nat Immunol 6(3): 314-322.

Ema, H., and Nakauchi, H. (2000). "Expansion of hematopoietic stem cells in the developing liver of a mouse embryo." Blood 95(7): 2284-2288.

Ema, H., Takano, H., Sudo, K., and Nakauchi, H. (2000). "In vitro self-renewal division of hematopoietic stem cells." J Exp Med 192(9): 1281-1288.

Eppert, K., Takenaka, K., Lechman, E.R., Waldron, L., Nilsson, B., van Galen, P., *et al.* (2011). "Stem cell gene expression programs influence clinical outcome in human leukemia." Nat Med 17(9): 1086-1093.

Faulkner, N.E., Dujardin, D.L., Tai, C.Y., Vaughan, K.T., O'Connell, C.B., Wang, Y., *et al.* (2000). "A role for the lissencephaly gene LIS1 in mitosis and cytoplasmic dynein function." Nat Cell Biol 2(11): 784-791.

Fleck, M.W., Hirotsune, S., Gambello, M.J., Phillips-Tansey, E., Suares, G., Mervis, R.F., *et al.* (2000). "Hippocampal abnormalities and enhanced excitability in a murine model of human lissencephaly." J Neurosci 20(7): 2439-2450.

Gardiol, D., Zacchi, A., Petrera, F., Stanta, G., and Banks, L. (2006). "Human discs large and scrib are localized at the same regions in colon mucosa and changes in their expression patterns are correlated with loss of tissue architecture during malignant progression." Int J Cancer 119(6): 1285-1290.

Gekas, C., Dieterlen-Lievre, F., Orkin, S.H., and Mikkola, H.K. (2005). "The placenta is a niche for hematopoietic stem cells." Dev Cell 8(3): 365-375.

Gekas, C., Rhodes, K.E., and Mikkola, H.K. (2008). "Isolation and visualization of mouse placental hematopoietic stem cells." Curr Protoc Stem Cell Biol Chapter 2(Unit 2A 8 1-2A 8 14.

Gerlitz, G., Darhin, E., Giorgio, G., Franco, B., and Reiner, O. (2005). "Novel functional features of the Lis-H domain: role in protein dimerization, half-life and cellular localization." Cell Cycle 4(11): 1632-1640.

Godin, I., Garcia-Porrero, J.A., Dieterlen-Lievre, F., and Cumano, A. (1999). "Stem cell emergence and hemopoietic activity are incompatible in mouse intraembryonic sites." J Exp Med 190(1): 43-52.

Gonzalez, C. (2007). "Spindle orientation, asymmetric division and tumour suppression in Drosophila stem cells." Nat Rev Genet 8(6): 462-472.

Grifoni, D., Garoia, F., Bellosta, P., Parisi, F., De Biase, D., Collina, G., *et al.* (2007). "aPKCzeta cortical loading is associated with Lgl cytoplasmic release and tumor growth in Drosophila and human epithelia." Oncogene 26(40): 5960-5965.

Gupta, A., Tsai, L.H., and Wynshaw-Boris, A. (2002). "Life is a journey: a genetic look at neocortical development." Nature Rev Genet 3(5): 342-355.

Harrison, D.E., Zhong, R.K., Jordan, C.T., Lemischka, I.R., and Astle, C.M. (1997). "Relative to adult marrow, fetal liver repopulates nearly five times more effectively long-term than short-term." Exp Hematol 25(4): 293-297.

Hattori, M., Adachi, H., Tsujimoto, M., Arai, H., and Inoue, K. (1994). "Miller-Dieker lissencephaly gene encodes a subunit of brain platelet-activating factor acetylhydrolase [corrected]." Nature 370(6486): 216-218.

Heidel, F.H., Bullinger, L., Arreba-Tutusaus, P., Wang, Z., Gaebel, J., Hirt, C., *et al.* (2013). "The cell fate determinant Llgl1 influences HSC fitness and prognosis in AML." J Exp Med 210(1): 15-22.

Hirotsune, S., Fleck, M.W., Gambello, M.J., Bix, G.J., Chen, A., Clark, G.D., *et al.* (1998). "Graded reduction of Pafah1b1 (Lis1) activity results in neuronal migration defects and early embryonic lethality." Nature Genet 19(4): 333-339.

Hisa, T., Spence, S.E., Rachel, R.A., Fujita, M., Nakamura, T., Ward, J.M., *et al.* (2004). "Hematopoietic, angiogenic and eye defects in Meis1 mutant animals." EMBO J 23(2): 450-459.

Hock, H., Hamblen, M.J., Rooke, H.M., Schindler, J.W., Saleque, S., Fujiwara, Y., *et al.* (2004a). "Gfi-1 restricts proliferation and preserves functional integrity of haematopoietic stem cells." Nature 431(7011): 1002-1007.

Hock, H., Meade, E., Medeiros, S., Schindler, J.W., Valk, P.J., Fujiwara, Y., *et al.* (2004b). "Tel/Etv6 is an essential and selective regulator of adult hematopoietic stem cell survival." Genes Dev 18(19): 2336-2341.

Hope, K.J., Cellot, S., Ting, S.B., MacRae, T., Mayotte, N., Iscove, N.N., *et al.* (2010). "An RNAi screen identifies Msi2 and Prox1 as having opposite roles in the regulation of hematopoietic stem cell activity." Cell Stem Cell 7(1): 101-113.

Ikuta, K., Kina, T., MacNeil, I., Uchida, N., Peault, B., Chien, Y.H., *et al.* (1990). "A developmental switch in thymic lymphocyte maturation potential occurs at the level of hematopoietic stem cells." Cell 62(5): 863-874.

Ito, K., Bernardi, R., Morotti, A., Matsuoka, S., Saglio, G., Ikeda, Y., *et al.* (2008). "PML targeting eradicates quiescent leukaemia-initiating cells." Nature 453(7198): 1072-1078.

Ito, K., Carracedo, A., Weiss, D., Arai, F., Ala, U., Avigan, D.E., *et al.* (2012). "A PML-PPAR-delta pathway for fatty acid oxidation regulates hematopoietic stem cell maintenance." Nat Med 18(9): 1350-1358.

Ito, T., Kwon, H.Y., Zimdahl, B., Congdon, K.L., Blum, J., Lento, W.E., *et al.* (2010). "Regulation of myeloid leukaemia by the cell-fate determinant Musashi." Nature 466(7307): 765-768.

Ivanova, N.B., Dimos, J.T., Schaniel, C., Hackney, J.A., Moore, K.A., and Lemischka, I.R. (2002). "A stem cell molecular signature." Science 298(5593): 601-604.

Kanda, T., Sullivan, K.F., and Wahl, G.M. (1998). "Histone-GFP fusion protein enables sensitive analysis of chromosome dynamics in living mammalian cells." Curr Biol 8(7): 377-385.

Kantor, A.B., Stall, A.M., Adams, S., Herzenberg, L.A., and Herzenberg, L.A. (1992). "Differential development of progenitor activity for three B-cell lineages." Proc Natl Acad Sci U S A 89(8): 3320-3324.

Katzav, S., Martin-Zanca, D., and Barbacid, M. (1989). "vav, a novel human oncogene derived from a locus ubiquitously expressed in hematopoietic cells." EMBO J 8(8): 2283-2290.

Keeshan, K., He, Y., Wouters, B.J., Shestova, O., Xu, L., Sai, H., *et al.* (2006). "Tribbles homolog 2 inactivates C/EBPalpha and causes acute myelogenous leukemia." Cancer Cell 10(5): 401-411.

Kharas, M.G., Lengner, C.J., Al-Shahrour, F., Bullinger, L., Ball, B., Zaidi, S., *et al.* (2010). "Musashi-2 regulates normal hematopoiesis and promotes aggressive myeloid leukemia." Nat Med 16(8): 903-908.

Kiel, M.J., Yilmaz, O.H., Iwashita, T., Yilmaz, O.H., Terhorst, C., and Morrison, S.J. (2005). "SLAM family receptors distinguish hematopoietic stem and progenitor cells and reveal endothelial niches for stem cells." Cell 121(7): 1109-1121.

Kim, I., Saunders, T.L., and Morrison, S.J. (2007). "Sox17 dependence distinguishes the transcriptional regulation of fetal from adult hematopoietic stem cells." Cell 130(3): 470-483.

Kim, I., Yilmaz, O.H., and Morrison, S.J. (2005). "CD144 (VE-cadherin) is transiently expressed by fetal liver hematopoietic stem cells." Blood 106(3): 903-905.

Kim, J.Y., Sawada, A., Tokimasa, S., Endo, H., Ozono, K., Hara, J., *et al.* (2004). "Defective long-term repopulating ability in hematopoietic stem cells lacking the Polycomb-group gene rae28." Eur J Haematol 73(2): 75-84.

Kirito, K., Fox, N., and Kaushansky, K. (2004). "Thrombopoietin induces HOXA9 nuclear transport in immature hematopoietic cells: potential mechanism by which the hormone favorably affects hematopoietic stem cells." Mol Cell Biol 24(15): 6751-6762.

Kitagawa, M., Umezu, M., Aoki, J., Koizumi, H., Arai, H., and Inoue, K. (2000). "Direct association of LIS1, the lissencephaly gene product, with a mammalian homologue of a fungal nuclear distribution protein, rNUDE." FEBS Lett 479(1-2): 57-62.

Knoblich, J.A. (2008). "Mechanisms of asymmetric stem cell division." Cell 132(4): 583-597.

Lapidot, T., Sirard, C., Vormoor, J., Murdoch, B., Hoang, T., Caceres-Cortes, J., *et al.* (1994). "A cell initiating human acute myeloid leukaemia after transplantation into SCID mice." Nature 367(6464): 645-648.

Lee, C.Y., Andersen, R.O., Cabernard, C., Manning, L., Tran, K.D., Lanskey, M.J., *et al.* (2006a). "Drosophila Aurora-A kinase inhibits neuroblast self-renewal by regulating aPKC/Numb cortical polarity and spindle orientation." Genes Dev 20(24): 3464-3474.

Lee, C.Y., Wilkinson, B.D., Siegrist, S.E., Wharton, R.P., and Doe, C.Q. (2006b). "Brat is a Miranda cargo protein that promotes neuronal differentiation and inhibits neuroblast self-renewal." Dev Cell 10(4): 441-449.

Lee, W.L., Oberle, J.R., and Cooper, J.A. (2003). "The role of the lissencephaly protein Pac1 during nuclear migration in budding yeast." J Cell Biol 160(3): 355-364.

Lei, Y., and Warrior, R. (2000). "The Drosophila Lissencephaly1 (DLis1) gene is required for nuclear migration." Dev Biol 226(1): 57-72.

Lessard, J., Faubert, A., and Sauvageau, G. (2004). "Genetic programs regulating HSC specification, maintenance and expansion." Oncogene 23(43): 7199-7209.

Lo Nigro, C., Chong, C.S., Smith, A.C., Dobyns, W.B., Carrozzo, R., and Ledbetter, D.H. (1997). "Point mutations and an intragenic deletion in LIS1, the lissencephaly causative gene in isolated lissencephaly sequence and Miller-Dieker syndrome." Hum Mol Genet 6(2): 157-164.

Maher, E.A., Furnari, F.B., Bachoo, R.M., Rowitch, D.H., Louis, D.N., Cavenee, W.K., *et al.* (2001). "Malignant glioma: genetics and biology of a grave matter." Genes Dev 15(11): 1311-1333.

Mayotte, N., Roy, D.C., Yao, J., Kroon, E., and Sauvageau, G. (2002). "Oncogenic interaction between BCR-ABL and NUP98-HOXA9 demonstrated by the use of an in vitro purging culture system." Blood 100(12): 4177-4184.

Medvinsky, A., and Dzierzak, E. (1996). "Definitive hematopoiesis is autonomously initiated by the AGM region." Cell 86(6): 897-906.

Merdes, A., Ramyar, K., Vechio, J.D., and Cleveland, D.W. (1996). "A complex of NuMA and cytoplasmic dynein is essential for mitotic spindle assembly." Cell 87(3): 447-458.

Metzeler, K.H., Hummel, M., Bloomfield, C.D., Spiekermann, K., Braess, J., Sauerland, M.C., *et al.* (2008). "An 86-probe-set gene-expression signature predicts survival in cytogenetically normal acute myeloid leukemia." Blood 112(10): 4193-4201.

Mikkola, H.K., and Orkin, S.H. (2006). "The journey of developing hematopoietic stem cells." Development 133(19): 3733-3744.

Miyamoto, K., Araki, K.Y., Naka, K., Arai, F., Takubo, K., Yamazaki, S., *et al.* (2007). "Foxo3a is essential for maintenance of the hematopoietic stem cell pool." Cell Stem Cell 1(1): 101-112.

Mizutani, K., Yoon, K., Dang, L., Tokunaga, A., and Gaiano, N. (2007). "Differential Notch signalling distinguishes neural stem cells from intermediate progenitors." Nature 449(7160): 351-355.

Morin, X., and Bellaiche, Y. (2011). "Mitotic spindle orientation in asymmetric and symmetric cell divisions during animal development." Dev Cell 21(1): 102-119.

Morris, S.M., Albrecht, U., Reiner, O., Eichele, G., and Yu-Lee, L.Y. (1998). "The lissencephaly gene product Lis1, a protein involved in neuronal migration, interacts with a nuclear movement protein, NudC." Curr Biol 8(10): 603-606.

Morrison, S.J. (2009). "Mechanisms of Stem Cell Self-Renewal." Annu Rev Cell Dev Biol

Morrison, S.J., Hemmati, H.D., Wandycz, A.M., and Weissman, I.L. (1995). "The purification and characterization of fetal liver hematopoietic stem cells." Proc Natl Acad Sci U S A 92(22): 10302-10306.

Morrison, S.J., and Kimble, J. (2006). "Asymmetric and symmetric stem-cell divisions in development and cancer." Nature 441(7097): 1068-1074.

Morrison, S.J., and Weissman, I.L. (1994). "The long-term repopulating subset of hematopoietic stem cells is deterministic and isolatable by phenotype." Immunity 1(8): 661-673.

Mucenski, M.L., McLain, K., Kier, A.B., Swerdlow, S.H., Schreiner, C.M., Miller, T.A., *et al.* (1991). "A functional c-myb gene is required for normal murine fetal hepatic hematopoiesis." Cell 65(4): 677-689.

Muller, A.M., Medvinsky, A., Strouboulis, J., Grosveld, F., and Dzierzak, E. (1994). "Development of hematopoietic stem cell activity in the mouse embryo." Immunity 1(4): 291-301.

Nagai, H., Li, Y., Hatano, S., Toshihito, O., Yuge, M., Ito, E., *et al.* (2003). "Mutations and aberrant DNA methylation of the PROX1 gene in hematologic malignancies." Genes Chromosomes Cancer 38(1): 13-21.

Naka, K., Hoshii, T., Muraguchi, T., Tadokoro, Y., Ooshio, T., Kondo, Y., *et al.* (2010). "TGF-beta-FOXO signalling maintains leukaemia-initiating cells in chronic myeloid leukaemia." Nature 463(7281): 676-680.

Nayernia, K., Vauti, F., Meinhardt, A., Cadenas, C., Schweyer, S., Meyer, B.I., *et al.* (2003). "Inactivation of a testis-specific Lis1 transcript in mice prevents spermatid differentiation and causes male infertility." J Biol Chem 278(48): 48377-48385.

Neer, E.J., Schmidt, C.J., Nambudripad, R., and Smith, T.F. (1994). "The ancient regulatory-protein family of WD-repeat proteins." Nature 371(6495): 297-300.

Neering, S.J., Bushnell, T., Sozer, S., Ashton, J., Rossi, R.M., Wang, P.Y., *et al.* (2007). "Leukemia stem cells in a genetically defined murine model of blast-crisis CML." Blood 110(7): 2578-2585.

Neumuller, R.A., and Knoblich, J.A. (2009). "Dividing cellular asymmetry: asymmetric cell division and its implications for stem cells and cancer." Genes Dev 23(23): 2675-2699.

Niethammer, M., Smith, D.S., Ayala, R., Peng, J., Ko, J., Lee, M.S., *et al.* (2000). "NUDEL is a novel Cdk5 substrate that associates with LIS1 and cytoplasmic dynein." Neuron 28(3): 697-711.

Ogilvy, S., Metcalf, D., Gibson, L., Bath, M.L., Harris, A.W., and Adams, J.M. (1999a). "Promoter elements of vav drive transgene expression in vivo throughout the hematopoietic compartment." Blood 94(6): 1855-1863.

Ogilvy, S., Metcalf, D., Print, C.G., Bath, M.L., Harris, A.W., and Adams, J.M. (1999b). "Constitutive Bcl-2 expression throughout the hematopoietic compartment affects multiple lineages and enhances progenitor cell survival." Proc Natl Acad Sci U S A 96(26): 14943-14948.

Ohta, H., Sawada, A., Kim, J.Y., Tokimasa, S., Nishiguchi, S., Humphries, R.K., *et al.* (2002). "Polycomb group gene rae28 is required for sustaining activity of hematopoietic stem cells." J Exp Med 195(6): 759-770.

Okuda, T., van Deursen, J., Hiebert, S.W., Grosveld, G., and Downing, J.R. (1996). "AML1, the target of multiple chromosomal translocations in human leukemia, is essential for normal fetal liver hematopoiesis." Cell 84(2): 321-330.

Orkin, S.H. (2000). "Diversification of haematopoietic stem cells to specific lineages." Nat Rev Genet 1(1): 57-64.

Orkin, S.H., and Zon, L.I. (2008). "Hematopoiesis: an evolving paradigm for stem cell biology." Cell 132(4): 631-644.

Ottersbach, K., and Dzierzak, E. (2005). "The murine placenta contains hematopoietic stem cells within the vascular labyrinth region." Dev Cell 8(3): 377-387.

Park, I.K., Qian, D., Kiel, M., Becker, M.W., Pihalja, M., Weissman, I.L., *et al.* (2003). "Bmi-1 is required for maintenance of adult self-renewing haematopoietic stem cells." Nature 423(6937): 302-305.

Paylor, R., Hirotsune, S., Gambello, M.J., Yuva-Paylor, L., Crawley, J.N., and Wynshaw-Boris, A. (1999). "Impaired learning and motor behavior in heterozygous Pafah1b1 (Lis1) mutant mice." Learn Mem 6(5): 521-537.

Pece, S., Serresi, M., Santolini, E., Capra, M., Hulleman, E., Galimberti, V., *et al.* (2004). "Loss of negative regulation by Numb over Notch is relevant to human breast carcinogenesis." J Cell Biol 167(2): 215-221.

Petronczki, M., and Knoblich, J.A. (2001). "DmPAR-6 directs epithelial polarity and asymmetric cell division of neuroblasts in Drosophila." Nat Cell Biol 3(1): 43-49.

Phillips, R.L., Ernst, R.E., Brunk, B., Ivanova, N., Mahan, M.A., Deanehan, J.K., *et al.* (2000). "The genetic program of hematopoietic stem cells." Science 288(5471): 1635-1640.

Porcher, C., Swat, W., Rockwell, K., Fujiwara, Y., Alt, F.W., and Orkin, S.H. (1996). "The T cell leukemia oncoprotein SCL/tal-1 is essential for development of all hematopoietic lineages." Cell 86(1): 47-57.

Punzel, M., Liu, D., Zhang, T., Eckstein, V., Miesala, K., and Ho, A.D. (2003). "The symmetry of initial divisions of human hematopoietic progenitors is altered only by the cellular microenvironment." Exp Hematol 31(4): 339-347.

Qin, X.F., An, D.S., Chen, I.S., and Baltimore, D. (2003). "Inhibiting HIV-1 infection in human T cells by lentiviral-mediated delivery of small interfering RNA against CCR5." Proc Natl Acad Sci U S A 100(1): 183-188.

Rebel, V.I., Kung, A.L., Tanner, E.A., Yang, H., Bronson, R.T., and Livingston, D.M. (2002). "Distinct roles for CREB-binding protein and p300 in hematopoietic stem cell self-renewal." Proc Natl Acad Sci U S A 99(23): 14789-14794.

Regala, R.P., Weems, C., Jamieson, L., Khoor, A., Edell, E.S., Lohse, C.M., *et al.* (2005). "Atypical protein kinase C iota is an oncogene in human non-small cell lung cancer." Cancer Res 65(19): 8905-8911.

Reiner, O., Carrozzo, R., Shen, Y., Wehnert, M., Faustinella, F., Dobyns, W.B., *et al.* (1993). "Isolation of a Miller-Dieker lissencephaly gene containing G protein beta-subunit-like repeats." Nature 364(6439): 717-721.

Reya, T. (2003). "Regulation of hematopoietic stem cell self-renewal." Recent Prog Horm Res 58(283-295.

Reya, T., Morrison, S.J., Clarke, M.F., and Weissman, I.L. (2001). "Stem cells, cancer, and cancer stem cells." Nature 414(6859): 105-111.

Rolls, M.M., Albertson, R., Shih, H.P., Lee, C.Y., and Doe, C.Q. (2003). "Drosophila aPKC regulates cell polarity and cell proliferation in neuroblasts and epithelia." J Cell Biol 163(5): 1089-1098.

Saito, T., and Yokosuka, T. (2006). "Immunological synapse and microclusters: the site for recognition and activation of T cells." Curr Opin Immunol 18(3): 305-313.

Sandberg, M.L., Sutton, S.E., Pletcher, M.T., Wiltshire, T., Tarantino, L.M., Hogenesch, J.B., *et al.* (2005). "c-Myb and p300 regulate hematopoietic stem cell proliferation and differentiation." Dev Cell 8(2): 153-166.

Sapir, T., Elbaum, M., and Reiner, O. (1997). "Reduction of microtubule catastrophe events by LIS1, platelet-activating factor acetylhydrolase subunit." EMBO J 16(23): 6977-6984.

Sasaki, S., Shionoya, A., Ishida, M., Gambello, M.J., Yingling, J., Wynshaw-Boris, A., *et al.* (2000). "A LIS1/NUDEL/cytoplasmic dynein heavy chain complex in the developing and adult nervous system." Neuron 28(3): 681-696.

Sasik, R., Woelk, C.H., and Corbeil, J. (2004). "Microarray truths and consequences." J Mol Endocrinol 33(1): 1-9.

Schober, M., Schaefer, M., and Knoblich, J.A. (1999). "Bazooka recruits Inscuteable to orient asymmetric cell divisions in Drosophila neuroblasts." Nature 402(6761): 548-551.

Shu, T., Ayala, R., Nguyen, M.D., Xie, Z., Gleeson, J.G., and Tsai, L.H. (2004). "Ndel1 operates in a common pathway with LIS1 and cytoplasmic dynein to regulate cortical neuronal positioning." Neuron 44(2): 263-277.

Siegrist, S.E., and Doe, C.Q. (2005). "Microtubule-induced Pins/Galphai cortical polarity in Drosophila neuroblasts." Cell 123(7): 1323-1335.

Siller, K.H., and Doe, C.Q. (2008a). "Lis1/dynactin regulates metaphase spindle orientation in Drosophila neuroblasts." Dev Biol 319(1): 1-9.

Siller, K.H., and Doe, C.Q. (2008b). "Lis1/dynactin regulates metaphase spindle orientation in Drosophila neuroblasts." Dev Biol 319(1): 1-9.

Siller, K.H., and Doe, C.Q. (2009). "Spindle orientation during asymmetric cell division." Nat Cell Biol 11(4): 365-374.

Smith, C.A., Lau, K.M., Rahmani, Z., Dho, S.E., Brothers, G., She, Y.M., *et al.* (2007). "aPKC-mediated phosphorylation regulates asymmetric membrane localization of the cell fate determinant Numb." EMBO J 26(2): 468-480.

Smith, D.S., Niethammer, M., Ayala, R., Zhou, Y., Gambello, M.J., Wynshaw-Boris, A., *et al.* (2000). "Regulation of cytoplasmic dynein behaviour and microtubule organization by mammalian Lis1." Nat Cell Biol 2(11): 767-775.

Somervaille, T.C., Matheny, C.J., Spencer, G.J., Iwasaki, M., Rinn, J.L., Witten, D.M., *et al.* (2009). "Hierarchical maintenance of MLL myeloid leukemia stem cells employs a transcriptional program shared with embryonic rather than adult stem cells." Cell Stem Cell 4(2): 129-140.

Srinivasan, D.G., Fisk, R.M., Xu, H., and van den Heuvel, S. (2003). "A complex of LIN-5 and GPR proteins regulates G protein signaling and spindle function in C elegans." Genes Dev 17(10): 1225-1239.

Stingl, J., and Caldas, C. (2007). "Molecular heterogeneity of breast carcinomas and the cancer stem cell hypothesis." Nature Rev Cancer 7(10): 791-799.

Subramanian, A., Tamayo, P., Mootha, V.K., Mukherjee, S., Ebert, B.L., Gillette, M.A., *et al.* (2005). "Gene set enrichment analysis: a knowledge-based approach for interpreting genome-wide expression profiles." Proc Natl Acad Sci U S A 102(43): 15545-15550.

Tai, C.Y., Dujardin, D.L., Faulkner, N.E., and Vallee, R.B. (2002). "Role of dynein, dynactin, and CLIP-170 interactions in LIS1 kinetochore function." J Cell Biol 156(6): 959-968.

Takano, H., Ema, H., Sudo, K., and Nakauchi, H. (2004). "Asymmetric division and lineage commitment at the level of hematopoietic stem cells: inference from differentiation in daughter cell and granddaughter cell pairs." J Exp Med 199(3): 295-302.

Tanaka, T., Serneo, F.F., Higgins, C., Gambello, M.J., Wynshaw-Boris, A., and Gleeson, J.G. (2004). "Lis1 and doublecortin function with dynein to mediate coupling of the nucleus to the centrosome in neuronal migration." J Cell Biol 165(5): 709-721.

Tarricone, C., Perrina, F., Monzani, S., Massimiliano, L., Kim, M.H., Derewenda, Z.S., *et al.* (2004). "Coupling PAF signaling to dynein regulation: structure of LIS1 in complex with PAF-acetylhydrolase." Neuron 44(5): 809-821.

Toyoshima, F., and Nishida, E. (2007). "Integrin-mediated adhesion orients the spindle parallel to the substratum in an EB1- and myosin X-dependent manner." EMBO J 26(6): 1487-1498.

Tsai, F.Y., Keller, G., Kuo, F.C., Weiss, M., Chen, J., Rosenblatt, M., *et al.* (1994). "An early haematopoietic defect in mice lacking the transcription factor GATA-2." Nature 371(6494): 221-226.

Tsai, J.W., Chen, Y., Kriegstein, A.R., and Vallee, R.B. (2005). "LIS1 RNA interference blocks neural stem cell division, morphogenesis, and motility at multiple stages." J Cell Biol 170(6): 935-945.

Tusher, V.G., Tibshirani, R., and Chu, G. (2001). "Significance analysis of microarrays applied to the ionizing radiation response." Proc Natl Acad Sci U S A 98(9): 5116-5121.

Venezia, T.A., Merchant, A.A., Ramos, C.A., Whitehouse, N.L., Young, A.S., Shaw, C.A., *et al.* (2004). "Molecular signatures of proliferation and quiescence in hematopoietic stem cells." PLoS Biol 2(10): e301.

Ventura, A., Kirsch, D.G., McLaughlin, M.E., Tuveson, D.A., Grimm, J., Lintault, L., *et al.* (2007). "Restoration of p53 function leads to tumour regression in vivo." Nature 445(7128): 661-665.

Wang, H., Ouyang, Y., Somers, W.G., Chia, W., and Lu, B. (2007). "Polo inhibits progenitor self-renewal and regulates Numb asymmetry by phosphorylating Pon." Nature 449(7158): 96-100.

Wang, H., Somers, G.W., Bashirullah, A., Heberlein, U., Yu, F., and Chia, W. (2006). "Aurora-A acts as a tumor suppressor and regulates self-renewal of Drosophila neuroblasts." Genes Dev 20(24): 3453-3463.

Wang, Q., Stacy, T., Binder, M., Marin-Padilla, M., Sharpe, A.H., and Speck, N.A. (1996). "Disruption of the Cbfa2 gene causes necrosis and hemorrhaging in the central nervous system and blocks definitive hematopoiesis." Proc Natl Acad Sci U S A 93(8): 3444-3449.

Weissman, I.L. (2000). "Stem cells: units of development, units of regeneration, and units in evolution." Cell 100(1): 157-168.

Willins, D.A., Liu, B., Xiang, X., and Morris, N.R. (1997). "Mutations in the heavy chain of cytoplasmic dynein suppress the nudF nuclear migration mutation of Aspergillus nidulans." Mol Gen Genet 255(2): 194-200.

Wirtz-Peitz, F., Nishimura, T., and Knoblich, J.A. (2008). "Linking cell cycle to asymmetric division: Aurora-A phosphorylates the Par complex to regulate Numb localization." Cell 135(1): 161-173.

Witte, O. (2001). "The role of Bcr-Abl in chronic myeloid leukemia and stem cell biology." Semin Hematol 38(3 Suppl 8): 3-8.

Wodarz, A., Ramrath, A., Grimm, A., and Knust, E. (2000). "Drosophila atypical protein kinase C associates with Bazooka and controls polarity of epithelia and neuroblasts." J Cell Biol 150(6): 1361-1374.

Wodarz, A., Ramrath, A., Kuchinke, U., and Knust, E. (1999). "Bazooka provides an apical cue for Inscuteable localization in Drosophila neuroblasts." Nature 402(6761): 544-547.

Wong, D.J., Liu, H., Ridky, T.W., Cassarino, D., Segal, E., and Chang, H.Y. (2008). "Module map of stem cell genes guides creation of epithelial cancer stem cells." Cell Stem Cell 2(4): 333-344.

Wu, M., Kwon, H.Y., Rattis, F., Blum, J., Zhao, C., Ashkenazi, R., *et al.* (2007). "Imaging hematopoietic precursor division in real time." Cell Stem Cell 1(5): 541-554.

Wynshaw-Boris, A. (2007). "Lissencephaly and LIS1: insights into the molecular mechanisms of neuronal migration and development." Clin Genet 72(4): 296-304.

Xiang, X., Osmani, A.H., Osmani, S.A., Xin, M., and Morris, N.R. (1995). "NudF, a nuclear migration gene in Aspergillus nidulans, is similar to the human LIS-1 gene required for neuronal migration." Mol Biol Cell 6(3): 297-310.

Yagi, T., Morimoto, A., Eguchi, M., Hibi, S., Sako, M., Ishii, E., *et al.* (2003). "Identification of a gene expression signature associated with pediatric AML prognosis." Blood 102(5): 1849-1856.

Yang, Z.J., Ellis, T., Markant, S.L., Read, T.A., Kessler, J.D., Bourboulas, M., *et al.* (2008). "Medulloblastoma can be initiated by deletion of Patched in lineage-restricted progenitors or stem cells." Cancer Cell 14(2): 135-145.

Yingling, J., Youn, Y.H., Darling, D., Toyo-Oka, K., Pramparo, T., Hirotsune, S., *et al.* (2008). "Neuroepithelial stem cell proliferation requires LIS1 for precise spindle orientation and symmetric division." Cell 132(3): 474-486.

Yoder, M.C., Hiatt, K., Dutt, P., Mukherjee, P., Bodine, D.M., and Orlic, D. (1997). "Characterization of definitive lymphohematopoietic stem cells in the day 9 murine yolk sac." Immunity 7(3): 335-344.

Youn, Y.H., Pramparo, T., Hirotsune, S., and Wynshaw-Boris, A. (2009). "Distinct dose-dependent cortical neuronal migration and neurite extension defects in Lis1 and Ndel1 mutant mice." J Neurosci 29(49): 15520-15530.

Zuber, J., Radtke, I., Pardee, T.S., Zhao, Z., Rappaport, A.R., Luo, W., *et al.* (2009). "Mouse models of human AML accurately predict chemotherapy response." Genes Dev 23(7): 877-889.

Biography

Bryan Zimdahl was born on January 12, 1985 in Syracuse, New York but spent the majority of his childhood and pre-college years in the small town of Mountainhome in the Pocono Mountains of Pennsylvania. After graduating high school as class valedictorian, Bryan attended Villanova University where in 2007, he graduated Phi Beta Kappa and magna cum laude with a Bachelor of Science degree in Biology and a minor in Chemistry. During his college years, Bryan completed a Howard Hughes Summer Research Fellowship at Princeton University in the Department of Molecular Biology where he worked on elucidating the role of microRNAs in breast cancer metastasis in Dr. Yibin Kang's laboratory. At Villanova, Bryan conducted research in the area of gene regulation under the late Dr. Mary Kay Francis and completed a senior thesis that involved characterizing the promoter region of a gene involved in wound healing. In 2007, Bryan was a finalist for the national Gates-Cambridge Scholarship and a recipient of the University of Cambridge Overseas Research Studentship Award. In 2011, as a graduate student, Bryan was invited to give a talk at the Keystone Symposia on Molecular and Cellular Biology: Hematopoiesis. To date, Bryan is a co-author on the following papers: 1) Ito, T, **Zimdahl, B** and Reya, T. (2012) aSIRTing control over cancer stem cells. *Cancer Cell*, 21(2):140-2. 2) Ito, T*, Kwon, HY*, **Zimdahl, B** et al. (2010) Regulation of myeloid leukaemia by the cell-fate determinant Musashi. *Nature* 466(7307):765-8.